Biochemical Characterization of Two Cytomegalovirus MHC Class I Homologs

Thesis by

Tara Lynn Chapman

In Partial Fulfillment of the Requirements

for the Degree of

Doctor of Philosophy

California Institute of Technology

Pasadena, California

2000

(Submitted December 15, 1999)

Acknowledgements

If there is anything I've learned over the past five years, it's the importance of working in a lab with people who are not only extremely talented, but who are also willing to share their expertise. My project would have been so much less without the input of my labmates and I would like to take some time now to acknowledge their contributions. First and foremost I would like to thank my advisor, Pamela J. Bjorkman, who has been an incredible source of inspiration and enthusiasm and given that I think she knows everything, a valuable source of scientific information. I would like to thank her for all the time she invested in teaching me how to design and interpret scientific experiments, for all her patience in helping me learn to talk and write about my work, and for all the advice she has given me regarding a career in science. I would also like to say that it has been really fun working with an advisor who is so willing to join into lab activities, whether it be ski vacations, dinner outings or Star Wars premiers.

I would next like to thank Astrid Heikema who has been integral in making the viral homolog project work. Let me just say right now that there is now way I can thank Astrid enough. She is as talented as any graduate student, understands the homolog project at least as well as I do and is exceptionally motivated - not to mention that she is a pleasure to work with and has an outlook on work in the sciences that is refreshing.

I am deeply indebted to Dr. Anthony West, most recently for his tireless efforts on the LIR-1 D1D2 structure project and previously for all his help with the Biacore. He is a very good and patient teacher and has spent many, many hours helping me at the expense of his own work. It is a real pleasure to work with Anthony and spending time with him has been rewarding as every now and then the taciturnity will fade and I'll catch a glimpse of the humorous, fun-loving individual underneath.

I would like to thank Zsuzsi Hamburger for being a really fantastic friend and for all her help with the LIR-1 D1D2 structure project. Zsuzsi is wonderful to have around as she is always encouraging and brings a tremendous amount of enthusiasm to any project or event. I have really enjoyed working with her and appreciate the hours she has spent processing data with me. I will miss her tremendously when I have to start my postdoctoral work.

I would like to thank Dr. Melanie Bennett for many things. First I would like to thank her for taking the time to look over my crystal trays; without her input I'm sure I would have completely overlooked many promising conditions. I would like to thank her for sharing with me a lot advice about applying for postdoctoral positions, applying for funding and for all the discussions I've subjected her to regarding a career in science. She is very knowledgeable, approachable and fair and in many ways she is the scientist I would like to be someday.

I would like to thank my baymate and friend, W. Lance Martin. When he joined the lab I asked Pamela if he could have the bench next to mine - looking back I realize that I had no idea what I was in for! Lance has been many things to me over the years including a walking textbook on molecular biology, an unabridged source of oftentimes pointless information, a moral compass, a pain in my ass, a means of support and sometimes prodding, a day laborer, a confidant, and above all a good friend. I greatly appreciate all the times he has helped me figure out why something wasn't working and his willingness to help me with the Biocad, but most of all I appreciate all the discussions and laughs we shared in the bay.

I would like to thank Dr. Art Chirino for help with crystallography, data collection and data processing and for advice regarding job searches and interview etiquette. I would like to thank Watson Shen for donating protein, for helping me move and for always being so good-natured. I would like to thank Dr. T.S. Ramalingam for sharing his expertise with cell staining studies and I would like to thank Dr. Luis Sánchez for protein donations and for help with protein chromatography and characterization. I would like to thank Dr. José Lébrón for providing HFE and for many helpful discussions regarding careers in science.

I would especially like to thank Marta Murphy. Never before has an administrative assistant been so committed to actually helping the people with whom she works. She is always good humored and will help when donuts are forgotten prior to

group meeting, will provide poster board for a retreat and will type numbers on the top several pages needed to complete a thesis.

I would like to thank Lynda Llamas for all the fun she brings into my life, for keeping the lab stocked and in working order, for sharing with me her love of music, dancing and all things Cuban (except Fidel of course!).

I would like to thank Peter Snow for making and expressing many protein constructs and for providing many, many liters of supernatants containing those proteins.

I would like to thank Dr. Ray Owen for introducing me to Caltech and to immunology, for letting me live with he and his wife, June, for many months, for sharing his Jelly Bellys and listening to my progress, for encouraging me to think about the implications of my work and for introducing me to other prominent members of the immunology field.

And thank you to Steve Arvedson. For many years now he has tolerated long hours and odd passions but still he is always on my side and is there to encourage me and bring out the brighter side of even the worst situation. Thank you Arv for all your love and support.

And finally, thank you to my parents Tom and Vicky Owen for all their love, support and the beef jerky.

Abstract

Cytomegaloviruses are ubiquitous host-specific pathogens that are capable of causing life-long persistent infections in immunocompetent hosts. To maintain this persistence in the presence of a functional immune system, both human and murine cytomegaloviruses (HCMV and MCMV, respectively) encode genes that modulate the host immune response. These genes include the MHC class I homologs UL18 from HCMV and m144 from MCMV. The host receptor for UL18 has been identified as LIR-1, a B cell, monocyte and dendritic cell inhibitory receptor related to natural killer cell inhibitory receptors, whereas the receptor for m144 remains unknown. In order to facilitate understanding of the functions of UL18 and m144 in viral pathogenesis and immune evasion, we have initiated structure/function analyses of m144, UL18 and LIR-1. We show that soluble m144 associates with the MHC class I light chain, ß2-microglobulin, but unlike UL18 and class I MHC proteins, m144 does not associate with endogenous peptides, presumably due to a large deletion in the peptide binding platform. Using soluble versions of UL18, class I MHC molecules and LIR-1, we find that LIR-1 interacts with the relatively non-polymorphic α3 domain of class I proteins and the analogous region of UL18 using its N-terminal immunoglobulin-like domain. Recognition of the α3 domain, which is relatively non-polymorphic in class I MHC molecules, predicts that LIR-1 can interact with most or all class I MHC molecules, consistent with previous observations that LIR-1 binds a wide range of class I proteins. We also find that LIR-1

binds UL18 with a >1000-fold higher affinity than it binds classical and non-classical class I MHC proteins, illustrating how a viral protein can effectively compete with host proteins to subvert the host immune response.

Table of Contents

Appendix B: Characterization of the Interaction Between the Herpes Simplex Virus Type I Fc Receptor and Immunoglobulin G

List of Figures

List of Tables

Chapter 1:

Introduction

Chapter 1: Introduction

1. Introduction

Cytomegaloviruses (CMVs) are ubiquitous, species-specific DNA viruses belonging to the Betaherpesvirinae subfamily of the herpesviridae family. Human cytomegalovirus (HCMV) is endemic in all human populations, infecting 50-90% of individuals in developed countries and up to 100% of those in developing countries (Britt and Alford, 1996). CMV infection in immunocompetant hosts is often subclinical, and while an immune response is made, it is insufficient to completely clear the infection. Instead, the virus persists, often in a state of latency, throughout the lifetime of the host. CMV infection in immunocompromised individuals such as neonates, transplant recipients and AIDS patients can cause severe to fatal disease. Due to the morbidity and mortality associated with CMV infection, strategies to prevent or resolve infection are of great importance. Characterization of viral genes responsible for CMV pathogenicity is necessary to advance the prevention and treatment of CMV disease.

2. Organization and Comparison of the Human and Murine CMV Genomes

The genomes of HCMV (strain AD169) and murine CMV (MCMV) (strain Smith) have both been sequenced (Chee et al., 1990; Rawlinson et al., 1996). Both contain a linear double stranded DNA molecule, approximately 230 kb in length. HCMV encodes 208 predicted ORFs, MCMV encodes 170 ORFs, of which 78 share significant amino acid

identity with HCMV genes. A common core of genes, conserved between CMVs, is found in the center of both CMV genomes and is flanked by genes lacking in homology to genes in other CMVs (Chee et al., 1990; Rawlinson et al., 1996). Many of the ORFs in HCMV share a high degree of identity with neighboring genes forming families that appear to be the result of gene duplication (Weber et al., 1988). The genome of HCMV is composed of two unique regions (U), designated as long (U_L) and short (U_S), flanked by inverted repeat sequences located internally (IR_L and IR_L) and terminally (TR_L and TR_S) (Figure 1-1). The MCMV genome has only one unique region flanked by direct repeats (Figure 1-1).

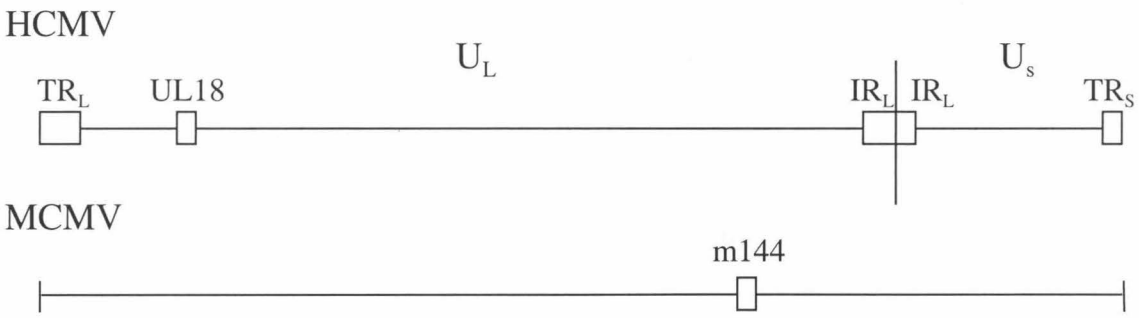

Figure 1-1. Schematic Representation of the Genomic Sequences of HCMV and MCMV.

3. Virion Structure

CMV DNA is enclosed within an icosahedral capsid, 100 nm in diameter, composed primarily of one protein, UL86. The capsid is surrounded by a tegument, an amorphous layer that fills the space between the nucleocapsid and an envelope. Neither the

structure nor the function of the tegument are clearly understood, although it contains 40% of the virion protein mass (Irmiere and Gibson, 1983), most of which is composed of phosphoproteins (Gibson, 1983). The major tegument proteins include pp65 (UL83) and pp150 (UL32). By comparison with other herpesviruses, it is predicted that pp150 and pp65 regulate viral gene expression and modify the host cell metabolism. Surrounding the tegument is an envelope composed of host lipids derived from nuclear, endosomal or cytoplasmic membranes (Mocarski, 1993; Tooze et al., 1993) and three to eight different viral proteins (Farrar and Oram, 1984). Glycoprotein B (gB, UL55) is the major envelope protein and the principal target of neutralizing antibodies (Britt et al., 1990; Rasmussen et al., 1991). Differences in virulency between HCMV strains have been attributed to differences in gB sequences (Bongarts et al., 1996; Fries et al., 1994); five different gB genotypes have been identified (Shepp et al., 1998). Glycoproteins H (gH, UL75) and L (gL, UL115) are also abundant in the viral envelope (Gretch et al., 1988).

4. Host Cell Adhesion and Entry

The viral ligands and host cell receptors responsible for attachment and entry of CMV into host cells have not been clearly defined. The initial event appears to be attachment to extracellular heparan sulfate (Compton et al., 1993) followed by interaction with a specific cellular receptor such as CD13 or annexin II (Sowadski, 1994; Wright et al.,

1995). The finding that HCMV is coated with the class I MHC light chain ß2-microglobulin led to the suggestion that MHC class I molecules were receptors for HCMV (Grundy et al., 1987); however, no correlation between HCMV infection and class I MHC expression has been observed (Polic et al., 1996). Instead gB is likely involved in host cell penetration (Navarro et al., 1993) and the covalently linked gH and gL together with gB are thought to contribute to fusion of the viral envelope with the host cell membrane (Milne et al., 1998).

5. Viral Replication

CMV replication is tightly regulated (Mocarski, 1993). Gene products are expressed at immediate early (IE), delayed early (E), and late (L) phases of the replication cycle in infected cells. IE genes are transcribed following virus entry, independent of de novo viral protein synthesis. E gene transcription then occurs only after expression of one or more IE genes as IE proteins are required to transactivate E gene promoters. The L phase of viral transcription is initiated by transactivation of L promoters by E gene products and marks the beginning of viral DNA replication and synthesis of virion structural proteins.

CMV has historically been described as a slow replicating virus based on the time to appearance of cytopathicity in cell culture. Recent experiments demonstrate,

however, that the doubling time of CMV is in fact more rapid than previously thought, being on the order of 1 day (Emery et al., 1999).

6. Viral Transmission

The high prevalence of CMVs is due to their efficient transmission between hosts. Once infected, viral shedding is observed for extensive periods of time and recurrent shedding is observed upon viral reactivation (Kumar et al., 1973). Humans are believed to be the only reservoir for HCMV. Spread of HCMV occurs through exposure to infected body secretions, including saliva, urine and milk (Britt and Alford, 1996). Children may acquire HCMV transplacentally, during birth, from breast-feeding, in day care centers, or in school (Britt and Alford, 1996). One study demonstrated that 80% of the children at a group day care center acquired HCMV as opposed to 20% of children who received care at home (Pass et al., 1984). While most individuals acquire HCMV during childhood, adults may acquire HCMV sexually or through blood, bone marrow or solid organ transplants (Britt and Alford, 1996).

7. Sites of Infection

It is not known how the virus moves from the site of infection into the bloodstream, although one theory suggests that the virus may be transported by phagocytes (Bevan et al., 1996). Once in the bloodstream CMV spreads to many tissues including the kidney,

liver, spleen, heart, brain, retina, esophagus, inner ear, lungs, colon and salivary glands (Sinzger and Jahn, 1996). HCMV DNA is also detectable in monocytes, lymphocytes and neutrophils, although the neutrophils are probably not infected, but are positive for viral DNA because of phagocytosis of intact virions (Turtinen et al., 1987).

8. Latency and Reactivation

After primary infection, the immune system effectively controls disease progression and terminates viral replication; however, the immune response is unable to completely eliminate the virus from all tissues in the host. In the tissues that remain infected it is unclear whether the virus establishes a chronic infection producing undetectable levels of virus or whether the virus is truly latent, remaining dormant in cells and producing virus only upon external stimulation. The prevailing theory is that CMV, at least in some cells, can assume a true latent state. The site of latency is also unclear, although HCMV transmission has been shown to occur through blood transfusions, bone marrow grafts and solid organ transplants (Britt and Alford, 1996). Examination of tissues obtained from infected individuals indicates that peripheral blood mononuclear cells are a viral reservoir (Meyers, 1986; Tegtmeier, 1989). Experiments suggest that myelomonocytic progenitor cells become infected early in their development (Taylor-Wiedeman et al., 1994) and HCMV persists in these cells in a non-lytic state, replicating along with them as they proliferate and differentiate. This enables virus to spread

throughout the host from a limited number of infected cells and to persist for long periods of time. While in the monocytic stage viral genes do not appear to be expressed; however, viral reactivation may be achieved by allogeneic stimulation of monocytes and infectious virus can be obtained from monocyte-derived macrophages (Soderberg-Naucler et al., 1997).

Vascular endothelial cells (VECs) may also be sites of latency. HCMV infection in vitro of VECs results in continuous release of infectious virus without inhibition of the cell cycle indicating that the virus and the cell coexist (Fish et al., 1998). VECs interact with cells trafficking in the bloodstream and migrating into tissues. If infected, they would provide an efficient means of disseminating virus.

9. Immune Response

Natural killer (NK) cells are important in restricting viral spread in the early phase (3-6 days) of viral infection. Their importance in control of HCMV infection was demonstrated by a patient with a complete NK cell deficiency who suffered from an unusually severe infection (Biron et al., 1989). They are also important in the control of MCMV as mice depleted of NK cells by treatment with anti-GM1 or anti-NK1.1 antibodies have increased levels of MCMV in the spleen, liver and lung (Tay et al., 1998) and genetic resistance to MCMV correlates with a single gene found within the NK gene complex (Scalzo et al., 1990). However, by themselves, NK cells are not

sufficient to clear MCMV infection. Recovery from MCMV disease is dependent upon a cellular immune response in which CD8+ T cells are dominant in limiting viral replication and preventing tissue destruction in all organs except for the salivary glands, where CD4+ T cells are necessary for viral control (Jonjic et al., 1990).

In humans, CD8+ and CD4+ T cells are also important in controlling HCMV infection. Adoptive transfer of HCMV-specific CTLs provides protection from HCMV disease (Reusser et al., 1991). The majority of the CTL response is directed against matrix proteins combined with fewer responses to gB, gH, pp50 (UL44) and pp28 (UL98) as well as CD4+ responses to IE-1, gB, IE-2, pp71 (UL82) and UL18 (He et al., 1995).

The importance of the antibody response to HCMV or MCMV is unclear. Antibodies have not been shown to be necessary in controlling the primary infection; however, they do appear to limit the severity of recurrent CMV disease (Winston et al., 1982).

10. T Cell Recognition of Virally Infected Cells

That the host immune response is highly effective in limiting CMV infection is evidenced by elimination of infectious virus from the bloodstream and restriction of viral replication in the tissues following primary infection and by prevention of widespread viral reactivation while the host remains immunocompetent. Therefore, to proliferate

and spread during acute infection and reactivation, CMV has developed a number of immune evasion mechanisms. As previously discussed, T cells are important in controlling CMV infection. T cells survey host cells for the presence of intracellular viruses, bacteria or other ills by expressing receptors that interact with either class I MHC or class II MHC molecules on the surface of host cells (Rammensee et al., 1993). Class I MHC molecules are expressed on nearly every cell in the body and are recognized by CD8+ T cells (also known as cytotoxic T cells or CTLs); MHC class II molecules are expressed on cells of the immune system and are recognized by CD4+ T cells. As the CMV immune evasion tactics discussed below focus primarily on modulating class I MHC expression and function, only class I MHC molecules will be discussed here

Class I MHC molecules are composed of two polypeptide chains. One is an MHC-encoded polymorphic heavy chain, typically 338 amino acids long with one N-linked glycosylation site and a molecular mass of 44 kDa (reviewed in (Bjorkman and Parham, 1990)). The extracellular region can be divided into three domains, α1, α2 and α3. The second polypeptide chain, ß2m, is a non MHC-encoded, non-polymorphic, non-glycosylated light chain, 99 amino acids in length with a molecular mass of 12 kDa. These two molecules associate in the ER where they complex with a third moiety, a peptide 8-9 amino acids in length that is derived from the degradation of cytosolic proteins (Rammensee et al., 1993). Peptides bind to class I MHC molecules in a groove

located between two α-helices that span an 8-stranded ß-pleated sheet. Peptide termini fit into pockets at each end of the groove that are lined with conserved residues (reviewed (Stern and Wiley, 1994)). There are additional pockets in the groove that, due to the chemical nature of the amino acids lining the pocket, can accommodate only specific side chains. The MHC molecule, once loaded with peptide, proceeds to the cell surface to present the peptide to the TCRs of CD8+ T cells; this is known as antigen presentation (reviewed in (Pamer and Cresswell, 1998)). Recognition of a peptide in the context of an MHC molecule may lead to the lysis of the host cell. It is therefore advantageous for a pathogen to interfere with antigen presentation, especially since CMV, due to its size, encodes many potential epitopes.

11. MCMV Immune Evasion Mechanisms

MCMV expresses a number of proteins that interfere with antigen presentation. The gene product of the E gene m152 retains class I MHC molecules in a post-ER/early Golgi compartment (Ziegler et al., 1997). gp48 (m06) binds ß2m and targets class I MHC molecules to the endosome/lysosome for degradation (Reusch et al., 1999). gp34 associates with class I MHC molecules and migrates with them to the cell surface, perhaps preventing them from being recognized by T cells (Kleijnen et al., 1997). MCMV also inhibits interferon (IFN)-γ-stimulated MHC class II expression on macrophages by inducing IFN-α or IFN-β (Heise et al., 1998). In addition, MCMV

encodes an immunoglobulin G receptor (Thale et al., 1994) that could prevent antibody-mediated detection of virally infected cells and possibly a chemokine receptor (Davis-Poynter et al., 1997) that could prevent attraction of immune effector cells to the site of infection.

12. HCMV Immune Evasion Mechanisms

To prevent antigen presentation throughout the HCMV replication cycle, HCMV encodes several different genes that are active at each stage of viral replication. In the IE stage, the matrix protein pp65 (UL83) inhibits presentation of the 72-kDa IE protein through phosphorylation (Gilbert et al., 1996). While this prevents peptide presentation, it does not affect the stability of the IE protein nor its ability to transactivate transcription. The US3 gene product is expressed during the E stage and retains MHC class I heterodimers in the ER (Ahn et al., 1996; Jones et al., 1996). The US2 and US11 gene products are also expressed during the E stage and direct newly synthesized MHC class I molecules from the ER to the cytosol where they are deglycosylated and then degraded by the proteasome (Wiertz et al., 1996). During the E/L phase, US6 is expressed, which inhibits TAP-mediated translocation of peptides into the ER (Ahn et al., 1997).

Other HCMV-mediated immune evasion strategies include interference with IFN-γ-stimulated MHC class II expression (Miller et al., 1998), expression of an

immunoglobulin G receptor (Murayama et al., 1989), expression of chemokine receptors that may be important in preventing leukocyte migration to the site of infection (Bodaghi et al., 1998) and expression of an α chemokine homolog that is hypothesized to attract neutrophils for subsequent infection (Penfold et al., 1999).

13. NK Cell Recognition of Cells with Down-Regulated Class I MHC Molecules

Another strategy used by both HCMV and MCMV to prevent antigen presentation is down-regulation of MHC class I expression. While this should hinder detection of virally infected cells by T cells, down-regulation of class I expression may also make virally-infected cells susceptible to NK cells lysis (Ljunggren et al., 1990). NK cells express both activating and inhibitory receptors (Lanier, 1997). The activating receptors may recognize either MHC or non MHC class I ligands, whereas the inhibitory receptors specifically recognize class I MHC molecules (Lanier, 1997). The inhibitory response is normally dominant; however, the target cell becomes susceptible to lysis if class I MHC expression levels decrease (Ljunggren and Kärre, 1990). In humans, NK cell inhibitory receptors belong to either the immunoglobulin (killer inhibitory receptors, KIRs) or C-type lectin (CD94 and NKG2) superfamilies (Yokoyama, 1998). In mice, inhibitory

receptors are primarily members of the C-type lectin (Ly49) superfamily (Yokoyama, 1998).

14. CMV-Encoded MHC Class I Homologs

MCMV, HCMV and rat CMV (RCMV) encode MHC class I heavy chain homologs (Beck and Barrell, 1988; Beisser et al., 1999; Rawlinson et al., 1996). The function of these MHC class I homologs is not known, but it is appealing to speculate that these proteins serve as decoy class I MHC molecules to engage NK cell inhibitory receptors, thereby preventing lysis of infected cells that have down-regulated their class I proteins. This idea, although attractive, has not been proven. Below is a summary of previous speculations and findings that shaped the questions I wanted to address with my thesis work.

The UL18 heavy chain was identified in HCMV by Beck and Barrel in 1988. In 1990 Browne et al. determined that the UL18 heavy chain associated with ß2m and also noted that endogenous MHC class I expression in HCMV-infected cells was severely decreased. Based on these observations Browne et al. suggested that UL18 expression might prevent surface MHC class I expression by sequestering ß2m from MHC class I heavy chains. However, a subsequent paper by Browne et al. (1992), using a mutant HCMV in which the UL18 gene had been deleted, demonstrated that the UL18 gene was

dispensible for replication and was not responsible for MHC class I down-regulation (Browne et al., 1992).

Further characterization of UL18 by Fahnestock et al. (1995) showed that UL18, like class I molecules, associates with peptides with characteristics similar to peptides found associated with classical MHC class I molecules (Fahnestock et al., 1995). At this time Fahnestock et al. also proposed that UL18 might be functioning as a surrogate class I molecule, engaging NK cell inhibitory receptors and protecting those cells that, due to down-regulation of surface MHC class I expression, would be susceptible to NK cell lysis.

m144 was identified by Rawlinson et al. (1996) and later work by Farrell et al. (1997), using a mutant MCMV lacking the m144 gene, demonstrated that m144 expression was important for preventing the clearance of virally infected cells by NK cells in infected mice (Farrell et al., 1997; Rawlinson et al., 1996). This work supported the hypothesis that the viral MHC class I homologs were modulating the anti-viral NK cell response.

In 1997 Cosman et al. identified the host receptor for UL18 and found surprisingly that it was not a KIR, but rather a member of the leukocyte immunoglobulin-like receptor (LIR) family, LIR-1. Unlike KIRs, which are expressed on NK cells and a subset of T cells (Lanier, 1998), LIR-1 is expressed predominantly on monocytes, B cells and dendritic cells and on only a subset of NK cells and T cells

(Borges et al., 1997; Colonna et al., 1997; Fanger et al., 1998). Despite the difference in expression of LIR-1 and KIRs, the LIR and KIR family share many similarities. The LIR family comprises nine members, each having either two or four extracellular Ig-like domains (Borges et al., 1997) encoded on human chromosome 19q13.4, in close proximity to the KIR genes (Wende et al., 1999). Five of the LIRs have intracellular ITIM motifs, three have short cytoplasmic tails with a charged arginine residue within the transmembrane domain and one is predicted to be secreted (reviewed in (Cosman et al., 1999)) (Figure 1-2). The function(s) of the LIR proteins are not known; however, both LIR-1 and LIR-2 have been demonstrated to associate with MHC class I molecules (Fanger et al., 1998).

LIR-1 shares ~40% overall sequence identity with the p58 NK cell killer inhibitory receptors (KIR) (Cosman et al., 1997). These KIRs encode two extracellular Ig-like domains; alignment of LIR-1 domains 1 and 2 (D1D2) with p58 KIRs reveals 37% identity and alignment of LIR-1 domains 3 and 4 (D3D4) with p58 KIRs reveals 44% identity (Figure 1-3).

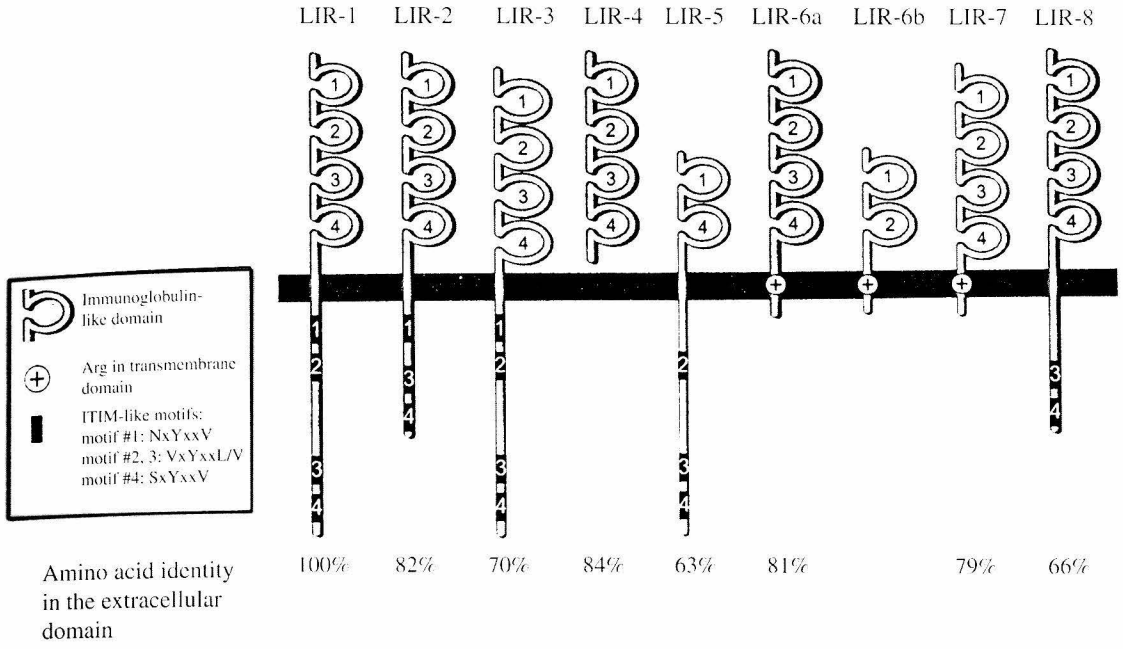

Figure 1-2. Schematic Representation of the LIR Family. Reproduced from (Cosman et al., 1999).

Alignment of KIR2DL3 with D1D2

36.9% identity

```
KIR2DL3 GFFLLQGAWPHEGVHRKPSLRAHPGPLVKSEETVILQCWSDVRFEHFLLHR
D1D2    GHL------P------KPTLWAEPGSVITQGSPVTLRCQGGQETQEYRLYR

KIR2DL3 EGKFKDTLRLIGEHHDGVSKANFSIGPMMQDLAGTYRCY-GSVTHSPYQLS
D1D2    EKKTAPWITRIPQ--ELVKKGQFPIPSITWEHAGRYRCYYGSDTAGR---S

KIR2DL3 APSDPLDIVITGLYEKPSLSAQPGPTVLAGESVTLSCSSRSSYDMYHLSRE
D1D2    ESSDPLELVVTGAYIKPTLSAQPSPVVNSGGNVTLQCDSQVAFDGFILCKE

KIR2DL3 GE-AHERRFSAGPKVNGTFQADFPLGPATHGGT--YRCFGSFRDSPYEWSN
D1D2    GEDEHPQCLNSQPHARGSSRAIFSVGPVSPSRRWWYRCYAYDSNSPYEWSL

KIR2DL3 SSD--PLLVS
D1D2    PSDLLELLVL
```

```
Alignment of KIR2DL3 with D3D4
43.7% identity

KIR2DL3 GFFLLQGAWPHEGVHRKPSLRAHPGPLVKSEETVILQCWSDVRFEHFLLHR
D3D4    G-----------VSKKPSLSVQPGPIVAPEETLTLQCGSDAGYNRFVLYK

KIR2DL3 EGKFKDTLRLIGEHHDGVSKANFSIGPMMQDLAGTYRCY-GSVTHSPYQLS
D3D4    DGE-RDFLQLAGAQPQAGLSQANFTLGPVSRSYGGQYRCYGAHNLSS-EWS

KIR2DL3 APSDPLDIVITGLYEKPSLSAQPGPTVLAGESVTLSCSSRSSYDMYHLSRE
D3D4    APSDPLDILIAGQFYDRVSLSVQPGPTVASGENVTLLCQSQGWMQTFLLTK

KIR2DL3 GE-AHERRFSAGPKVNGTFQADFPLGPATHGGT--YRCFGSFRDSPYEWSN
D3D4    EGAADDPWRLRSTYQSQKYQAE-PMGPVTSAHAGTYRCYGSQSSKPYLLTH

KIR2DL3 SSDPL-LVS
D3D4    PSDPLELVV
```

Figure 1-3. Alignment of p58 KIR2DL3 with LIR-1 D1D2 and D3D4.

KIRs inhibit NK cell activation by engaging MHC class molecules followed by association of their ITIM sequences with the tyrosine phosphatases, SHP-1 and/or SHP-2 (Leibson, 1997). The ITIM domains of LIR-1 also associate with SHP-1 (Cosman et al., 1997) and LIR-1 has been shown to function as an inhibitory receptor capable of preventing calcium mobilization in monocytes and B cells, inhibiting target cell lysis by NK cells and increasing the activation threshold of cytotoxic T cells (Colonna et al., 1997; Fanger et al., 1998).

Yet unlike KIRs, which bind MHC class I molecules with allelic specificity, LIR-1 and LIR-2 recognize a broad range of MHC class I molecules (Fanger et al., 1998;

Navarro et al., 1999; Vitale et al., 1999). It is not known why monocytes, B cells and dendritic cells would express an inhibitory receptor for MHC class I molecules or why it would be advantageous for HCMV to express a molecule that specifically recognizes this receptor. A portion of my thesis work was devoted to characterizing the UL18/LIR-1 interaction in comparison to the MHC class I/LIR-1 interaction in an effort to address these questions.

15. Goals of m144 Characterization

To characterize m144, my approach was to express m144 and compare the properties of the purified protein to those of classical MHC class I molecules and UL18; e.g., analyze the secondary structure, determine whether it associates with ß2m and/or peptides. I also wanted to crystallize m144 and compare the three-dimensional structure to that of conventional MHC class I molecules and to generate reagents that could be used to identify the m144 ligand (e.g., anti-m144 antibodies, m144-GFP fusion proteins, biotinylated m144).

16. Characterization of m144

In my characterization of m144 I compared soluble versions of m144, UL18 and classical MHC class I molecules expressed in Chinese hamster ovary (CHO) cells. As mentioned above, both conventional MHC class I molecules and UL18 associate with

ß2m and peptides derived from the degradation of cytosolic proteins, and while m144 does associate with ß2m, I discovered that it does not associate with peptides. Furthermore, m144 is stably folded in the absence of bound peptides, a property not shared by either UL18 or class I MHC molecules (Chapman and Bjorkman, 1997; Fahnestock et al., 1992). This suggested that either peptide binding was not a required feature in the function of viral MHC class I homologs or that m144 and UL18 function differently. In addition to lacking a peptide binding function, measurement of the far UV CD spectrum of m144 revealed that m144 possesses secondary structural features that distinguish it further from molecules with a canonical class I MHC fold (e.g., UL18, H-2K^d, and FcRn). These studies are described in Chapter 2.

Determination of whether these structural differences between UL18 and m144 are indicative of a functional difference between the two viral homologs would be greatly facilitated by identification of the m144 host receptor. In collaboration with several other researchers, I have tried a number of different approaches without success. Thus at this time the m144 field is still filled with more questions than answers, many of which will be addressed in further detail in Chapter 3.

17. Experiments to Test Whether UL18 Engages NK Cell Inhibitory Receptors

Prior to the discovery of LIR-1 as the UL18 receptor, I attempted to test the theory that UL18 modulates the host immune response by interfering with the anti-viral NK response (Fahnestock et al., 1995). My approach was to express UL18 in HLA class I-null cells and determine whether or not UL18 expression in these cells provided protection against NK cell lysis. These experiments were hampered by the fact that UL18 is not expressed on the surface of these cells (Chapter 5). This problem was also encountered by our collaborators who were attempting the same experiment (L.L. Lanier, personal communication). In contrast, another laboratory published results suggesting that UL18 expressed on the surface of the same class I negative cell line did provide protection against NK cell lysis (Reyburn et al., 1997). This paper has been called into question by a number of subsequent studies and is discussed in detail in Chapter 5.

18. Goals of UL18/LIR-1 and MHC Class I/LIR-1 Characterization

To characterize the UL18/LIR-1 interaction in comparison to the MHC class I/LIR-1 interaction, my approach was to first express soluble versions of each of the proteins: UL18, LIR-1 and several classical and nonclassical MHC class I proteins. I then measured the affinity of the UL18/LIR-1 interaction, and determined whether variations

in the degree of glycosylation of UL18 or peptide binding by UL18 would affect the UL18/LIR-1 interaction. I also wanted to map which domain(s) on LIR-1 encoded the UL18 binding site and determine whether this is the same site recognized by MHC class I molecules. And reciprocally, I wanted to identify the domain used for LIR-1 binding on UL18 and determine whether this is the same domain used for LIR-1 binding of MHC class I molecules. Similar experiments could not be done with m144 since the ligand for m144 has not yet been identified.

19. Characterization of the UL18/LIR-1 and MHC Class I/LIR-1 Interactions

Using soluble versions of UL18, LIR-1 and several different classical and nonclassical MHC class I molecules, I determined that LIR-1 binds UL18 with an affinity >1000 fold higher than LIR-1 binds MHC class I molecules. I also determined that neither peptide binding nor variations in the degree of glycosylation of UL18 were factors in LIR-1 recognition. I identified the N-terminal domain of LIR-1 to be the UL18 and MHC class I binding site, and in collaboration with Astrid Heikema, a technician in the Bjorkman lab, identified the $\alpha 3$ domain of UL18 and MHC class I molecules as the binding site for LIR-1. Recognition of the $\alpha 3$ domain of class I molecules, which is relatively nonpolymorphic, predicts that LIR-1 can interact with most or all MHC class I molecules. Several previous studies have demonstrated that LIR-1 recognizes a wide

range of molecules (Colonna et al., 1997; Fanger et al., 1998; Navarro et al., 1999) and indeed I found that LIR-1 recognized all the classical and nonclassical class I molecules I tested. LIR-1 did not, however, recognize three MHC class I homologs that are structurally similar to, but functionally different from MHC class I molecules: the hemochromatosis protein (HFE) (Lebrón et al., 1998), the neonatal Fc receptor (FcRn) (Burmeister et al., 1994) and the Zn-α2-glycoprotein (ZAG) (Sánchez et al., 1997). None of these molecules associate with peptides and hence do not have a role in antigen presentation and while HFE and FcRn associate with ß2m, ZAG does not. Thus, from these examples, it appears that LIR-1 is specific for peptide-binding class I molecules that function in the immune system (Figure 1-4).

20. Implications of the UL18/LIR-1, MHC Class I/LIR-1 Characterization

The UL18 molecule was likely acquired as an MHC class I molecule from an infected host at a point during the evolution of HCMV with humans (Wiley, 1988). The fact that there is now such a dramatic difference in the LIR-1/UL18 and LIR-1/MHC class I interactions suggests that the original MHC class I molecule was modified to be specific for LIR-1 and implies that there is a benefit for HCMV in modulating LIR-1 expression and/or function. Yet before one can know what benefit UL18 is providing by derailing normal LIR-1 function, one needs to know what that normal LIR-1 function is.

As mentioned previously, LIR-1 is expressed on monocytes, B cells and dendritic cells and recognizes MHC class I molecules. By expressing a receptor that is specific

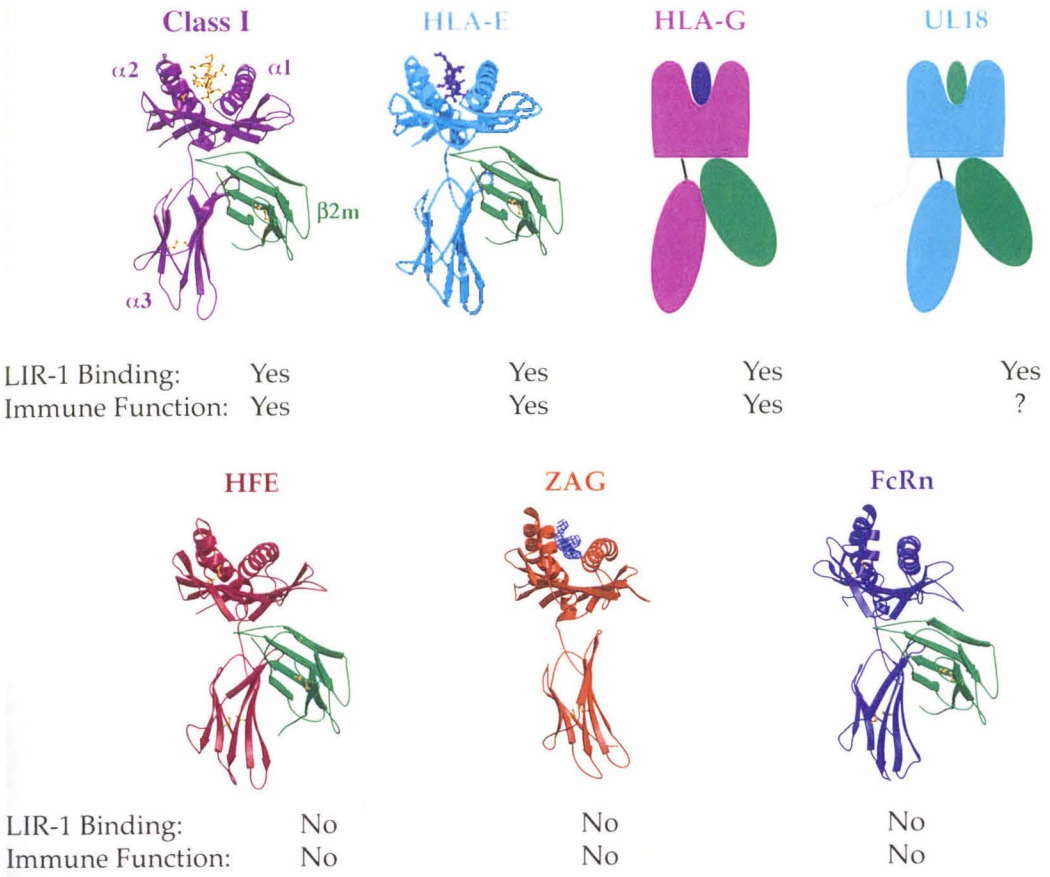

Figure 1-4. Schematic Showing the Molecules Tested for LIR-1 Binding, Their Functional Status in the Immune System and Ability to Bind Peptides.

for class I molecules, LIR-1-expressing cells are able to monitor the MHC class I expression of cells surrounding them. As T cells are effective at recognizing and eliminating infected or defective cells by surveying peptides displayed in MHC class I molecules, if a particular cell is expressing class I molecules and has not been eliminated

by T cells, MHC class I expression is probably a good indicator that the cell is in good health. As LIR-1 is an inhibitory receptor and interaction with MHC class I molecules triggers an inhibitory response, interaction with cells expressing normal MHC class I levels would presumably increase the activation threshold of LIR-1-expressing cells, decreasing the likelihood of immune effector cell activation and protecting healthy cells (Figure 1-5A). In contrast, interaction with cells expressing decreased class I expression

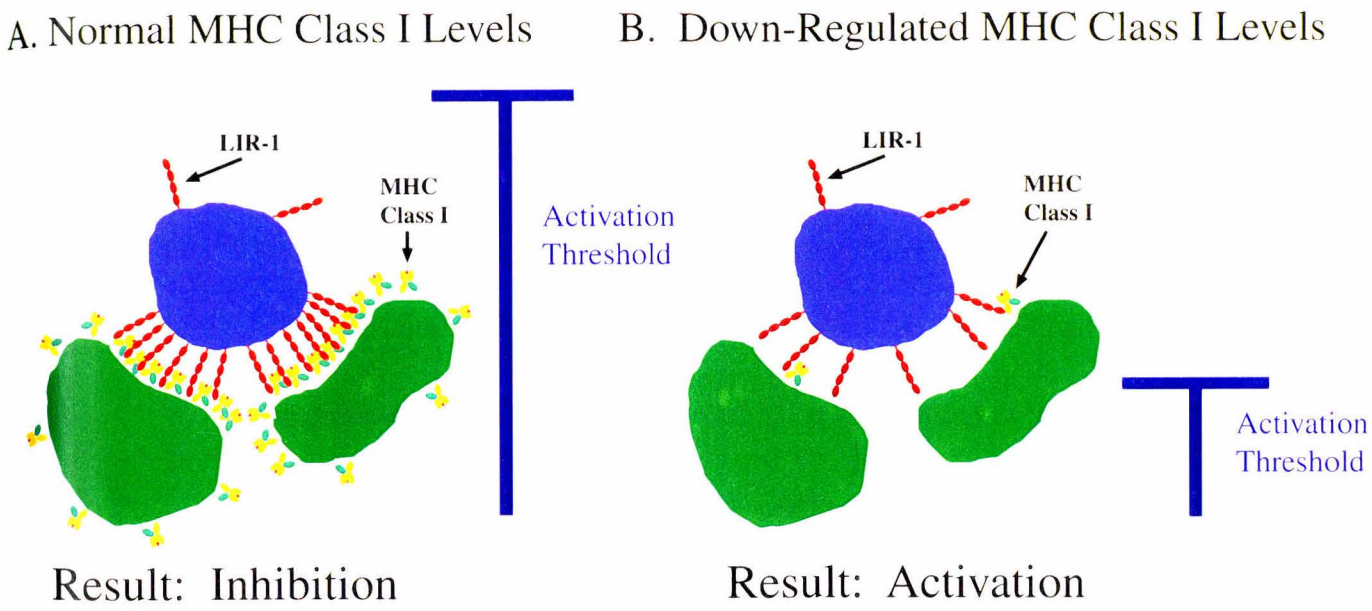

Figure 1-5. (A) Interaction of a LIR-1-expressing cell with cells expressing high levels of MHC class I molecules results in an increased activation threshold and a decreased likelihood of cell activation. (B) Interaction of a LIR-1-expressing cell with cells expressing low levels of MHC class I molecules results in a decreased activation threshold and an increased likelihood of cell activation.

levels (e.g., tumors, virally infected cells) would presumably decrease the activation threshold of LIR-1 expressing cells, increasing the likelihood of immune effector cell

activation and leading to elimination of defective cells (Figure 1-5B). The ability of LIR-1 to recognize the α3 domain of class I molecules presents a means for LIR-1-expressing cells to monitor the overall class I expression levels rather than the expression levels of specific molecules or alleles. The weakness of the LIR-1/MHC class I affinity requires that there be a high density of MHC class I expression in order to trigger LIR-1-mediated inhibition.

The UL18 molecule binds LIR-1 specifically and with high affinity, implying that the UL18 function is to modify either the expression and/or signaling of LIR-1. Based upon the results described in Chapter 4, I have thought of three possibilities to explain how UL18 could influence LIR-1 expression and signaling to benefit HCMV.

(1) UL18 substitutes for class I MHC molecules on the infected cell and binds LIR-1 expressed on immune effector cells. It is known that only very low levels of UL18 are expressed on the surface of virally infected cells (Leong et al., 1998). However, due to the the high affinity interaction of UL18 with LIR-1 only low levels of UL18 would be needed to elicit a similar effect on LIR-1-bearing cells as high numbers of MHC class I molecules. This may be a ploy used by HCMV to prevent activation of LIR-1-expressing immune effector cells, perhaps to prevent cytolysis of the infected cell or to prevent cytokine secretion that would attract other immune effector cells to the site of infection (Figure 1-6A).

(2) UL18 and LIR-1 bind to each other on the surface of the same cell. HCMV is known to infect both B cells and monocytes (Zhuravskaya et al., 1997), thus these cells will express both LIR-1 and UL18. By contrast, MHC class I molecules expressed on the same cells as LIR-1 would not be expected to constantly engage LIR-1 proteins on the same membrane because of their lower affinity for LIR-1 compared to that of UL18 for LIR-1. By continuously engaging LIR-1 molecules on the surface of an infected cell, LIR-1-expressing immune effector cells could be made oblivious to the MHC class I expression state of surrounding cells, possibly allowing infection to go unchecked (Figure 1-6B). This sort of scenario would have a particular role in regulation of HCMV latency and reactivation in monocytes, which are a reservoir of latent CMV infection (Taylor-Wiedman et al., 1991). Virus is not produced in monocytes, but when these cells are stimulated to progress to macrophages, infectious virus is expressed and released (Soderberg-Naucler et al., 1997). If UL18 binds LIR-1 on the surface of a monocyte, the monocyte is less likely to become activated and therefore HCMV would remain latent.

(3) UL18 prevents expression of LIR-1 on the surface of an infected cell by retaining it in an intracellular compartment. The majority of UL18 staining in virally infected cells is intracellular (E. Mocarski, personal communication), thus it appears that most UL18 molecules do not reach the surface of the cell, perhaps

being retained in the ER/Golgi region. If newly synthesized UL18 binds LIR-1 in the ER/Golgi, the high affinity of this interaction could trap LIR-1, preventing it from reaching the cell surface. Class I MHC molecules expressed in the same cell as LIR-1 would not be expected to trap LIR-1 intracellularly because class I molecules themselves are not retained. In contrast to the previous two scenarios, which propose that UL18 expression results in enhanced LIR-1 activity, in this scenario, UL18 expression results in decreased LIR-1 activity and therefore increased likelihood of activation of the LIR-1-expressing cell. Activation could result in cytokine production and attraction of immune effector cells, which could themselves be infected, to the site of infection (Figure 1-6C). In monocytes, retention of LIR-1 along with UL18 would lead to an increased likelihood of activation, resulting in increased likelihood of HCMV replication and viral production. Figure 1-6 can be found on the next page.

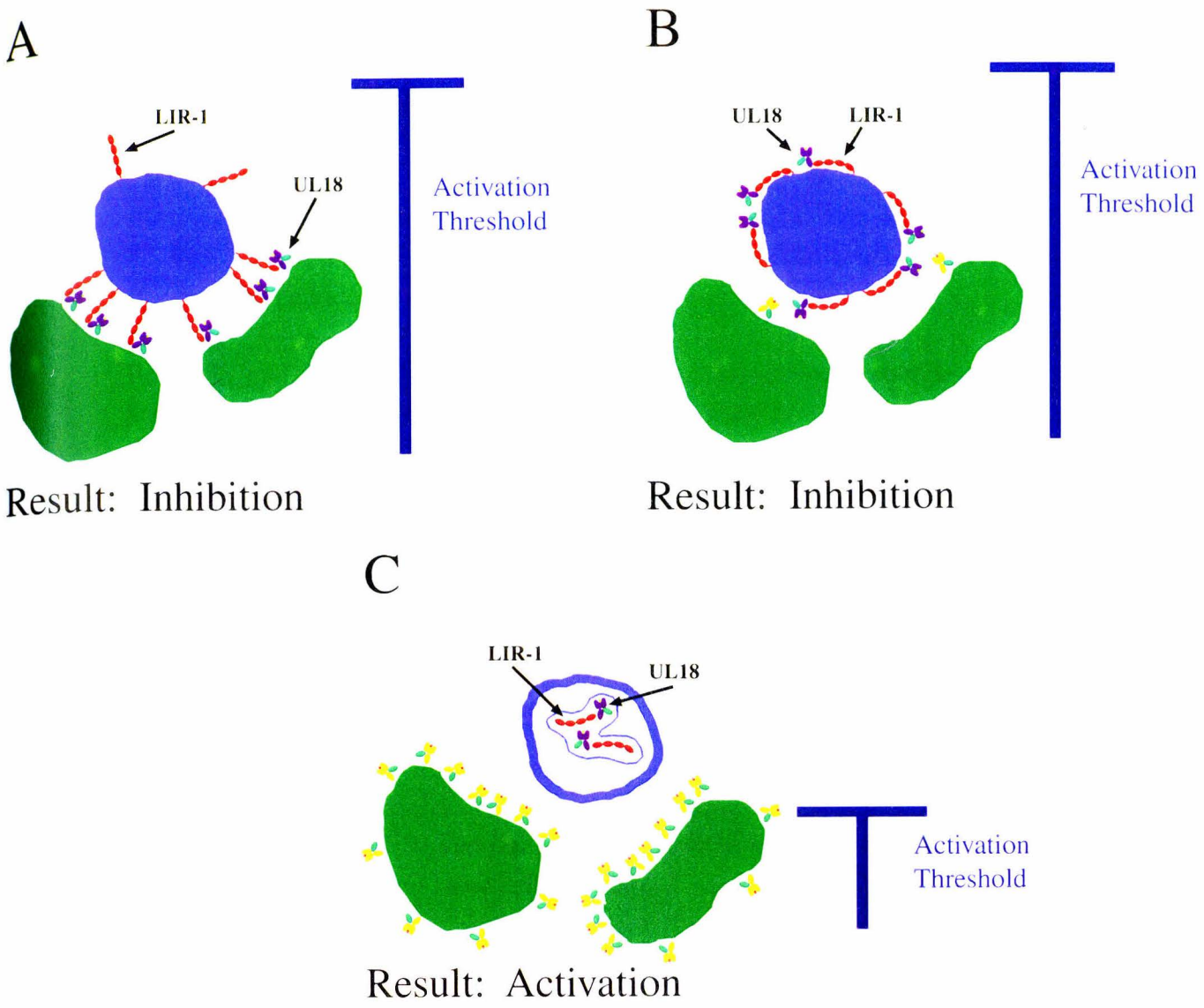

Figure 1-6. (A) Interaction of a LIR-1-expressing cell with cells expressing UL18 in place of MHC class I molecules could result in an increased activation threshold and a decreased likelihood of cell activation. (B) UL18 and LIR-1 expression on the same cell could result in high LIR-1 activation producing an increased activation threshold and decreased likelihood of activation of the LIR-1-expressing cell. (C) UL18-mediated retention of LIR-1 in the interior of the cell could prevent LIR-1-mediated signaling, lowering the activation threshold of the LIR-1-expressing cell and increasing the likelihood of cell activation.

21. References

Ahn, K., Angulo, A., Ghazal, P., Peterson, P. A., Yang, Y., and Fruh, K. (1996). Human cytomegalovirus inhibits antigen presentation by a sequential multistep process. Proc. Natl. Acad. Sci. U. S. A. *93*, 10990-10995.

Ahn, K., Gruhler, A., Galocha, B., Jones, T. R., Wiertz, E. J., Ploegh, H. L., Peterson, P. A., Yang, Y., and Fruh, K. (1997). The ER-luminal domain of the HCMV glycoprotein US6 inhibits peptide translocation by TAP. Immunity *6*, 613-621.

Beck, S., and Barrell, B. G. (1988). Human cytomegalovirus encodes a glycoprotein homologous to MHC class I antigens. Nature *331*, 269-272.

Beisser, P. S., Kloover, J. S., Grauls, G. E. L. M., Blok, M. J., Bruggeman, C. A., and Vink, C. (1999). The r144 MHC class I-like gene of rat cytomegalovirus is dispensable for both acute and long-term infection in the immunocompromised host. J. Virol. *In Press*.

Bevan, I. S., Sammons, C. C., and Sweet, C. (1996). Investigation of murine cytomegalovirus latency and reactivation in mice using viral mutants and the polymerase chain reaction. J. Med. Virol. *48*, 308-320.

Biron, C. A., Byron, K. S., and Sullivan, J. L. (1989). Severe herpesvirus infections in an adolescent without natural killer cells. N. Engl. J. Med. *320*, 1731-1735.

Bjorkman, P. J., and Parham, P. (1990). Structure, function and diversity of class I major histocompatibility complex molecules. Ann. Rev. Biochem. *90*, 253-88.

Bodaghi, B., Jones, T. R., Zipeto, D., Vita, C., Sun, L., Laurent, L., Arenzana-Seisdedos, F., Virelizier, J. L., and Michelson, S. (1998). Chemokine sequestration by viral chemoreceptors as a novel viral escape strategy: withdrawal of chemokines from the environment of cytomegalovirus-infected cells. J. Exp. Med. *188*, 855-866.

Bongarts, A., Von Laer, D., Vogelberg, C., Ebert, K., Van Lunzen, J., Garweg, J., Vaith, P., Hufert, F. T., Haller, O., and Meyer-Konig, U. (1996). Glycoprotein B genotype of human cytomegalovirus: distribution in HIV-infected patients. Scand. J. Infect. Dis. *28*, 447-449.

Borges, L., Hsu, M. L., Fanger, N., Kubin, M., and Cosman, D. (1997). A family of human lymphoid and myeloid Ig-like receptors, some of which bind to MHC class I molecules. J. Immunol. *159*, 5192-5196.

Britt, W. J., and Alford, C. A. (1996). Cytomegalovirus. In Fields Virology, B. N. Fields, D. M. Knipe, P. M. Howley, R. M. Chanock, J. L. Melnick, T. P. Monath, B. Roizman and S. E. Straus, eds. (Philadelphia, PA: Lippincott-Raven), pp. 2493-2523.

Britt, W. J., Vugler, L., Butfiloski, E. J., and Stephens, E. B. (1990). Cell surface expression of human cytomegalovirus (HCMV) gp55-116 (gB): use of HCMV-recombinant vaccinia virus-infected cells in analysis of the human neutralizing antibody response. J. Virol. *64*, 1079-1085.

Browne, H., Churcher, M., and Minson, T. (1992). Construction and characterization of a human cytomegalovirus mutant with the UL18 (class I homolog) gene deleted. J. Virol. *66*, 6784-6787.

Browne, H., Smith, G., Beck, S., and Minson, T. (1990). A complex between the MHC class I homologue encoded by human cytomegalovirus and ß2 microglobulin. Nature *347*, 770-772.

Burmeister, W. P., Gastinel, L. N., Simister, N. E., Blum, M. L., and Bjorkman, P. J. (1994). Crystal structure at 2.2 Å resolution of the MHC-related neonatal Fc receptor. Nature *372*, 336-343.

Chapman, T. L., and Bjorkman, P. J. (1997). Characterization of a murine cytomegalovirus class I MHC homolog: Comparison to MHC molecules and to the human cytomegalovirus MHC homolog. J. Virol., in press.

Chee, M. S., Bankier, A. T., Beck, S., Bohni, R., Brown, C. M., Cerny, R., Horsnell, T., Hutchison, C. A. D., Kouzarides, T., and Martignetti, J. A. (1990). Analysis of the protein-coding content of the sequence of human cytomegalovirus strain AD169. Curr Top Microbiol Immunol *154*, 125-169.

Colonna, M., Navarro, F., Bellon, T., Llano, M., Garcia, P., Samaridis, J., Angman, L., Cella, M., and Lopez-Botet, M. (1997). A common inhibitory receptor for major histocompatibility complex class I molecules on human lymphoid and myelomonocytic cells. J. Exp. Med. *186*, 1809-1818.

Compton, T., Nowlin, D. M., and Cooper, N. R. (1993). Initiation of human cytomegalovirus infection requires initial interaction with cell surface heparan sulfate. Virology *193*, 834-841.

Cosman, D., Fanger, N., and Borges, L. (1999). Human cytomegalovirus, MHC class I and inhibitory signalling receptors: more questions than answers. Immunological Reviews *168*, 177-185.

Davis-Poynter, N. J., Lynch, D. M., Vally, H., Shellam, G. R., Rawlinson, W. D., Barrell, B. G., and Farrell, H. E. (1997). Identification and characterization of a G protein-coupled receptor homolog encoded by murine cytomegalovirus. J. Virol. *71*, 1521-1529.

Emery, V. C., Cope, A. V., Bowen, E. F., Gor, D., and Griffiths, P. D. (1999). The dynamics of human cytomegalovirus replication in vivo. J. Exp. Med. *190*, 177-182.

Fahnestock, M. L., Johnson, J. L., Feldman, R. M. R., Neveu, J. M., Lane, W. S., and Bjorkman, P. J. (1995). The MHC class I homolog encoded by human cytomegalovirus binds endogenous peptides. Immunity *3*, 583-590.

Fahnestock, M. L., Tamir, I., Narhi, L., and Bjorkman, P. J. (1992). Thermal stability comparison of purified empty and peptide filled forms of a class I MHC molecule. Science *258*, 1658-1662.

Fanger, N. A., Cosman, D., Peterson, L., Braddy, S. C., Maliszewski, C. R., and Borges, L. (1998). The MHC class I binding proteins LIR-1 and LIR-2 inhibit Fc receptor-mediated signaling in monocytes. Eur. J. Immunol. *28*, 3423-3434.

Farrar, G. H., and Oram, J. D. (1984). Characterization of the human cytomegalovirus envelope glycoproteins. J Gen Virol *65*, 1991-2001.

Farrell, H. E., Vally, H., Lynch, D. M., Fleming, P., Shellam, G. R., Scalzo, A. A., and Davis-Poynter, N. J. (1997). Inhibition of natural killer cells by a cytomegalovirus MHC class I homologue in vivo. Nature *386*, 510-514.

Fish, K. N., Soderberg-Naucler, C., Mills, L. K., Stenglein, S., and Nelson, J. A. (1998). Human cytomegalovirus persistently infects aortic endothelial cells. J. Virol. *72*, 5661-5668.

Fries, B. C., Chou, S., Boeckh, M., and Torok-Storb, B. (1994). Frequency distribution of cytomegalovirus envelope glycoprotein genotypes in bone marrow transplant recipients. J Infect Dis *169*, 769-774.

Gibson, W. (1983). Protein counterparts of human and simian cytomegaloviruses. Virology *128*, 391-406.

Gilbert, M. J., Riddell, S. R., Plachter, B., and Greenberg, P. D. (1996). Cytomegalovirus selectively blocks antigen processing and presentation of its immediate-early gene product. Nature *383*, 720-722.

Gretch, D. R., Kari, B., Rasmussen, L., Gehrz, R. C., and Stinski, M. F. (1988). Identification and characterization of three distinct families of glycoprotein complexes in the envelopes of human cytomegalovirus. J. Virol. *62*, 875-881.

Grundy, J. E., J.A., M., Ward, P. J., Sanderson, A. R., and Griffiths, P. D. (1987). Beta 2 microglobulin enhances the infectivity of cytomegalovirus and when bound to the virus enables class I HLA molecules to be used as a virus receptor. J. Gen. Virol. *68*, 793-803.

He, H., Rinaldo, C. R. J., and Morel, P. A. (1995). T cell proliferative responses to five human cytomegalovirus proteins in healthy seropositive individuals: implications for vaccine development. J. Gen. Virol. *76*, 1603-1610.

Heise, M. T., Pollock, J. L., O'Guin, A., Barkon, M. L., Bormley, S., and Virgin, H. W. T. (1998). Murine cytomegalovirus infection inhibits IFN gamma-induced MHC class II expression on macrophages: the role of type I interferon. Virology *241*, 331-344.

Irmiere, A., and Gibson, W. (1983). Isolation and characterization of a noninfectious virion-like particle released from cells infected with human strains of cytomegalovirus. Virology *130*, 118-133.

Jones, T. R., Wiertz, E. J., Sun, L., Fish, K. N., Nelson, J. A., and Ploegh, H. L. (1996). Human cytomegalovirus US3 impairs transport and maturation of major histocompatibility complex class I heavy chains. Proc. Natl. Sci. U. S. A. *93*, 11327-11333.

Jonjic, S., Pavic, I., Lucin, P., Rukavina, D., and Koszinowski, U. H. (1990). Efficacious control of cytomegalovirus infection after long-term depletion of CD8+ T lymphocytes. J. Virol. *64*, 5457-5464.

Kleijnen, M. F., Huppa, J. B., Lucin, P., Mukherjee, S., Farrell, H., Campbell, A. E., Koszinowski, U. H., Hill, A. B., and Ploegh, H. L. (1997). A mouse cytomegalovirus glycoprotein, gp34, forms a complex with folded class I MHC molecules in the ER which is not retained but is transported to the cell surface. EMBO *16*, 685-694.

Kumar, M. L., Nankervis, G. A., and Gold, E. (1973). Inapparent congenital cytomegalovirus infection. A follow-up study. N. Engl. J. Med. *288*, 1370-1372.

Lanier, L. L. (1997). Natural killer cells: from no receptors to too many. Immunity *6*, 371-378.

Lanier, L. L. (1998). NK cell receptors. Annu. Rev. Immunol. *16*, 359-393.

Lebrón, J. A., Bennett, M. J., Vaughn, D. E., Chirino, A. J., Snow, P. M., Mintier, G. A., Feder, J. N., and Bjorkman, P. J. (1998). Crystal structure of the hemochromatosis protein HFE and characterization of its interaction with transferrin receptor. Cell *93*, 111-123.

Leibson, P. J. (1997). Signal transduction during natural killer cell activation: inside the mind of a killer. Immunity *6*, 655-661.

Leong, C. C., Chapman, T. L., Bjorkman, P. J., Formankova, D., Mocarski, E. S., Phillips, J. H., and Lanier, L. L. (1998). Modulation of natural killer cell cytotoxicity in human cytomegalovirus infection: the role of endogenous class I major histocompatibility complex and a viral class I homolog. J. Exp. Med. *187*, 1681-1687.

Ljunggren, H.-G., and Kärre, K. (1990). In search of the "missing self": MHC molecules and NK cell recognition. Immunol. Today *11*, 237-244.

Ljunggren, H. G., Stam, N. J., Öhlén, C., Neefjes, J. J., Höglund, P., Heemels, M. T., Bastin, J., Schumacher, T. N. M., Townsend, A., Kärre, K., and Ploegh, H. L. (1990). Empty MHC class I molecules come out in the cold. Nature *346*, 476-480.

Meyers, J. D. (1986). Infection in bone marrow transplant recipients. Am. J. Med. *81*, 27-38.

Milne, R. S., Paterson, D. A., and Booth, J. C. (1998). Human cytomegalovirus glycoprotein H/glycoprotein L complex modulates fusion-from-without. J. Gen. Virol. *79*, 855-865.

Mocarski, E. (1993). Cytomegalovirus biology and replication. In The Human Herpesviruses., B. Roizman, R. J. Whitley and C. Lopez, eds. (New York: Raven Press), pp. 173-236.

Murayama, T., Natsuume-Sakai, S., Xu, B., Furukawa, T., and Rinaldo, C. R. J. (1989). Biological response modifier enhances the activity of natural killer cell against human cytomegalovirus-infected cells. J. Med. Virol. *29*, 102-108.

Navarro, D., Paz, P., Tugizov, S., Topp, K., La Vail, J., and Pereira, L. (1993). Glycoprotein B of human cytomegalovirus promotes virion penetration into cells, transmission of infection from cell to cell, and fusion of infected cells. Virology *197*, 143-158.

Navarro, F., Llano, M., Bellon, T., Colonna, M., Geraghty, D. E., and Lopez-Botet, M. (1999). The ILT2(LIR1) and CD94/NKG2A NK cell receptors respectively recognize HLA-G1 and HLA-E molecules co-expressed on target cells. Eur. J. Immunol *29*, 277-283.

Pamer, E., and Cresswell, P. (1998). Mechanisms of MHC class I--restricted antigen processing. Annu. Rev. Immunol. *16*, 323-358.

Pass, R. F., Hutto, S. C., Reynolds, D. W., and Polhill, R. B. (1984). Increased frequency of cytomegalovirus infection in children in group day care. Pediatrics *74*, 121-126.

Penfold, M. E., Dairaghi, D., Duke, G. M., Saederup, N., Mocarski, E. S., Kemble, G. W., and Schall, T. J. (1999). Cytomegalovirus encodes a potent alpha chemokine. Proc. Natl. Acad. Sci. U. S. A . *96*, 9839-9844.

Polic, B., Jonjic, S., Pavic, I., Crnkovic, I., Zorica, I., Hengel, H., Lucin, P., and Koszinowski, U. H. (1996). Lack of MHC class I complex expression has no effect on spread and control of cytomegalovirus infection in vivo. J. Gen. Virol. *77*, 217-225.

Rammensee, H. G., Falk, K., and Rotzschke, O. (1993). Peptides naturally presented by MHC class I molecules. Annu. Rev. Immunol. *11*, 213-244.

Rasmussen, L., Matkin, C., Spaete, R., Pachl, C., and Merigan, T. C. (1991). Antibody response to human cytomegalovirus glycoproteins gB and gH after natural infection in humans. J. Infect. Dis. *164*, 835-842.

Rawlinson, W. D., Farrell, H. E., and Barrell, B. G. (1996). Analysis of the complete DNA sequence of murine cytomegalovirus. J. Virol *70*, 8833-8849.

Reusch, U., Muranyi, W., Lucin, P., Burgert, H. G., Hengel, H., and Koszinowski, U. H. (1999). A cytomegalovirus glycoprotein re-routes MHC class I complexes to lysosomes for degradation. EMBO *18*, 1081-1091.

Reusser, P., Riddell, S. R., Meyers, J. D., and Greenberg, P. D. (1991). Cytotoxic T-lymphocyte response to cytomegalovirus after human allogeneic bone marrow transplantation: pattern of recovery and correlation with cytomegalovirus infection and disease. Blood *78*, 1373-1380.

Reyburn, H. T., Mandelboim, O., Valez-Gomez, M., Davis, D. M., Pazmany, L., and Strominger, J. L. (1997). The class I MHC homologue of human cytomegalovirus inhibits attack by natural killer cells. Nature *386*, 514-519.

Sánchez, L. M., López-Otín, C., and Bjorkman, P. J. (1997). Characterization and crystallization of human Zn-α2-glycoprotein, a soluble class I MHC homolog. Proc. Natl. Acad. Sci. U.S.A. *94*, 4626-4630.

Scalzo, A. A., Fitzgerald, N. A., Simmons, A., La Vista, A. B., and Shellam, G. R. (1990). Cmv-1, a genetic locus that controls murine cytomegalovirus replication in the spleen. J. Exp. Med. *171*, 1469-1483.

Shepp, D. H., Match, M. E., Lipson, S. M., and Pergolizzi, R. G. (1998). A fifth human cytomegalovirus glycoprotein B genotype. Res. Virol. *149*, 109-114.

Sinzger, C., and Jahn, G. (1996). Human cytomegalovirus cell tropism and pathogenesis. Intervirology *39*, 302-319.

Soderberg-Naucler, C., Fish, K. N., and Nelson, J. A. (1997). Reactivation of latent human cytomegalovirus by allogeneic stimulation of blood cells from healthy donors. Cell *91*, 119-126.

Sowadski, J. M. (1994). Crystallization of membrane proteins. Curr. Opin. Struct. Biol. *4*, 761-764.

Stern, L. J., and Wiley, D. C. (1994). Antigenic peptide binding by class I and class II histocompatibility proteins. Structure *15*, 245-251.

Tay, C. H., Szomolanyi-Tsuda, E., and Welsh, R. M. (1998). Control of infections by NK cells. Curr. Top. Microbiol. Immunol. *230*, 193-220.

Taylor-Wiedman, J., Sissons, J. G., Borysiewicz, L. K., and Sinclair, J. (1991). Monocytes are a major site of persistence of human cytomegalovirus in peripheral blood mononuclear cells. J. Gen. Virol. *72*, 2059-2068.

Taylor-Wiedeman, J., Sissons, P., and Sinclair, J. (1994). Induction of endogenous human cytomegalovirus gene expression after differentiation of monocytes from healthy carriers. J. Virol. *98*, 1597-1604.

Tegtmeier, G. E. (1989). Posttransfusion cytomegalovirus infections. Arch. Pathol. Lab. Med. *113*, 236-245.

Thale, R., Lucin, P., Schneider, K., Eggers, M., and Koszinowski, U. H. (1994). Identification and expression of a murine cytomegalovirus early gene coding for an Fc receptor. J. Virol. *68*, 7757-7765.

Tooze, J., Hollinshead, M., Reis, B., Radsak, K., and Kern, H. (1993). Progeny vaccinia and human cytomegalovirus particles utilize early endosomal cisternae for their envelopes. Eur J Cell Biol *60*, 163-178.

Turtinen, L. W., Saltzman, R., Jordan, M. C., and Haase, A. T. (1987). Interactions of human cytomegalovirus with leukocytes in vivo: analysis by in situ hybridization. Microb. Pathog. *3*, 287-297.

Vitale, M., Castriconi, R., Parolini, S., Pende, D., Hsu, M. L., Moretta, L., Cosman, D., and Moretta, A. (1999). The leukocyte Ig-like receptor (LIR)-1 for the cytomegalovirus UL18 protein displays a broad specificity for different HLA class I alleles: analysis of LIR-1 + NK cell clones. Int. Immunol. *11*, 29-35.

Weber, P. C., Challberg, M. D., Nelson, N. J., Levine, M., and Glorioso, J. C. (1988). Inversion events in the HSV-1 genome are directly mediated by the viral DNA replication machinery and lack sequence specificity. Cell *54*, 369-381.

Wende, H., Colonna, M., Ziegler, A., and Volz, A. (1999). Organization of the leukocyte receptor cluster (LRC) on human chromosome 19q13.4. Mamm. Genome *10*, 154-160.

Wiertz, E. J., Jones, T. R., Sun, L., Bogyo, M., Geuze, H. J., and Ploegh, H. L. (1996). The human cytomegalovirus US11 gene product dislocates MHC class I heavy chains from the endoplasmic reticulum to the cytosol. Cell *84*, 769-779.

Wiley, D. (1988). MHC gene in cytomegalovirus. Nature *331*, 209-210.

Winston, D. J., Pollard, R. B., Ho, W. G., Gallagher, J. G., Rasmussen, L. E., Huang, S. N., Lin, C. H., Gossett, T. G., Merigan, T. C., and Gale, R. P. (1982). Cytomegalovirus immune plasma in bone marrow transplant recipients. Ann. Intern. Med. *97*, 11-18.

Wright, J. F., Kurosky, A., Pryzdial, E. L., and Wasi, S. (1995). Host cellular annexin II is associated with cytomegalovirus particles isolated from cultured human fibroblasts. J. Virol. *69*, 4784-4791.

Yokoyama, W. M. (1998). Natural killer cell receptors. Curr. Opin. Immunol. *10*, 298-305.

Zhuravskaya, T., Maciejewski, J. P., Netski, D. M., Bruening, E., Mackintosh, F. R., and St Jeor, S. (1997). Spread of human cytomegalovirus (HCMV) after infection of human hematopoietic progenitor cells: model of HCMV latency. Blood *90*, 2482-2491.

Ziegler, H., Thale, R., Lucin, P., Muranyi, W., Flohr, T., Hengel, H., Farrell, H., Rawlinson, W., and Koszinowski, U. H. (1997). A mouse cytomegalovirus glycoprotein retains MHC class I complexes in the ERGIC/cis-Golgi compartments. Immunity *6*, 57-66.

Chapter 2:

Characterization of a Murine Cytomegalovirus Class I Major Histocompatibility Complex (MHC) Homolog: Comparison to MHC Molecules and to the Human Cytomegalovirus MHC Homolog

JOURNAL OF VIROLOGY, Jan. 1998, p. 460–466
0022-538X/98/$04.00+0

Vol. 72, No. 1

Characterization of a Murine Cytomegalovirus Class I Major Histocompatibility Complex (MHC) Homolog: Comparison to MHC Molecules and to the Human Cytomegalovirus MHC Homolog

TARA L. CHAPMAN[1] AND PAMELA J. BJORKMAN[1,2]*

Division of Biology 156-29[1] and Howard Hughes Medical Institute,[2] California Institute of Technology, Pasadena, California 91125

Received 5 August 1997/Accepted 6 October 1997

Both human and murine cytomegaloviruses (HCMV and MCMV) down-regulate expression of conventional class I major histocompatibility complex (MHC) molecules at the surfaces of infected cells. This allows the infected cells to evade recognition by cytotoxic T cells but leaves them susceptible to natural killer cells, which lyse cells that lack class I molecules. Both HCMV and MCMV encode class I MHC heavy-chain homologs that may function in immune response evasion. We previously showed that a soluble form of the HCMV class I homolog (U_L18) expressed in Chinese hamster ovary cells binds the class I MHC light-chain β2-microglobulin and a mixture of endogenous peptides (M. L. Fahnestock, J. L. Johnson, R. M. R. Feldman, J. M. Neveu, W. S. Lane, and P. J. Bjorkman, Immunity 3:583–590, 1995). Consistent with this observation, sequence comparisons suggest that U_L18 contains the well-characterized groove that serves as the binding site in MHC molecules for peptides derived from endogenous and foreign proteins. By contrast, the MCMV homolog (m144) contains a substantial deletion within the counterpart of its α2 domain and might not be expected to contain a groove capable of binding peptides. We have now expressed a soluble version of m144 and verified that it forms a heavy chain–β2-microglobulin complex. By contrast to U_L18 and classical class I MHC molecules, m144 does not associate with endogenous peptides yet is thermally stable. These results suggest that U_L18 and m144 differ structurally and might therefore serve different functions for their respective viruses.

Cytomegaloviruses (CMVs) are ubiquitous, host-specific pathogens that are capable of establishing lifelong infections in immunocompetent hosts. Although acute infection will elicit an immune response, this response usually fails to completely resolve the infection. Instead, the virus persists in the host, often in a state of latency, and recurrent infections may be observed if the animal becomes immunocompromised (5). In order to maintain this degree of persistence, especially in the face of a fully primed immune system, CMVs have developed various means of modulating the host immune system. One strategy used by both human and murine CMVs (HCMV and MCMV) is the down-regulation of host class I major histocompatibility complex (MHC) molecules (6). Class I MHC molecules are polymorphic glycoproteins composed of a membrane-bound heavy chain associated with a nonpolymorphic light chain, β2-microglobulin (β2m). Class I molecules present peptides derived from the degradation of cytoplasmic proteins to cytotoxic T cells, thus enabling them to survey the status of the interior of the cell (49). In an uninfected cell, MHC molecules bind peptides derived from self proteins to which T cells are tolerant. However, in an infected cell, some MHC molecules are occupied by peptides derived from viral proteins, to which T cells react by killing the cell. By down-regulating MHC class I molecules, viruses are able to elude viral-antigen-specific cytotoxic T cells.

Although interference with class I-mediated antigen presentation or class I expression may enable infected cells to evade virus-specific T cells, it may also render these cells susceptible to detection and lysis by NK cells. NK cells express both activating and inhibitory surface receptors (31). The activating receptors are predominantly triggered by non-MHC molecules, while the inhibitory receptors recognize class I MHC molecules (31). Stimulation of activating receptors leads to target cell lysis unless the NK cell inhibitory receptors are able to engage an adequate level of self class I molecules on the target cell (27). Therefore, those cells that have down-regulated their class I molecules to a level sufficient to avoid T cells can be recognized and eliminated by NK cells.

As a possible means of undermining the host NK cell response, both HCMV and MCMV encode MHC class I homologs (2, 14, 39). It has been hypothesized that the role of these homologs in a virus-infected cell is to engage NK cell inhibitory receptors, thereby preventing the lysis that would normally occur due to down-regulation of class I molecules (11, 14, 40). In this way virus-infected cells are less susceptible to lysis by both cytotoxic T lymphocytes and NK cells. The HCMV-encoded homolog, U_L18, is a 348-residue type I transmembrane glycoprotein whose extracellular region shares ~25% amino acid sequence identity with the extracellular regions of human class I molecules (2) (Fig. 1A). Like class I MHC molecules, U_L18 associates with β2m (6). We previously showed that a soluble form of U_L18 expressed in Chinese hamster ovary (CHO) cells binds a mixture of endogenous peptides with characteristics similar to those of peptides eluted from class I molecules, that is, "anchor" residues, and a predominance of short peptides derived from cytoplasmic proteins (11). The MCMV-encoded MHC homolog, m144, is a 383-residue type I transmembrane glycoprotein whose extracellular region shares ~25% amino acid sequence identity with the corresponding part of murine class I MHC extracellular re-

* Corresponding author. Mailing address: Division of Biology 156-29, Caltech, Pasadena, CA 91125. Phone: (626) 395-8350. Fax: (626) 792-3683. E-mail: bjorkman@cco.caltech.edu.

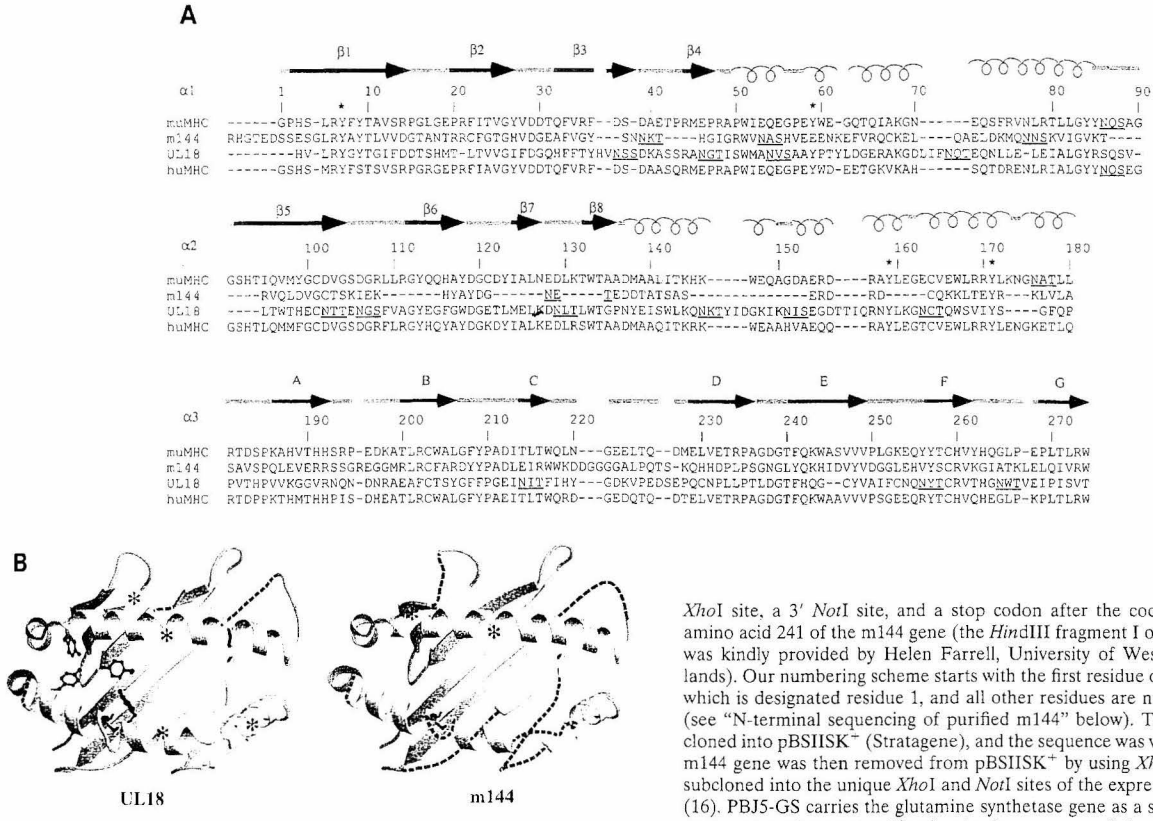

FIG. 1. Comparison of MCMV and HCMV class I homologs with class I MHC molecules. (A) Sequence alignment of the mature extracellular regions of m144 with a murine class I molecule (muMHC) and of U_L18 with a human class I MHC molecule (huMHC) (based on data from Fig. 1 in reference 14). Numbering is with reference to class I MHC molecules. Crystallographically determined secondary-structural elements in class I MHC molecules (3) are shown above the sequences as arrows for β strands (strands 1 through 8 within the α1 and α2 domains are labeled β1 to β8, and strands 1 through 7 within the α3 domain are labeled A to G) and spirals for α-helical regions. Positions of conserved tyrosines in the pocket that accommodates peptide N termini (pocket A in class I MHC molecules [45, 47]) are marked with an asterisk, and potential N-linked glycosylation sites are underlined. (B) Locations of U_L18 and m144 sequence insertions and deletions on the class I MHC structure. Ribbon diagrams of the carbon-α backbone of the α1 and α2 domains of HLA-A2 (4, 45) are shown with the locations of U_L18 or m144 insertions indicated by asterisks; class I regions that are deleted in U_L18 or m144 are indicated by dashed lines. Conserved tyrosines shared between U_L18 and class I molecules are highlighted in the left panel. This figure was generated by using Molscript (28) and Raster-3D (34).

gions (14, 39) (Fig. 1A). The two viral homologs are not closely related to each other, sharing only 18% sequence identity, thus requiring that m144 be separately characterized.

In this paper we describe the expression and biochemical characterization of a soluble version of m144. We find that, like U_L18 and class I MHC molecules, m144 binds β2m, but unlike these other proteins, it does not associate with endogenous peptides. We further demonstrate that m144 is thermally stable in the absence of bound peptide, unlike both class I MHC molecules (13, 33, 46, 50) and U_L18. Taken together with a sequence comparison of m144 with class I MHC molecules, these results suggest that the m144 counterpart of the MHC peptide-binding site differs from those of both class I molecules and U_L18 (Fig. 1B).

MATERIALS AND METHODS

Construction of the m144 expression plasmid. Molecular cloning manipulations were performed by standard protocols (43). PCR was used to insert a 5′ *Xho*I site, a 3′ *Not*I site, and a stop codon after the codon corresponding to amino acid 241 of the m144 gene (the *Hin*dIII fragment I of MCMV strain K181 was kindly provided by Helen Farrell, University of Western Australia, Nedlands). Our numbering scheme starts with the first residue of the mature protein, which is designated residue 1, and all other residues are numbered sequentially (see "N-terminal sequencing of purified m144" below). The PCR product was cloned into pBSIISK$^-$ (Stratagene), and the sequence was verified. The modified m144 gene was then removed from pBSIISK$^+$ by using *Xho*I and *Not*I and was subcloned into the unique *Xho*I and *Not*I sites of the expression vector PBJ5-GS (16). PBJ5-GS carries the glutamine synthetase gene as a selectable marker and as a means of gene amplification in the presence of the drug methionine sulfoximine, a system developed by Celltech (1).

Construction of the murine β2m (b allele) expression plasmid. An expression plasmid containing the a allele of murine β2m (mβ2m^a) was previously constructed in our laboratory (12). This allele of β2m, however, is not recognized by the anti-mβ2m monoclonal antibody (MAb) S19.8 (48). Originally anticipating that m144-mβ2m heterodimers could be purified by S19.8 immunoaffinity chromatography, we used site-directed mutagenesis to change mβ2m^a to mβ2m^b. This mβ2m^a gene was excised by using *Xba*I and *Xho*I and was subcloned into the same sites in pBSKS+ (Stratagene). The a and b alleles of mβ2m differ by only 1 nucleotide, which changes residue 85 from Asp to Ala (15). The single nucleotide was altered by oligonucleotide-directed in vitro mutagenesis (29), and the sequence was verified. The modified mβ2m gene was then removed from pBSKS$^+$ by using *Xba*I and *Xho*I and was subcloned into the unique *Xba*I and *Xho*I sites of the expression vector PBJ1 (32). Unfortunately, the mβ2m^b epitope recognized by the antibody S19.8 is inaccessible when the protein is complexed to the m144 heavy chain, as verified in immunoprecipitation experiments (data not shown).

Cell culture and transfection. The m144 expression plasmid was cotransfected with either a human β2m (hβ2m) (13) expression vector or the previously described mβ2m expression vector into CHO cells by a Lipofectin procedure (GIBCO BRL). Cells resistant to 100 μM methionine sulfoximine were selected according to the protocol established by Celltech, modification of which has been previously described (16). Transfected CHO cells were maintained in glutamine-free α minimal essential medium (Irvine Scientific) supplemented with 5% dialyzed fetal bovine serum (GIBCO BRL), 100 μM methionine sulfoximine (Sigma), penicillin (100 U/ml), and streptomycin (100 μg/ml). Cells secreting m144-β2m heterodimers were identified by immunoprecipitation of supernatants of cells metabolically labeled with [^{35}S]methionine and [^{35}S]cysteine (see below) by using either an antibody against hβ2m (BBM.1) (36) or anti-m144 antiserum. Clones were considered positive if immunoprecipitation yielded a heavy chain of 44 kDa and a light chain of 12 kDa. The heavy chain was verified to be m144 by N-terminal sequencing (see below).

^{35}S metabolic labeling. m144-transfected CHO cell lines derived from colonies were expanded into 12-well trays, grown to confluence, and incubated for 5 h in 1.0 ml of methionine- and cysteine-free medium (GIBCO BRL) plus 1% dialyzed fetal bovine serum including 5 μCi of a [^{35}S]methionine and [^{35}S]cysteine (ICN) mixture. Supernatants were clarified by a 5-min spin in a microcentrifuge, and either BBM.1 or anti-m144 antiserum (see below) was added. Immunoprecipitations were carried out by standard methods (21) with protein G-bearing Sepharose beads (Pharmacia). Samples were boiled in sodium dodecyl sulfate-polyacrylamide gel electrophoresis (SDS-PAGE) running buffer and loaded onto 15% polyacrylamide gels, which were fixed, dried, and exposed to a Phosphor-

Imager screen (Molecular Dynamics). The image was then developed with a Molecular Dynamics 425E phosphorimage scanner.

Protein purification. m144-hβ2m- and m144-mβ2m-secreting CHO cell lines were grown to confluence in 50 10-cm plates. Supernatants were collected every 3 days for 1 month. Soluble m144-hβ2m heterodimers were purified from the supernatants on a BBM.1 immunoaffinity column. This affinity column was prepared by coupling 70 mg of the BBM.1 MAb to cyanogen bromide-treated Sepharose 4B (Pharmacia) at approximately 10 mg of antibody/ml of resin according to the protocol of the manufacturer. Supernatants were passed over the affinity column, which was then washed with 50 column volumes of a solution consisting of 50 mM Tris (pH 7.4), 0.1% NaN_3, and 1 mM EDTA. Free β2m and m144-hβ2m heterodimers were eluted from the BBM.1 column with 50 mM diethylamine (pH 11.5) into tubes containing 1.0 M Tris (pH 7.4). Free hβ2m was separated from m144-hβ2m heterodimers by using a Superdex 200 HR 10/30 fast protein liquid chromatography (FPLC) filtration column. Approximately 3 mg of m144-hβ2m heterodimers was recovered per liter of transfected cell supernatants. Soluble m144-mβ2m heterodimers were purified from the supernatants on a 15C6 immunoaffinity column made by coupling an anti-m144 MAb (see below) to Sepharose beads as described above. Supernatants from m144-mβ2m-secreting CHO cell lines were passed over the column, the column was washed, and the protein was eluted as described above. A second protein migrating with an apparent molecular mass of 93 kDa coeluted with the m144-mβ2m heterodimer and was separated by using a Superdex 200 HR 10/30 FPLC filtration column. Approximately 1 mg of m144-mβ2m heterodimer was recovered per liter of transfected cell supernatants.

N-terminal sequencing of purified m144. N-terminal sequencing was performed on 2.3 μg of purified soluble m144-hβ2m or m144-mβ2m in a phosphate buffer dried onto a poly(vinylidene difluoride) membrane and inserted into an Applied Biosystems model 476A sequencer reaction cartridge. Two sequences were isolated from the m144-hβ2m sample: the sequence IQRTPKIQVYSRH PAEN, corresponding to the first 17 residues of mature hβ2m (26), and the sequence HGTEDSSESGLRYAYT, corresponding to the first 17 residues of the mature m144 heavy chain (reference 14 and data not shown). Two sequences were also isolated from the m144-mβ2m sample: the sequence IQKTPQIQVYS RHPPEN, corresponding to the first 17 residues of mature mβ2m (17), and the residues given above for the m144 heavy chain.

Acid elution and characterization of peptides. Purified secreted U_L18, m144-hβ2m, m144-mβ2m, FcRn (a class I MHC homolog that functions as a receptor for the Fc portions of immunoglobulin G [16]), and H2-K^d-hβ2m (a murine class I MHC heavy chain complexed with hβ2m [13]) proteins were analyzed for the presence of bound peptides. All these proteins were produced in CHO cells as described above for m144. In these experiments, FcRn served as the negative control, since it had previously been established by biochemical and crystallographic methods that it does not associate with endogenous peptides (7, 37), while U_L18 and K^d served as positive controls, since endogenous peptides had previously been characterized from samples of these proteins (11, 37). Acid elutions and sequencing were performed by established methods (24, 42, 51). Briefly, 0.25 mg of protein was concentrated to 100 μl in a Centricon 3 (molecular weight cutoff, 3,000) ultrafiltration device (Amicon; Beverly, Mass.). After dilution with 1.0 ml of 50 mM ammonium acetate (pH 7.5), the proteins were again concentrated to 100 μl, and this procedure was repeated. The washed protein was then treated with 1.0 ml of 12% acetic acid, heated to 70°C for 5 min, and subsequently concentrated again to 100 μl in the ultrafiltration unit, with the filtrate containing any eluted material. This elution step was then repeated. The acid eluates were lyophilized and analyzed by automated Edman degradation with an Applied Biosystems model 476A protein sequencer (see Table 1). Eluates were also analyzed with a Perkin-Elmer/Applied Biosystems Inc. model 172A microbore high-pressure liquid chromatograph (HPLC) and a Reliasil C_{18} (Reliasil Column Engineering) column. Material was eluted by using a 3-ml gradient from 0.05% trifluoroacetic acid in water to 0.05% trifluoroacetic acid in 40% acetonitrile. Absorbance was monitored at 200 nm. The fractions containing peaks were analyzed by matrix-assisted, laser desorption, time-of-flight mass spectrometry with a PerSeptive Biosystems (Farmingham, Mass.) ELITE mass spectrometer.

CD analyses. An Aviv 62A DS spectropolarimeter equipped with a thermoelectric cell holder was used for circular dichroism (CD) measurements. Wavelength scans and thermal denaturation curves were obtained from samples containing 10 μM protein in 5 mM phosphate at pH 7 by using a 0.1-mm path length cell for wavelength scans and a 1-mm path length cell for thermal denaturation measurements. The heat-induced unfolding of U_L18, m144-hβ2m, m144-mβ2m, and H2-K^d-hβ2m was monitored by recording the CD signal at 223 nm while the sample temperature was raised from 25 to 75°C at a rate of approximately 0.7°C/min. The transition midpoint (T_m) for each curve was determined by taking the maximum of a plot of $d\theta/dT$ versus T (where θ is ellipticity) after averaging the data with a moving window of 5 points.

Production of MAbs and polyclonal antiserum. Three MAbs were generated for the studies presented here, two specific for m144-β2m and one specific for the U_L18 heavy chain. Of those that recognize m144-β2m, 15C6 was raised against a gel slice of the m144 heavy chain and 19G4 was raised against the m144-hβ2m heterodimer. Female BALB/c mice (5 weeks old) were primed and twice boosted at 2-week intervals by intraperitoneal injection of either a 5- by 10- by 1.5-mm homogenized gel slice containing m144 or 100 μg of purified soluble m144-hβ2m. Serum was screened 1 week after each injection by enzyme-linked immunosorbent assay (ELISA). Three days preceding the fusion, one mouse was boosted with a gel slice or 100 μg of purified m144 in phosphate-buffered saline. Splenocytes from the boosted mouse were fused with HL-1 murine myeloma cells, and media from the hybridoma cultures were tested for antibodies against the m144 heavy chain by ELISA. After subcloning of positive clones at clonal density, ascites tumors were produced in pristane-primed BALB/c mice. In addition, a rabbit antiserum recognizing m144 was raised against a gel slice of the m144 heavy chain (Antibodies Incorporated, Davis, Calif.). Both MAbs and the antiserum are effective reagents in an ELISA for detection of m144-β2m, immunoprecipitation of soluble m144-β2m heterodimers, and Western blotting. The U_L18-specific MAb, 10C7, was prepared similarly to m144-specific MAbs; however, the mice used were female OLA × BL6 hβ2m transgenic mice (a kind gift of H. Ploegh, Massachusetts Institute of Technology) injected with enzymatically deglycosylated U_L18-hβ2m heterodimers. Several previous attempts to isolate an antibody against the U_L18 heavy chain in nontransgenic mice failed, presumably because U_L18 is heavily glycosylated (13 potential N-linked glycosylation sites [2]), so that an antibody recognizing a protein epitope within U_L18 rather than β2m was difficult to isolate. Indeed, all hybridomas screened from nontransgenic mice produced antibodies that recognized hβ2m instead of the heavy chain. By using hβ2m transgenic mice, many potential MAbs against the heavy chain were generated. A rabbit antiserum recognizing U_L18 was raised against a gel slice of the U_L18 heavy chain (HRP Inc., Denver, Pa.). Both the MAb and the antiserum are effective reagents in an ELISA for detection of U_L18-hβ2m, immunoprecipitation of soluble U_L18-hβ2m heterodimers, and Western blotting.

Preparation of peptide-filled U_L18 and H-2K^d. U_L18 was purified from the supernatants of U_L18-hβ2m-secreting cells (11) grown in a hollow-fiber bioreactor device (Cell Pharm I; Unisyn Fibertec, San Diego, Calif.). Using this system, only 35 to 40% of the molecules appear to contain endogenous peptides, compared to U_L18 produced from transfected cells grown on plates, which appears to be fully occupied (11). As previously described (11), we calculated the percent of U_L18 occupied with peptide by comparing the amount of peptide material eluted from H-2K^d with the amount eluted from U_L18 when the number of picomoles of starting protein is the same. The peptide ALPHAILRL, previously identified as a major component of U_L18 acid eluates (11), was synthesized with an Applied Biosystems 433A peptide synthesizer. The peptide was incubated with U_L18 at a 20:1 molar ratio for 12 h at room temperature. Unbound peptides were separated from U_L18 by passing the mixture over a Superdex 200 HR 10/30 FPLC size exclusion column. H-2K^d was purified from supernatants of K^d-hβ2m-secreting cells grown on 10-cm plates. Previous characterization of soluble K^d established that ~70% of the protein is empty and ~30% is occupied by endogenous peptide (13). The peptide SYIPSAEKI, previously identified as a K^d-binding peptide (12, 41), was synthesized and incubated with partially empty K^d, and unbound peptide was separated from K^d-peptide complexes as described above for preparation of peptide-filled U_L18.

RESULTS

Soluble m144 associates with hβ2m and mβ2m. To investigate whether m144 binds β2m and serves as a peptide receptor, we expressed a soluble version of m144 in CHO cells together with hβ2m or mβ2m. The soluble version of m144 was constructed by truncating the gene prior to the predicted transmembrane region (following residue 241 of the mature protein). Initial experiments were performed with the hβ2m gene in order to facilitate detection of the protein product with the antibody BBM.1 (36), which binds to hβ2m but not to mβ2m. Transfected cells were screened by immunoprecipitating metabolically labeled supernatants with BBM.1. SDS-PAGE analysis of protein from positive clones revealed two bands, one having an apparent molecular mass of 45 kDa (consistent with its identity as truncated m144) and the other having an apparent molecular mass of 12 kDa, corresponding to β2m. The calculated molecular mass of truncated m144 is 27 kDa, but the protein is glycosylated (4 potential N-linked glycosylation sites [14, 39]) and would be expected to migrate with a higher apparent molecular mass. Supernatants from positive clones were passed over a BBM.1 immunoaffinity column, eluted, then passed over a size exclusion column to separate free β2m from β2m-heavy chain heterodimers. An SDS-PAGE gel of the resulting purified protein is shown in Fig. 2. N-terminal sequencing of purified heterodimers confirmed the sequences of the first 17 residues of the mature forms of hβ2m (26) and m144 (14, 39).

Soluble m144 was used to produce MAbs that could be used

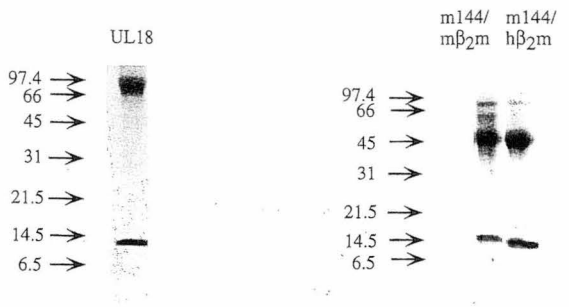

FIG. 2. SDS-PAGE (15% polyacrylamide) analysis of U_L18 and the two forms of m144. Proteins were purified from the supernatants of transfected CHO cells by passage over an immunoaffinity column followed by size exclusion chromatography. The heavy chains of both heterodimers migrate with a higher apparent molecular mass than is suggested by the mass of their protein backbones due to the addition of N-linked glycosides (U_L18 contains 13, and m144 contains 4, potential N-linked glycosylation sites).

to recognize m144 when complexed with mβ2m. Two antibodies were produced: 15C6, which was raised against a gel slice of the m144 heavy chain, and 19G4, which was raised against purified m144-hβ2m heterodimers. CHO cells were transfected with genes encoding truncated m144 and the b allele of mβ2m. Cells expressing m144-mβ2m heterodimers could be identified by immunoprecipitation with either the anti-m144 MAbs or a polyclonal anti-β2m antiserum that recognizes mβ2m, but not by immunoprecipitation with the MAb S19.8 (48), which apparently does not react with $m\beta2m^b$ complexed with m144. SDS-PAGE analysis of immunoprecipitated protein from cells expressing m144 and mβ2m also reveals two bands migrating at 45 and 12 kDa (data not shown). m144-mβ2m was purified from transfected cell supernatants on an immunoaffinity column constructed with MAb 15C6 (Fig. 2). N-terminal sequencing of purified protein established that the heterodimer was composed of the mature forms of m144 and mβ2m. Sequences of hamster (16) and bovine (20) β2m were not detected, indicating that m144 was not associating with endogenous hamster β2m or exchanging with bovine β2m in the medium, as can occur when mouse class I MHC proteins are expressed with mβ2m in CHO cells (13).

m144 does not bind endogenous peptides. To determine if either m144-hβ2m or m144-mβ2m binds peptides, purified proteins were treated with acetic acid to dissociate potential peptide material (24, 42, 51). Acid eluates were characterized by N-terminal sequencing (see Table 1), HPLC, and mass spectrometry. Soluble versions of other proteins expressed in CHO cells (the murine class I MHC molecule H2-K^d and two other MHC class I homologs, U_L18 from HCMV and the rat neonatal Fc receptor, FcRn) were subjected to the same treatment. K^d and U_L18 had previously been shown to bind peptides and were used as positive controls (10, 11, 37). FcRn does not bind peptides (7, 37) and was used as a negative control.

The characteristics of the peptides isolated from K^d and U_L18 were similar to those previously reported (11, 37) and consistent with the known requirement for a tyrosine anchor at position 2 for K^d (38) and a leucine or methionine anchor at position 2 for U_L18 (11) (Table 1). An aliquot of the U_L18 acid eluate was passed over a reverse-phase HPLC column, several peaks were collected, and a number of these were characterized by mass spectrometry. This procedure resulted in identification of multiple peptides in the U_L18 acid eluate whose exact molecular weights corresponded to the sequences of peptides previously shown to be associated with U_L18 (reference 11 and data not shown).

By contrast, the low-molecular-weight acid eluates from m144-hβ2m, m144-mβ2m, and FcRn did not show the presence of peptides (Table 1). With the exception of cycle 1, which is typically subject to high backgrounds, the total yield of the amino acids from each cycle of pool sequencing of the acid eluates remained nearly constant, and this yield was only slightly above background. In addition, most of the peaks in the HPLC profile of the m144-hβ2m acid eluate were also apparent in eluates extracted from FcRn, and all were barely notable above the background. When the few peaks that differed between the m144-hβm and FcRn eluates were collected and characterized by mass spectrometry, these peaks were found to contain low-molecular-weight material that did not show proteinaceous characteristics (data not shown).

m144, but not U_L18, is thermally stable in the absence of peptides. Class I MHC heavy chains show decreased stability in the absence of bound peptide (13, 33, 50). To ascertain if m144-hβ2m or m144-mβ2m is unstable due to the absence of bound peptide, we monitored the heat-induced unfolding of these proteins by recording the CD signal at 223 nm while increasing the sample temperature from 25 to 75°C (Fig. 3A). The results were compared with melting curves of partially empty and peptide-filled forms of the class I MHC molecule H-2K^d (Fig. 3B) (13). Two unfolding transitions are evident in the curve derived from m144-hβ2m. The first, with a T_m of 55°C, corresponds to the unfolding of the m144 heavy chain, while the second, with a T_m of 64°C, corresponds to the previously observed T_m for hβ2m (13) and represents the independent unfolding of the light chain subsequent to heavy-chain denaturation. m144-mβ2m melts less cooperatively than m144-hβ2m and the derived T_m for the heavy-chain unfolding (52°C) is slightly lower, indicating that m144 complexed with mβ2m is somewhat less stable than m144 complexed with hβ2m. In addition, the downward-sloping transition for the melting of β2m is not apparent in the melting curve of m144-mβ2m, perhaps being obscured by the CD signal from the melted m144 heavy chain. Similar results were obtained for the melting of K^d complexed with mβ2m (12). The melting behavior of

TABLE 1. Amino acids recovered from acid elutions[a]

Cycle	Yield (pmol) of:				
	U_L18	H-2K^d-hβ2m	FcRn	m144-hβ2m	m144-mβ2m[b]
1	86	84.5	5.9	13.7	7.3
2	75.1[c]	51.1[d]	4.7	0	1.5
3	36.9[e]	33.6	0.7	0.5	0.3
4	19.8	12.3	7.6	1.2	0.3
5	11.3	18.2	0	0.7	0.2
6	4.0	30.8	0	1.0	0.1
7	3.7	1.1	0.2	1.6	0.1
8	6.5	3.1	0.6	2.0	1.6
9	4.3	12.1	9.5	0.2	0.3
10	1.3	7.5	0.3	0.1	1.2
11	0.4	10.1	0.5	0.3	0.2
12	2.5	6.7	0.8	0.1	0.5

[a] The total yield of amino acids from each sequencing cycle is presented for acid eluates derived from equivalent amounts of soluble U_L18, K^d-hβ2m, FcRn, m144-hβ2m, and m144-mβ2m heterodimers. Only those amino acid residues that showed an increase in the absolute amount recovered compared to the previous cycle were considered significant. Results for the FcRn, K^d, and U_L18 eluates are similar to those previously reported (11, 37) in which soluble U_L18 and K^d, but not FcRn, were shown to bind endogenous peptides.

[b] Acid elution contributions from Asp, Glu, and Gly were not included in the m144-mβ2m tabulation because the first four cycles showed unusually high yields that were also present in the negative control.

[c] Leu, Met = 71.

[d] Tyr = 25.

[e] Pro = 19.

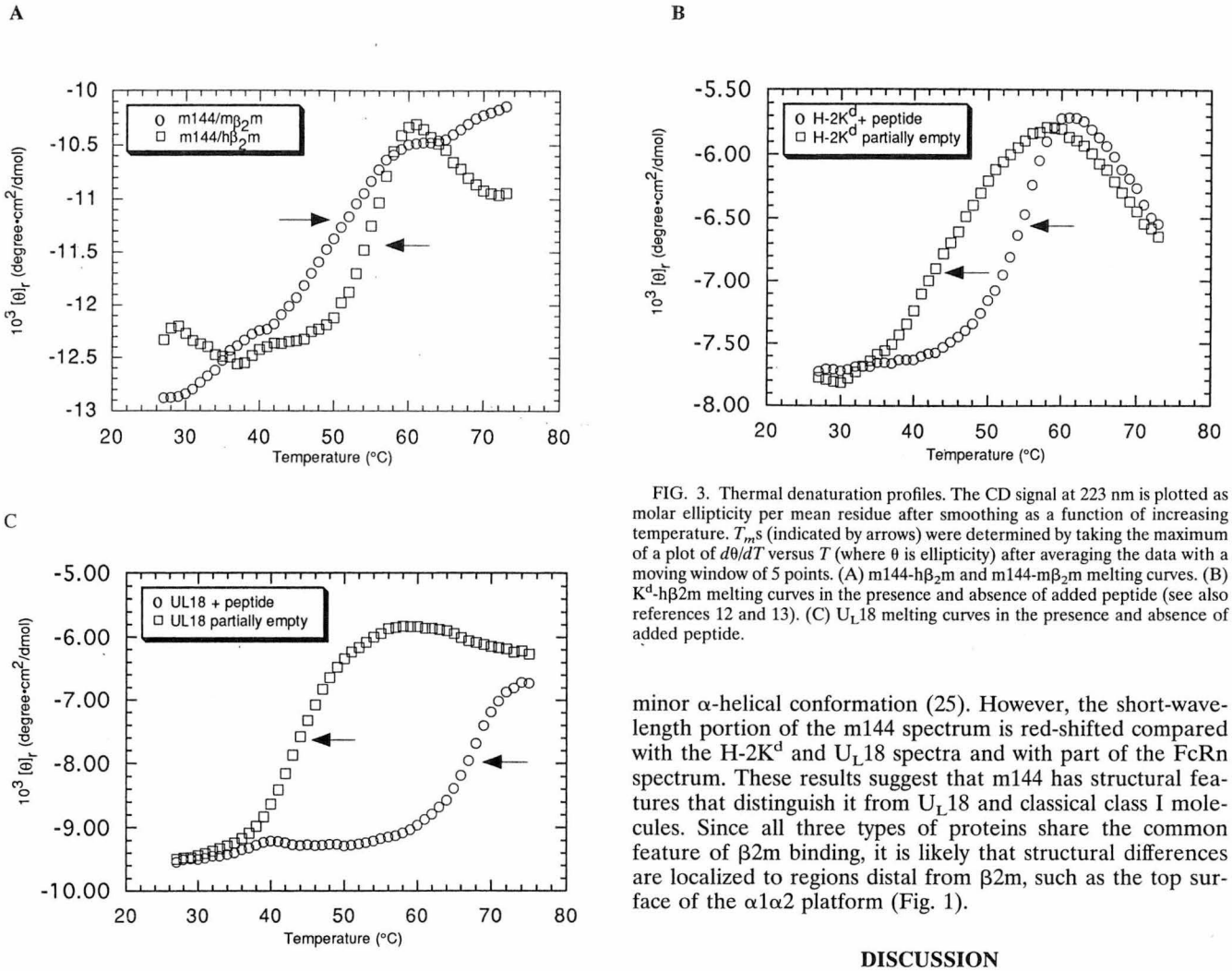

FIG. 3. Thermal denaturation profiles. The CD signal at 223 nm is plotted as molar ellipticity per mean residue after smoothing as a function of increasing temperature. T_ms (indicated by arrows) were determined by taking the maximum of a plot of $d\theta/dT$ versus T (where θ is ellipticity) after averaging the data with a moving window of 5 points. (A) m144-hβ$_2$m and m144-mβ$_2$m melting curves. (B) K^d-hβ2m melting curves in the presence and absence of added peptide (see also references 12 and 13). (C) U$_L$18 melting curves in the presence and absence of added peptide.

both forms of m144 is more similar to that of peptide-filled K^d (T_m = 56°C for K^d-mβ2m; T_m = 57°C for K^d-hβ2m) than to that of empty K^d (T_m = 42°C for K^d-mβ2m; T_m = 45°C for K^d-hβ2m) (12, 13) (compare Fig. 3A and B), suggesting that m144 is thermally stable in the absence of peptide.

By contrast, thermal-stability profiles of U$_L$18 indicate that U$_L$18 is only marginally stable in the absence of added peptide (Fig. 3C). The U$_L$18 protein produced from transfected CHO cells grown in a hollow-fiber bioreactor is estimated to be only 40% occupied with endogenous peptide (see Materials and Methods). This form of U$_L$18 melts with a T_m of 41°C. Upon addition of a known U$_L$18-binding peptide (11), the T_m increases to 66°C (Fig. 3C).

CD spectral comparison of m144, U$_L$18, FcRn, and class I MHC. The far-UV CD spectrum of m144 was compared with spectra of other MHC homologs and a classical class I molecule (Fig. 4). Far-UV CD spectra were previously used to characterize the secondary structures of class I MHC molecules and FcRn (16, 18, 30). The available crystal structures of FcRn and class I molecules (7, 47) can be used to verify the conclusion derived from the CD spectra that the secondary-structure arrangement of FcRn resembles, but is not identical to, class I MHC structures. The spectra of all four molecules (m144-hβ2m, U$_L$18, FcRn, and H-2K^d) show characteristics of proteins that are composed primarily of β-structure with a minor α-helical conformation (25). However, the short-wavelength portion of the m144 spectrum is red-shifted compared with the H-2K^d and U$_L$18 spectra and with part of the FcRn spectrum. These results suggest that m144 has structural features that distinguish it from U$_L$18 and classical class I molecules. Since all three types of proteins share the common feature of β2m binding, it is likely that structural differences are localized to regions distal from β2m, such as the top surface of the α1α2 platform (Fig. 1).

DISCUSSION

HCMV and MCMV both encode class I MHC homologs. Previous studies indicated that U$_L$18, the HCMV class I homolog, binds the class I light chain β2m (6) and associates with endogenous peptides (11). In this study, we expressed a soluble version of the MCMV class I homolog m144 and compared its biochemical characteristics to those of class I molecules and U$_L$18. We found that m144 expressed in CHO cells associates with both hβ2m and mβ2m, implying that m144 heterodimerizes with host-derived β2m in virus-infected cells. However, unlike U$_L$18 and class I molecules, m144 does not bind endogenous peptides, since we do not detect peptide material associated with either form of m144-β2m. Other class I MHC homologs for which biochemical or structural studies do not reveal the presence of endogenous peptides include FcRn (7, 37), human Zn-α2-glycoprotein (44), and the hemochromatosis gene product HFE (31a). In addition, human MICA and mouse H-2T region-encoded molecules are stably expressed in cells that lack a functional peptide transporter, suggesting that they too do not bind conventional class I peptide ligands (9, 19, 23, 52).

A comparison of alignments of the m144 and U$_L$18 sequences with class I MHC sequences reveals that U$_L$18 is more likely than m144 to adopt a fold that includes an MHC-like peptide-binding groove (Fig. 1B). Peptides bind to class I MHC molecules in a groove located between two α-helices that span an 8-stranded β-pleated sheet. Peptide termini are

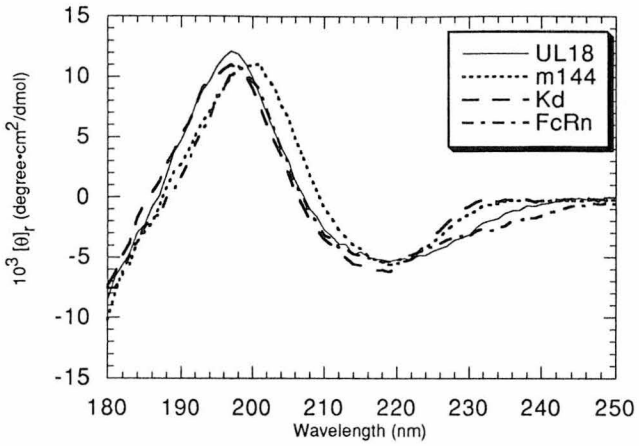

FIG. 4. Far-UV CD spectra of peptide-filled U_L18, peptide-filled K^d, FcRn, and m144 expressed as ellipticity per mean residue. CD spectra of the partially empty versions of U_L18 and K^d superimpose almost perfectly upon spectra of their peptide-filled counterparts (data not shown).

accommodated in pockets at each end of the groove that are lined with conserved residues (reviewed in reference 47). The peptide N terminus binds in pocket A on the left side of the groove (as depicted in Fig. 1B), in which four conserved tyrosines make critical hydrogen bonds to main-chain atoms of the peptide (residues 7, 59, 159, and 171; class I numbering) (Fig. 1A). These tyrosines are also found in the U_L18 sequence, suggesting a similar mechanism for interaction with peptide N termini (11). While the U_L18 sequence shows some gaps and insertions compared to class I sequences, these are primarily confined to regions corresponding to the right side of the groove and suggest that the U_L18 structure may differ from MHC structures in the region of the groove that interacts with peptide C termini. Indeed, analysis of endogenous peptides associated with U_L18 revealed variability in the length of bound peptides (11), whereas classical class I molecules show a strong preference for binding octamer and nonamer peptides (reviewed in reference 47). By contrast, only two of the four pocket A tyrosines are conserved in the m144 sequence (Fig. 1A). Furthermore, the α2 domain of m144 is significantly truncated compared to those of class I and U_L18 molecules, such that β strands 6 and 8 are much shorter, there is no predicted seventh strand, and there is a large deletion within the predicted α2 domain helix. These characteristics do not seem compatible with formation of a functional peptide-binding groove, and they imply that this region of m144 is structurally distinct from class I molecules and U_L18. Far-UV CD spectral differences support this prediction (Fig. 4).

Our finding that m144, unlike class I MHC molecules and U_L18, is thermally stable in the absence of bound peptide is also consistent with a structural rearrangement in the counterpart of its peptide-binding region. CD melting curves of m144 complexed with either hβ2m or mβ2m show that it is more stable than either an empty class I molecule or partially empty U_L18 (Fig. 3). The melting curves of the empty forms of class I and U_L18 were characterized by T_ms between 42 and 45°C, while the T_m of the m144-hβ2m curve was 55°C, closer to the T_m for peptide-filled K^d (56 to 57°C) (12, 13). m144 is slightly less stable when complexed with mβ2m (T_m = 52°C). This effect was also noted for the complex of mβ2m with K^d, compared with the complex of hβ2m with K^d (12), and more dramatically, for the complex of mβ2m with the nonclassical murine class I protein T10 (9). We were able to analyze the effect of bound peptide on U_L18 stability by taking advantage of the fact that soluble U_L18 is only partially occupied with endogenous peptides when it is expressed at high levels. Addition of a synthetic peptide corresponding to the sequence of an endogenous peptide eluted from U_L18 shifts the T_m to 66°C, thus formally demonstrating that U_L18 binds this peptide and suggesting a general method for assaying peptide binding by U_L18.

The different properties of U_L18 and m144 revealed by this study do not, in and of themselves, undermine the contention that these molecules both function as surrogate class I proteins, capable of engaging NK cell inhibitory receptors and protecting cells that lack class I surface expression. Murine NK cell inhibitory receptors are homodimeric C-type lectin superfamily proteins, whereas the majority of characterized human inhibitory receptors are members of the immunoglobulin superfamily (reviewed in references 22 and 35). It is therefore conceivable that mouse NK inhibitory receptors would recognize features of mouse class I MHC molecules different from those recognized on human class I molecules by human inhibitory receptors. While there is no evidence yet of a direct interaction between a mouse inhibitory receptor and m144, recent results demonstrate that the presence of m144 interferes with NK cell-mediated clearance of virus-infected cells in vivo (14). The connection between U_L18 and human NK cells is less straightforward. A recent study reported that U_L18 expressed on a human class I-negative B-lymphoblastoid cell line inhibited NK cell lysis through interaction with the C-lectin-like inhibitory receptor CD94 (40). However, we and investigators at other laboratories have been unable to detect cell surface expression of U_L18 when its gene was transfected into the same B-cell line (31b). Additional results indicate that the presence of U_L18 on virus-infected fibroblasts slightly augments, rather than inhibits, NK cell-mediated lysis (31b). A probable host ligand for U_L18 was recently identified as LIR-1, a new immunoglobulin superfamily member related to human NK inhibitory receptors (8). LIR-1 is expressed mainly on B cells and monocytes, but only on a subset of NK cells; thus, it is possible that the HCMV MHC homolog exerts its primary effects on host cells other than NK cells. Further studies will be necessary to resolve the roles of both m144 and U_L18 in the interactions of their respective viruses with the immune systems of the infected hosts. However, currently available data suggest that the two homologs function differently, a hypothesis that is consistent with the biochemical and structural differences between m144 and U_L18 observed in the present study.

ACKNOWLEDGMENTS

This work was supported by the Howard Hughes Medical Institute and by a grant from the Arthritis Foundation to P.J.B. T.L.C. is supported by a National Defense Science and Engineering Pre-Doctoral Fellowship.

We thank H. Farrell and N. Davis-Poynter for providing the m144 gene and for helpful discussions and critical reading of the manuscript. We also thank G. Hathaway and the Caltech Protein Peptide Micro Analytical Laboratory for peptide analysis, and members of the Bjorkman laboratory for critical reading of the manuscript.

REFERENCES

1. **Bebbington, C. R., and C. C. G. Hentschel.** 1987. The use of vectors based on gene amplification for the expression of cloned genes in mammalian cells, p. 163–188. *In* D. M. Glover (ed.), DNA cloning: a practical approach. IRL Press, Oxford, United Kingdom.
2. **Beck, S., and B. G. Barrell.** 1988. Human cytomegalovirus encodes a glycoprotein homologous to MHC class I antigens. Nature **331**:269–272.
3. **Bjorkman, P. J., and P. Parham.** 1990. Structure, function and diversity of class I major histocompatibility complex molecules. Annu. Rev. Biochem. **90**:253–288.

4. **Bjorkman, P. J., M. A. Saper, B. Samraoui, W. S. Bennett, J. L. Strominger, and D. C. Wiley.** 1987. Structure of the human class I histocompatibility antigen, HLA-A2. Nature **329:**506–512.
5. **Britt, W. J., and C. A. Alford.** 1996. Cytomegalovirus, p. 2493–2523. *In* B. N. Fields, D. M. Knipe, P. M. Howley, R. M. Chanock, J. L. Melnick, T. P. Monath, B. Roizman, and S. E. Straus (ed.), Fields Virology. Lippincott-Raven, Philadelphia, Pa.
6. **Browne, H., G. Smith, S. Beck, and T. Minson.** 1990. A complex between the MHC class I homologue encoded by human cytomegalovirus and β2 microglobulin. Nature **347:**770–772.
7. **Burmeister, W. P., L. N. Gastinel, N. E. Simister, M. L. Blum, and P. J. Bjorkman.** 1994. Crystal structure at 2.2 Å resolution of the MHC-related neonatal Fc receptor. Nature **372:**336–343.
8. **Cosman, D., N. Fanger, L. Borges, M. Kubin, W. Chin, L. Peterson, and M.-L. Hsu.** 1997. A novel immunoglobulin superfamily receptor for cellular and viral MHC class I molecules. Immunity **7:**273–282.
9. **Crowley, M. P., Z. Reich, N. Mavaddat, J. D. Altmann, and Y.-H. Chien.** 1997. The recognition of the nonclassical major histocompatibility complex (MHC) class I molecule, T10, by the γδ T cell, G8. J. Exp. Med. **185:**1223–1230.
10. **Fahnestock, M. L., J. M. Dadgari, M. McMillan, and P. J. Bjorkman.** 1994. Phosphatidyl inositol-linked forms of a murine class I MHC molecule expressed on CHO cells retain peptide binding capability and alloreactivity. Int. Immunol. **6:**307–314.
11. **Fahnestock, M. L., J. L. Johnson, R. M. R. Feldman, J. M. Neveu, W. S. Lane, and P. J. Bjorkman.** 1995. The MHC class I homolog encoded by human cytomegalovirus binds endogenous peptides. Immunity **3:**583–590.
12. **Fahnestock, M. L., J. L. Johnson, R. M. R. Feldman, T. J. Tsomides, J. Mayer, L. O. Narhi, and P. J. Bjorkman.** 1994. Effects of peptide length and composition on binding to an empty class I MHC heterodimer. Biochemistry **33:**8149–8158.
13. **Fahnestock, M. L., I. Tamir, L. Narhi, and P. J. Bjorkman.** 1992. Thermal stability comparison of purified empty and peptide filled forms of a class I MHC molecule. Science **258:**1658–1662.
14. **Farrell, H. E., H. Vally, D. M. Lynch, P. Fleming, G. R. Shellam, A. A. Scalzo, and N. J. Davis-Poynter.** 1997. Inhibition of natural killer cells by a cytomegalovirus MHC class I homologue in vivo. Nature **386:**510–514.
15. **Gasser, D. L., K. A. Klein, E. Choi, and J. G. Seidman.** 1985. A new beta-2 microglobulin allele in mice defined by DNA sequencing. Immunogenetics **22:**413–416.
16. **Gastinel, L. N., N. E. Simister, and P. J. Bjorkman.** 1992. Expression and crystallization of a soluble and functional form of an Fc receptor related to class I histocompatibility molecules. Proc. Natl. Acad. Sci. USA **89:**638–642.
17. **Gates, F. T., J. E. Coligan, and T. J. Kindt.** 1981. Complete amino acid sequence of murine β2-microglobulin: structural evidence for strain-related polymorphism. Proc. Natl. Acad. Sci. USA **78:**554–558.
18. **Gorga, J. C., A. Dong, M. C. Manning, R. W. Woody, W. S. Caughey, and J. L. Strominger.** 1989. Comparison of the secondary structures of human class I and class II major histocompatibility complex antigens by Fourier-transform infrared and circular dichroism spectroscopy. Proc. Natl. Acad. Sci. USA **86:**2321–2325.
19. **Groh, V., S. Bahram, S. Bauer, A. Herman, M. Beauchamp, and T. Spies.** 1996. Cell stress-regulated human major histocompatibility complex class I gene expressed in gastrointestinal epithelium. Proc. Natl. Acad. Sci. USA **93:**12445–12450.
20. **Groves, M. L., and R. Greenberg.** 1982. Complete amino acid sequence of bovine β2-microglobulin. J. Biol. Chem. **257:**2619–2626.
21. **Harlow, E., and D. Lane.** 1988. Antibodies: a laboratory manual. Cold Spring Harbor Laboratory Press, Cold Spring Harbor, N.Y.
22. **Höglund, P., J. Sundback, M. Y. Olsson-Anheim, M. Johansson, M. Salcedo, C. Öhlén, H. G. Ljunggren, C. L. Sentman, and K. Kärre.** 1997. Host MHC class I control of NK-cell specificity in the mouse. Immunol. Rev. **155:**11–28.
23. **Holcombe, H. R., A. R. Castano, H. Cheroutre, M. Teitell, J. K. Maher, P. A. Peterson, and M. Kronenberg.** 1995. Nonclassical behavior of the thymus leukemia antigen—peptide transporter-independent expression of a non-classical class I molecule. J. Exp. Med. **181:**1433–1443.
24. **Jardetzky, T. S., W. S. Lane, R. A. Robinson, D. R. Madden, and D. C. Wiley.** 1991. Identification of self peptides bound to purified HLA-B27. Nature **353:**325–330.
25. **Johnson, C. W.** 1990. Protein secondary structure and circular dichroism: a practical guide. Proteins Struct. Funct. Genet. **7:**205–214.
26. **Kabat, E. A., T. T. Wu, H. M. Perry, K. S. Gottesman, and C. Foeller.** 1991. Sequences of proteins of immunological interest. U.S. Department of Health and Human Services, Bethesda, Md.
27. **Kärre, K., H.-G. Ljunggren, G. Piontek, and R. Kiessling.** 1986. Selective rejection of H-2 deficient lymphoma variants suggest alternative immune defense strategy. Nature **319:**675–678.
28. **Kraulis, P. J.** 1991. MOLSCRIPT: a program to produce both detailed and schematic plots of protein structures. J. Appl. Crystallogr. **24:**946–950.
29. **Kunkel, T. A., J. D. Roberts, and R. A. Zakour.** 1987. Rapid and efficient site directed mutagenesis without phenotypic selection. Methods Enzymol. **154:**367–382.
30. **Lancet, D., P. Parham, and J. L. Strominger.** 1979. Heavy chain of HLA-A and HLA-B antigens is conformationally labile: a possible role for β2-microglobulin. Proc. Natl. Acad. Sci. USA **76:**3844–3848.
31. **Lanier, L. L., B. Corliss, and J. H. Phillips.** 1997. Arousal and inhibition of human NK cells. Immunol. Rev. **155:**145–154.

31a. **Lebrón, J. A., and P. J. Bjorkman.** Unpublished data.

31b. **Leong, C., T. L. Chapman, P. J. Bjorkman, E. Mocarski, and L. L. Lanier.** Unpublished data.

32. **Lin, A. Y., B. Devaux, A. Green, C. Sagerström, J. F. Elliott, and M. M. Davis.** 1990. Expression of T cell antigen receptor heterodimers in a lipid-linked form. Science **249:**677–679.
33. **Ljunggren, H. G., N. J. Stam, C. Öhlén, J. J. Neefjes, P. Höglund, M. T. Heemels, J. Bastin, T. N. M. Schumacher, A. Townsend, K. Kärre, and H. L. Ploegh.** 1990. Empty MHC class I molecules come out in the cold. Nature **346:**476–480.
34. **Merritt, E. A., and M. E. P. Murphy.** 1994. Raster3D version 2.0, a program for photorealistic molecular graphics. Acta Crystallogr. Sect. D **50:**869–873.
35. **Moretta, A., R. Biassoni, C. Bottino, D. Pende, M. Vitale, A. Poggi, M. C. Mingari, and L. Moretta.** 1997. Major histocompatibility complex class I-specific receptors on human natural killer and T lymphocytes. Immunol. Rev. **155:**105–117.
36. **Parham, P., M. J. Androlewicz, N. J. Holmes, and B. E. Rothenberg.** 1983. Arginine-45 is a major part of the determinant of human β2-microglobulin recognized by mouse monoclonal antibody BBM.1. J. Biol. Chem. **258:**6179–6186.
37. **Raghavan, M., L. N. Gastinel, and P. J. Bjorkman.** 1993. The class I MHC-related Fc receptor shows pH dependent stability differences correlating with immunoglobulin binding and release. Biochemistry **32:**8654–8660.
38. **Rammensee, H.-G., K. Falk, and O. Rötzschke.** 1993. Peptides naturally presented by MHC class I molecules. Annu. Rev. Immunol. **11:**213–244.
39. **Rawlinson, W. D., H. E. Farrell, and B. G. Barrell.** 1996. Analysis of the complete DNA sequence of murine cytomegalovirus. J. Virol. **70:**8833–8849.
40. **Reyburn, H. T., O. Mandelboim, M. Valez-Gomez, D. M. Davis, L. Pazmany, and J. L. Strominger.** 1997. The class I MHC homologue of human cytomegalovirus inhibits attack by natural killer cells. Nature **386:**514–519.
41. **Romero, P., G. Corradin, I. F. Luescher, and J. L. Maryanski.** 1991. H-2K^d restricted antigenic peptides share a simple binding motif. J. Exp. Med. **174:**603–612.
42. **Rötzschke, O., K. Falk, K. Deres, H. Schild, M. Norda, J. Metzger, G. Jung, and H.-G. Rammensee.** 1990. Isolation and analysis of naturally processed viral peptides as recognized by cytotoxic T cells. Nature **348:**252–257.
43. **Sambrook, J., E. F. Fritsch, and T. Maniatis.** 1989. Molecular cloning: a laboratory manual, 2nd ed. Cold Spring Harbor Laboratory Press, Cold Spring Harbor, N.Y.
44. **Sánchez, L. M., C. López-Otín, and P. J. Bjorkman.** 1997. Characterization and crystallization of human Zn-α2-glycoprotein, a soluble class I MHC homolog. Proc. Natl. Acad. Sci. USA **94:**4626–4630.
45. **Saper, M. A., P. J. Bjorkman, and D. C. Wiley.** 1991. Refined structure of the human histocompatibility antigen HLA-A2 at 2.6 Å resolution. J. Mol. Biol. **219:**277–319.
46. **Schumacher, T. N. M., M. T. Heemels, J. J. Neefjes, W. M. Kast, C. J. M. Melief, and H. L. Ploegh.** 1990. Direct binding of peptide to empty MHC class I molecules on intact cells and in vitro. Cell **62:**563–567.
47. **Stern, L. J., and D. C. Wiley.** 1994. Antigenic peptide binding by class I and class II histocompatibility proteins. Structure **15:**245–251.
48. **Tada, N., S. Kimura, A. Hatzfeld, and U. Hammerling.** 1980. Ly-m11: the H-3 region of mouse chromosome 2 controls a new surface alloantigen. Immunogenetics **11:**441–449.
49. **Townsend, A., and H. Bodmer.** 1989. Antigen recognition by class I-restricted T lymphocytes. Annu. Rev. Immunol. **7:**601–624.
50. **Townsend, A., T. Elliott, V. Cerundolo, L. Foster, B. Barber, and A. Tse.** 1990. Assembly of MHC class I molecules analyzed in vitro. Cell **62:**285–295.
51. **Van Bleek, G. M., and S. G. Nathenson.** 1990. Isolation of an endogenously processed immunodominant viral peptide from the class I H-2K^b molecule. Nature **348:**213–216.
52. **Weintraub, B. C., M. R. Jackson, and S. M. Hedrick.** 1994. Gamma-delta T-cells can recognize nonclassical MHC in the absence of conventional antigenic peptides. J. Immunol. **153:**3051–3058.

Chapter 3:

Efforts to Isolate the m144 Ligand and Advances in the m144 Field

In this chapter I discuss my continuing efforts to identify the m144 ligand and recent developments in the study of m144 and its function.

Chapter 3

1. Continuing Efforts to Identify the m144 Receptor

As mentioned in the discussion of the previous chapter, the study by Farrell et al. (1997) determined that m144 expression is important in protecting virally infected cells *in vivo* from clearance by NK cells in the liver, spleen and lung during early points of infection. Given the similarity between m144 and class I MHC molecules, it was hypothesized that m144 could inhibit NK cell lysis by engaging NK cell inhibitory receptors. To test this hypothesis, I tested m144 for binding to soluble versions of murine NK cell inhibitory receptors expressed by Yang Liu, a fellow graduate student in the Bjorkman lab. I also tested the interaction between m144 and PIR-A and PIR-B as the PIR proteins are a family of receptors expressed by mice that share significant sequence identity with LIRs (Kubagawa et al., 1999) and LIR-1 is the receptor for UL18. Like LIRs, some PIR proteins have long cytoplasmic tails that encode ITIMs while others are short with a charged amino acid in the transmembrane domain (Kubagawa et al., 1999). In addition the expression pattern of PIR-A and PIR-B are similar to LIR-1 (monocytes, macrophages, dendritic cells and mast cells) and the location of the PIR genes in the mouse genome is sytenic to that of the LIR genes in the human genome (Kubagawa et al., 1999). In collaboration with Dr. Peter Snow (Caltech Protein Expression Facility) and Dr. Clinton White (previous Postdoctoral Fellow in the Bjorkman lab), we expressed

soluble versions of both PIR-A and PIR-B using a baculovirus expression system and tested both PIR-A and PIR-B for interaction with m144.

1.1. Protein Expression. Soluble versions of the murine NK cell inhibitory receptors Ly49A and Ly49I, each with an N-terminal histidine tag, were expressed by Yang Liu using a baculovirus expression system. Both proteins were verified to be dimers. Soluble m144 was produced as described in Chapman & Bjorkman, 1998 (Chapter 2). PIR-A and PIR-B were expressed with C-terminal histidine tags by Dr. Peter Snow using a baculovirus expression system.

1.2. Binding Assays. I combined soluble m144 with either Ly49A or Ly49I, incubated with mixing, followed by addition of either anti-His antibody or BBM.1, an antibody specific for ß2m (Parham et al., 1983). The antibody complex was precipitated, after washing, with protein G-immobilized sepharose and analyzed by SDS-PAGE. Neither assay revealed any indication of an interaction between either Ly49 construct and m144 (data not shown). As this assay does not rule out the possibility of a low affinity m144/Ly 49 interaction, I also tested the ability of m144 to associate with Ly49A and Ly49I using a biosensor based assay. Ly49A and Ly49I were each immobilized on a separate biosensor chip to a high density (1500 RU) using standard amine chemistry and m144 was passed over at concentrations ranging from 100

nM to 10 μM. Even at micromolar concentrations of m144, no apparent interaction was observed between the proteins (data not shown).

To test binding of m144 to PIR-A and PIR-B, I combined soluble m144 with either PIR-A or PIR-B, incubated with mixing followed by addition of BBM.1, an antibody specific for ß2m (Parham et al., 1983). The antibody complex was precipitated, after washing, with protein G-immobilized sepharose and analyzed by SDS-PAGE. Neither PIR-A nor PIR-B associated with m144 (data not shown).

1.3. Results. Neither the Ly-49 molecules nor the PIR molecules were recognized by m144. The assays I used could not have detected very low affinity interactions; however, they would have been sufficient to detect an interaction between MHC molecules and TCRs (K_D ~ 2-60 μM) (Alam et al., 1996; Garcia et al., 1996; Matsui et al., 1991) or class I MHC molecules and KIRs (K_D ~ 10 μM) (Vales-Gomez et al., 1998). If there is an interaction between m144 and either the Ly49 molecules or the PIRs, it is of lower affinity than ~60μM. I therefore doubt that Ly49A or I or PIR-A or -B are the ligand for m144. To make a comparison with the UL18/LIR-1 interaction (Chapter 4 and 5), in which I believe it is the high affinity of LIR-1 for UL18 compared to MHC class I molecules that is the basis of UL18's proposed immunomodulary effect, I would expect m144 to have a high affinity for its ligand. It remains to be seen whether the PIRs are actually murine analogs of the LIRs and whether there are other PIR family

members that have not yet been isolated. Of the nine LIR molecules, only LIR-1 interacts with UL18; it is therefore not unreasonable that one PIR protein would recognize m144 while another would not. In addition, there may be other unidentified molecules that are analogous to the LIRs and bind m144, or it is possible that the m144 ligand is structurally and, possibly functionally, unrelated to LIRs.

1.4. Cell Based Assays Using m144 Tetramers. In collaboration with Dr. Chris McMahon, a postdoctoral fellow in Dr. David Raulet's laboratory (UC Berkeley), I have continued studies to identify the m144 counterstructure. Using m144 expressed in either insect cells or bacteria, complexed with either human or murine ß2m, Dr. McMahon and I have generated tetramers of m144 using a biotinylated version of m144 bound to tetrameric streptavidin (Braud et al., 1998).

Tetramers have previously been used to identify ligands in low affinity interactions (Braud et al., 1998). Using the m144 tetramers, Dr. McMahon has screened Cos-7 cells that transiently express high levels of Ly49 A, B, C, D, F, G2, H or I molecules; but did not see any indication of binding. He has also screened B, T and NK cells, macrophages and activated peripheral blood cells in addition to NK cell libraries from CB17 and B6 mice. In each instance the m144 tetramers did not specifically recognize any of the surface proteins expressed by these cells. He repeatedly observes

weak staining of J774 macrophages, but has been unable to identify what is being recognized.

2. Recent Studies of m144 Function

Recently published studies regarding the function of m144 continue to address the hypothesis that m144 modulates the host anti-viral NK response. Kubota et al. (1999) provided results which they argue demonstrate that m144 expression in the human Burkitt lymphoma line, Raji, partially inhibited antibody-dependent cell-mediated cytotoxic activity by IL-2-activated murine NK cells. However, the observed inhibition was not complete (11.3-31.5%) and the difference in percent specific lysis between m144 transfected cells as compared to vector alone-transfected controls was constant throughout the range of effector to target cell ratios, not even decreasing at low effector to target cells ratios as one would expect if m144 was really providing protection from lysis. I therefore doubt the authors' conclusion that m144 expression protects target cells from lysis by NK cells and suspect that their results are due to an inherent difference in the stability of the m144- and vector alone-transfected clonal lines in the ^{51}Cr assays they used rather than an effect of NK cell lysis susceptibility. In addition, the m144-mediated inhibitory effect was not reversed by addition of antibodies against Ly49 molecules A, C or G, nor was it affected by the addition of the anti-m144 antibody 15C6 (Chapman and Bjorkman, 1997). I would expect an antibody against m144 to block the

inhibition, although it is possible that the anti-m144 antibody does not block the functional epitope of m144 and would therefore not inhibit the observed inhibition. I have sent the authors of this paper an anti-m144 antiserum, but have not yet heard whether it was effective at blocking inhibition.

Cretney et al. recently published a paper investigating the effects of m144 expression in *in vivo* NK-mediated clearance of class I-negative cells (Cretney et al., 1999). Their results show that NK-cell mediated rejection of RMA-S cells expressing m144 (RMA-S-m144) was reduced compared to wild type RMA-S cells. RMA-S cells are defective in peptide loading of class I MHC molecules and express only low levels of surface class I. As a result, they are highly susceptible to NK cell-mediated lysis. The authors argue that the basis of the reduced rejection is that the number of NK cells accumulating around the injected RMA-S-m144 cells was reduced and that the lytic capacity of these NK cells was also reduced. However, analysis of the peritoneal lavages collected from mice injected with RMA-S-m144 cells reveals that the total number of cells, not just the number of NK cells, was reduced at the site of injection. In my opinion, these results suggest that the effect mediated by m144 may affect a larger body of immune effector cells and may not be specific for NK cells. This would explain a second observation made in this same paper that *in vitro*, RMA-S-m144 cells were only slightly protected against activated NK cells and even less protected against resting NK cells.

At this point the data regarding the function of m144 are difficult to interpret. Despite the strength of the results by Farrell et al. (1997) correlating m144 expression with protection against NK cell-mediated clearance in infected mice (Farrell et al., 1997), it is not clear how m144 is providing this protection. *In vitro* experiments designed to demonstrate a cell-cell interaction between m144-expressing cells and NK cells have been difficult as m144 is not readily expressed on the surface of laboratory cell lines (T. Chapman, P. Bjorkman unpublished observations; (Kubota et al., 1999)) and all previous studies presume that m144 is a cell surface ligand. However, there is little evidence to suggest that m144 is expressed on the surface of virally infected cells (Farrell et al., 1999). It is possible that m144 remains intracellular during MCMV infection, despite its cell surface glycoprotein characteristics.

It is my opinion that m144 may be modulating the cytokine profile at the site of infection. The results by Cretney et al. (1999) described above indicate that fewer infiltrating and activated immune effector cells are found at the site of injected $m144^+$ tumor cells suggesting that m144 expression may prevent the attraction and activation of immune effector cells. In addition, continuing studies by Farrell et al. using wild type MCMV and the m144-deletion virus suggest that m144 expression may affect the cytokine profile in MCMV-infected mice (Farrell et al., 1999). In the original paper by Farrell et al. (1997) which described the pathogenicity of wildtype MCMV compared to the mutant m144 deletion virus, the replication rate of the mutant virus was restored to

that of the wildtype virus by eliminating the NK cell population using an antibody against an NK cell-specific protein. Although it was not demonstrated, the authors suggested that m144 was able to protect infected cells from NK cell-mediated clearance through direct interaction with NK cells, e.g., interaction of m144 with an NK cell inhibitory receptor. Recent results, however, show that the replication rate of the mutant virus can be restored by eliminating IL-12 or IFN-γ levels. IL-12 stimulates NK cells to produce IFN-γ and NK cell-produced-IFN-γ has been shown to reduce MCMV viral titers. The significance of this result is twofold: one, it suggests that NK cell clearance of MCMV-infected cells is mediated through cytokines as opposed to a direct protein:protein interaction and two, it suggests that m144 may modulate the anti-viral NK cell response by modulating the cytokines that affect NK cell activation, e.g., IL-12. Both monocytes and macrophages are important sources of IL-12 and both are sites of MCMV infection.

Recently the role of the RCMV MHC class I homolog, r144, in RCMV pathogenicity was addressed by comparing replication, dissemination and tissue destruction of wild type RCMV with an r144-null mutant RCMV, RCMVΔr144 (Beisser et al., 1999). r144 and m144 appear to be closely related as they occupy similar locations in the genomes of RCMV and MCMV, respectively, share 30% sequence identity (as compared to 18% shared sequence identity between r144 and UL18) and

both have large deletions in the α2 domain (Beisser et al., 1999). It is enticing to think that analysis of the r144 function might shed some light on the m144 function.

3. r144 in RCMV Infection

While the authors observed no major differences between wild type RCMV and the mutant RCMVΔr144, the authors did note that there were fewer infiltrating leukocytes in the footpads of rats infected with RCMVΔr144 as compared to the footpads of rats infected with wild type RCMV (Beisser et al., 1999). This result is reminiscent of that found by Cretney et al. who demonstrated fewer infiltrating immune effector cells surrounding the injection site of m144-expressing tumor cells (Cretney et al., 1999). Beisser et al. suggest that the presence of fewer infiltrating leukocytes in the footpads of rats infected with RCMVΔr144 is due to an interaction, either direct or indirect, between r144 and macrophages (Beisser et al., 1999). Thus, limited data describing the function of both m144 and r144 seem to imply a function in the modulation of cytokine production. However, in the absence of knowing the identity of either the m144 or r144 ligand, it is difficult to speculate about the function(s) of these proteins.

4. Are UL18 and m144 Performing Similar Functions?

Like m144, I think that UL18 may be important in modulating the cytokine profile at the site of CMV infection. However, as described in the previous chapter, m144 and UL18

are significantly different structurally (e.g., UL18 binds peptides, m144 does not; m144 and UL18 are composed of different secondary structural elements as indicated by differences in their far UV CD spectrums), and one needs to ask whether this structural disparity implies a functional disparity as well. In addition a phylogenetic tree, comparing the sequences of m144, UL18 and r144 with classical class I MHC molecules from mice, humans and rats indicates that while m144 and r144 are closely related, UL18 is relatively divergent from either m144 or r144 (Figure 2-1). This, coupled with the observation that the m144 and r144 genes are located at similar locations in the

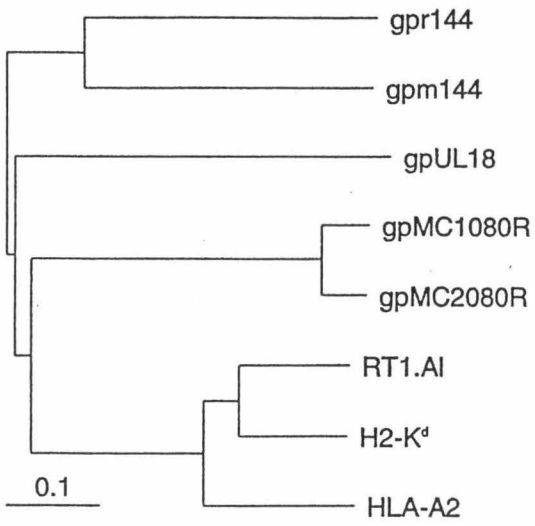

Figure 1. A phylogenetic tree comparing UL18, m144, and r144 to three mammalian MHC class I proteins as produced in (Beisser et al., 1999). gpMC1080R and gpMC2080R are MHC class I homologs from molluscum contagiosum virus type 1 and 2 (Senkevich et al., 1996; Senkevich and Moss, 1998).

MCMV and RCMV genomes, respectively, while the UL18 gene is located at different position in the HCMV genome, suggests that acquisition of UL18 for HCMV and m144

and r144 for an ancestral rodent CMV were separate events (Beisser et al., 1999; Chee et al., 1990; Rawlinson et al., 1996).

However, it has not been shown that different acquistion times necessarily correlate with different functions for two separate proteins. Therefore, the fact that m144 and UL18 were acquired separately is not sufficient to prove that m144 and UL18 are performing different functions. With respect to the structural differences between m144 and UL18, it is unknown whether the locations of these structural differences are actually relevant to the function of the molecules. I demonstrated that m144 does not bind peptides due to a large deletion in the α2 region of the molecule. However, as will be shown in Chapter 4, the primary LIR-1 binding site on UL18 and class I MHC is located within the α3 domain of these molecules and, presumably, structural deviations in the α2 region of UL18 or MHC class I molecules would not affect LIR-1 recognition of these proteins. If the binding site of the m144 ligand is also in the α3 domain, deletions in the α2 domain would probably be inconsequential for function. Amino acid sequence comparisons of the extracellular region of m144 with that of murine MHC class I molecules reveal that the α3 domain of m144 shares a much higher degree of identity with murine class I molecules (32%) than either the α1 or α2 domain (23% and 20%, respectively) (Farrell et al., 1997). It is possible that the functional epitope of m144, like that of UL18, is located in the α3 domain and that there is an analogous

receptor to LIR-1 in mice. Therefore, despite structural differences between UL18 and m144, it is possible that both molecules may be performing similar functions for their respective viruses.

5. References

Alam, S. M., Travers, P. J., Wung, J. L., Nasholds, W., Redpath, S., Jameson, S. C., and Gascoigne, N. R. (1996). T-cell-receptor affinity and thymocyte positive selection. Nature *381*, 616-620.

Beisser, P. S., Kloover, J. S., Grauls, G. E. L. M., Blok, M. J., Bruggeman, C. A., and Vink, C. (1999). The r144 MHC class I-like gene of rat cytomegalovirus is dispensable for both acute and long-term infection in the immunocompromised host. J. Virol. *In Press*.

Braud, V. M., Allan, D. S., O'Callaghan, C. A., Soderstrom, K., D'Andrea, A., Ogg, G. S., Lazetic, S., Young, N. T., Bell, J. I., Phillips, J. H., Lanier, L. L., and McMichael, A. J. (1998). HLA-E binds to natural killer cell receptors CD94/NKG2A, B and C. Nature *391*, 795-799.

Chapman, T. L., and Bjorkman, P. J. (1997). Characterization of a murine cytomegalovirus class I MHC homolog: Comparison to MHC molecules and to the human cytomegalovirus MHC homolog. J. Virol., in press.

Chee, M. S., Bankier, A. T., Beck, S., Bohni, R., Brown, C. M., Cerny, R., Horsnell, T., Hutchison, C. A. D., Kouzarides, T., and Martignetti, J. A. (1990). Analysis of the protein-coding content of the sequence of human cytomegalovirus strain AD169. Curr Top Microbiol Immunol *154*, 125-169.

Cretney, E., Degli-Esposti, M., A, Densley, E. H., Farrell, H. E., Davis-Poynter, N. J., and Smyth, M. J. (1999). m144, a murine cytomegalovirus (MCMV)-encoded major histocompatibility complex class I homologue, confers tumor resistance to natural killer cell-mediated rejection. J. Exp. Med *190*, 435-444.

Farrell, H. E., Degli-Esposti, M. A., and Davis-Poynter, N. J. (1999). Cytomegalovirus evasion of natural killer cell responses. Immunol. Rev. *168*, 187-197.

Farrell, H. E., Vally, H., Lynch, D. M., Fleming, P., Shellam, G. R., Scalzo, A. A., and Davis-Poynter, N. J. (1997). Inhibition of natural killer cells by a cytomegalovirus MHC class I homologue in vivo. Nature *386*, 510-514.

Garcia, K. C., Scott, C. A., Brunmark, A., Carbone, F. R., Peterson, P. A., Wilson, I. A., and Teyton, L. (1996). CD8 enhances formation of stable T-cell receptor/MHC

class I molecule complexes. Nature *384*, 577-581.

Kubagawa, H., Chen, C. C., Ho, L. H., Shimada, T. S., Gartland, L., Mashburn, C., Uehara, T., Ravetch, J. V., and Cooper, M. D. (1999). Biochemical nature and cellular distribution of the paired immunoglobulin-like receptors, PIR-A and PIR-B. J. Exp. Med. *189*, 309-318.

Kubota, A., Kubota, S., Farrell, H. E., Davis-Poynter, N., and Takei, F. (1999). Inhibition of NK cells by murine CMV-encoded class I MHC homologue m144. Cell. Immunol *191*, 145-151.

Matsui, K., Boniface, J. J., Reay, P. A., Schild, H., Fazekas de St. Groth, B., and Davis, M. M. (1991). Low affinity interactions of peptide-MHC complexes with T cell receptors. Science *254*, 1788-1791.

Parham, P., Androlewicz, M. J., Holmes, N. J., and Rothenberg, B. E. (1983). Arginine-45 is a major part of the determinant of human ß2-microglobulin recognized by mouse monoclonal antibody BBM.1. J. Biol. Chem. *258*, 6179-6186.

Rawlinson, W. D., Farrell, H. E., and Barrell, B. G. (1996). Analysis of the complete DNA sequence of murine cytomegalovirus. J. Virol *70*, 8833-8849.

Senkevich, T. G., Bugert, J. J., Sisler, J. R., Koonin, E. V., Darai, G., and Moss, B. (1996). Genome sequence of a human tumorigenic poxvirus: prediction of specific host response-evasion genes. Science *273*, 813-816.

Senkevich, T. G., and Moss, B. (1998). Domain structure, intracellular trafficking, and beta2-microglobulin binding of a major histocompatibility complex class I homolog encoded by molluscum contagiosum virus. Virology *250*, 397-407.

Vales-Gomez, M., Reyburn, H. T., Mandelboim, M., and Strominger, J. L. (1998). Kinetics of interaction of HLA-C ligands with natural killer cell inhibitory receptors (erratum). Immunity *9*, 892.

Chapter 4:

The Inhibitory Receptor LIR-1 Uses a Common Binding Interaction to Recognize Class I MHC Molecules and the Viral Homolog UL18

In this chapter I determine the affinities of the LIR-1/UL18 and LIR-1/MHC class I interactions using a biosensor based assay. I also identify the binding site on LIR-1 for UL18 and MHC class I molecules and in collaboration with Astrid Heikema, a technician in the Bjorkman lab, identify the binding site on UL18 and MHC class I molecules for LIR-1. The cell staining assays, as well as preparation of the DNA constructs used in the cell staining assays, were done by Astrid Heikema.

Immunity, Vol. 11, 603–613, November, 1999, Copyright ©1999 by Cell Press

The Inhibitory Receptor LIR-1 Uses a Common Binding Interaction to Recognize Class I MHC Molecules and the Viral Homolog UL18

Tara L. Chapman,* Astrid P. Heikema,† and Pamela J. Bjorkman†‡
*Graduate Option in Biochemistry
†Division of Biology 156-29
and Howard Hughes Medical Institute
California Institute of Technology
Pasadena, California 91125

Summary

LIR-1 is a class I MHC receptor related to natural killer inhibitory receptors (KIRs). Binding of LIR-1 or KIRs to class I molecules results in inhibitory signals. Unlike individual KIRs, LIR-1 recognizes many class I alleles and also binds UL18, a human cytomegalovirus class I MHC homolog. Here, we show that LIR-1 interacts with the relatively nonpolymorphic α3 domain of class I proteins and the analogous region of UL18 using its N-terminal immunoglobulin-like domain. The >1000-fold higher affinity of LIR-1 for UL18 than for class I illustrates how a viral protein competes with host proteins to subvert the host immune response. LIR-1 recognition of class I molecules resembles the CD4–class II MHC interaction more than the KIR–class I interaction, implying a functional distinction between LIR-1 and KIRs.

Introduction

Human cytomegalovirus (HCMV) is a widespread infectious agent that infects 70%–90% of immunocompetent adults (Wentworth and Alexander, 1971). While primary infection elicits an immune response, the response is insufficient to clear the virus, and lifelong infection ensues. To maintain viral persistence in the presence of a fully primed immune system, HCMV has evolved strategies that subvert the host immune system, including downregulation of cell surface expression of host class I MHC molecules (reviewed in Wiertz et al., 1997). Class I MHC molecules are heterodimers composed of a polymorphic membrane-bound heavy chain associated with the nonpolymorphic light chain β_2-microglobulin (β_2m). Peptides derived from degradation of cytoplasmic proteins are presented to cytotoxic T cells bound to class I molecules in a groove within the α1 and α2 domains of the heavy chain (reviewed in Bjorkman and Parham, 1990). While downregulation of surface class I expression hinders recognition of infected cells by virus-specific T cells, cells that lack surface class I MHC expression are potential targets for natural killer (NK) cells. NK cells express activating receptors, which can be triggered by both non-MHC and MHC molecules, and inhibitory receptors, which recognize class I MHC molecules (reviewed in Lanier et al., 1997). Stimulation of activating receptors leads to target cell lysis unless the NK cell inhibitory receptors engage an adequate level of class I molecules on the target cell. Thus, the host immune system ensures that those cells that have downregulated their class I MHC molecules to a level sufficient to avoid detection by T cells can be recognized and eliminated by NK cells.

As a strategy that may be involved in modulation of the host immune response, HCMV expresses UL18, a class I MHC homolog (Beck and Barrell, 1988). The predicted extracellular portion of UL18 can be divided into three domains (α1, α2, and α3) that share ~25% amino acid sequence identity with their class I counterparts. Like host class I molecules, UL18 associates with β_2m (Browne et al., 1990) and endogenously derived peptides (Fahnestock et al., 1995). UL18 was proposed to function as a decoy class I molecule capable of binding NK cell inhibitory receptors and preventing lysis of infected cells lacking surface class I expression (Fahnestock et al., 1995). However, the host cell ligand of UL18 was identified as leukocyte immunoglobulin-like receptor-1 (LIR-1 or ILT2), a membrane glycoprotein expressed on only a subset of NK cells (Cosman et al., 1997) and most or all monocytes, dendritic and B cells, and some T cells (Borges et al., 1997; Colonna et al., 1997; Fanger et al., 1998). LIR-1 is a member of a family of proteins (LIR-1 to LIR-8) that contain two or four extracellular immunoglobulin (Ig)-like domains related to NK cell killer inhibitory receptor (KIR) domains (Borges et al., 1997). The endogenous ligands of LIR-1, LIR-2, and KIRs are class I MHC molecules. However, while individual KIRs show allele-specific recognition of class I molecules, LIR-1 and LIR-2 interact with a broad range of classical and nonclassical class I MHC molecules (Fanger et al., 1998; Navarro et al., 1999; Vitale et al., 1999). Despite a high level of sequence identity between LIR family members, only LIR-1 binds UL18 (Borges et al., 1997).

The role of LIR-1 in the immune response to viruses in general and HCMV in particular has not yet been elucidated, but LIR-1 shows properties consistent with an inhibitory function. In common with KIRs, several LIR proteins contain inhibitory motifs in their cytoplasmic tails, and LIR-1 associates with SHP-1, a tyrosine phosphatase that inhibits activating signals (Cosman et al., 1997). LIR-1 engagement on NK and T cells by class I MHC molecules protects target cells from lysis, and concurrent recognition of LIR-1 with other receptors results in inhibition of intracellular Ca^{2+} mobilization (Colonna et al., 1997). These studies demonstrate that LIR-1 can function as an inhibitory receptor and might therefore modulate activation signals in response to recognition of host cell class I molecules or UL18.

To better understand the functions of UL18 in evasion of the host immune response and LIR-1 in the presence and absence of CMV infection, we characterized the LIR-1/UL18 and LIR-1/class I MHC interactions. We find that LIR-1 binds UL18 with greater than 1000-fold higher affinity than it binds classical and nonclassical class I proteins; thus, even low levels of UL18 can efficiently compete with residual host cell class I proteins on

‡To whom correspondence should be addressed (e-mail: bjorkman@cco.caltech.edu).

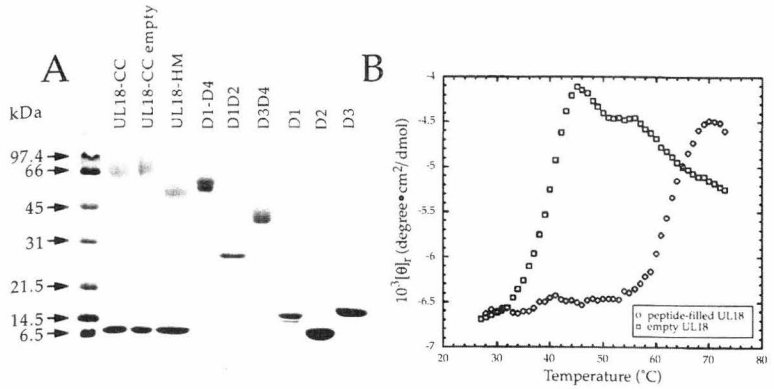

Figure 1. Characterization of Proteins

(A) Purified proteins analyzed on 15% reducing SDS-PAGE. The ~10 kDa contaminant in the D1D2 and D1 preparations is not responsible for the observed interaction between D1D2 and UL18 or D1 and UL18, since it is not coprecipitated with UL18 and either LIR-1 fragment using reagents that bind to UL18 (an anti-β_2m monoclonal antibody or Ni-NTA beads) (data not shown).

(B) Thermal denaturation of peptide-filled and empty forms of UL18-CC monitored by the CD signal at 223 nm. Transition midpoints (T_m), 35°C, empty UL18-CC; 60°C, peptide-filled UL18-CC.

HCMV-infected cells for LIR-1 binding. The primary binding site on LIR-1 for both class I molecules and UL18 is its N-terminal domain, and this region interacts with the α3 domain of class I proteins and UL18. Recognition of the α3 domain, which is relatively nonpolymorphic, predicts that LIR-1 can interact with most or all class I MHC molecules, consistent with previous observations that LIR-1 binds a wide range of class I proteins (Colonna et al., 1997; Lanier et al., 1997; Fanger et al., 1998; Navarro et al., 1999). These results suggest that LIR-1 differs in recognition properties from KIRs, sharing more characteristics with the T cell coreceptor CD4-class II MHC interaction than with the KIR-class I MHC interaction.

Results

Production of Peptide-Filled, Empty, and Different Carbohydrate-Containing Forms of Soluble UL18

We previously demonstrated that soluble UL18 produced in CHO cells associates with endogenously derived peptides (Fahnestock et al., 1995). To investigate the role of bound peptide in LIR-1 recognition of UL18, we prepared peptide-filled and empty forms of soluble UL18-human β_2m heterodimers produced in CHO cells (hereafter referred to as UL18-complex carbohydrate or UL18-CC [see below]) (Figure 1A). The empty form of UL18-CC was prepared by removing endogenous peptides from the peptide-filled form under denaturing conditions and then refolding the protein in the absence of peptide. Empty UL18-CC is thermally unstable compared with the peptide-filled form (Figure 1B).

The extracellular portion of the UL18 heavy chain contains 13 potential N-linked carbohydrate sites (Beck and Barrell, 1988). The majority of these sites appear to be utilized when the protein is produced in infected or transfected cells since the heavy chain migrates on SDS polyacrylamide gels with a higher than predicted apparent molecular mass (Browne et al., 1990; Fahnestock et al., 1995; Leong et al., 1998) (Figure 1A). Because a large proportion of the surface of UL18 is likely to be occluded by carbohydrate, we wished to examine the role of carbohydrate in recognition of UL18 by LIR-1. We therefore expressed UL18 in insect cells, which attach high mannose or truncated trimannosyl N-linked glycans (Jenkins et al., 1996), to compare with UL18 produced in CHO cells, which attach complex N-linked carbohydrates (Davis et al., 1993). A previously identified UL18-binding peptide (Fahnestock et al., 1995) was added to insect cell supernatants, resulting in peptide-filled UL18, hereafter referred to as UL18-high mannose or UL18-HM (see the Experimental Procedures). The heavy chains of UL18-CC and UL18-HM migrate with different apparent molecular masses on an SDS-acrylamide gel: 77 to 97 kDa for UL18-CC and 50 to 53 kDa for UL18-HM (Figure 1A), consistent with molecular weights derived by mass spectrometry (76 kDa for UL18-CC and 57 kDa for UL18-HM; data not shown). The molecular weight difference indicates that the two forms of UL18 differ in the composition of carbohydrates attached to potential N-linked glycosylation sites.

Production of Soluble Forms of LIR-1 Containing One, Two, and Four Ig-like Domains

The extracellular region of LIR-1 comprises four Ig-like domains (D1, D2, D3, and D4). A soluble version of the entire extracellular region (D1-D4) was expressed in baculovirus-infected insect cells. Equilibrium analytical ultracentrifugation demonstrated that purified D1-D4 is monomeric at μM concentrations (data not shown). To determine which region of LIR-1 interacts with UL18 and class I MHC molecules, we prepared smaller versions of LIR-1 corresponding to single domains (D1, D2, and D3) or tandem domains (D1D2 and D3D4) (see the Experimental Procedures). All of the fragments run in the expected position on a gel filtration column, and far UV circular dichroism (CD) spectra indicate that each fragment contains mainly β-sheet secondary structure (data not shown); thus, the fragments retain their native folds. These results suggest that interdomain interactions are not required for correct folding of the LIR-1 domains and are consistent with an elongated structure for D1-D4 (Figure 5).

LIR-1 and UL18 Form a 1:1 Complex in Solution

To determine the stoichiometry of the interaction between UL18 and LIR-1 in solution, various molar ratios of UL18-HM and D1-D4 were passed over a Superose 6B column. When UL18-HM and D1-D4 were present at equimolar ratios, a single peak corresponding to the UL18/LIR-1 complex eluted from the column (Figure 2). The 1:1 stoichiometry of the UL18/LIR-1 complex was verified by equilibrium analytical ultracentrifugation, which yielded molecular weights of 59 kDa (UL18-HM),

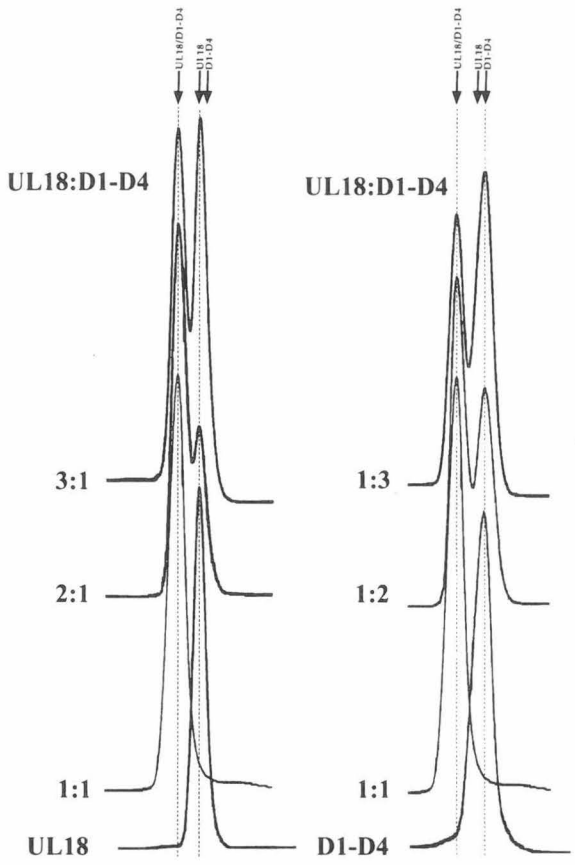

Figure 2. Gel Filtration Chromatographic Demonstration that UL18 and D1-D4 Bind with 1:1 Stoichiometry

UL18-HM and D1-D4 were incubated at the indicated molar ratios and then passed over a sizing column to separate UL18:D1-D4 complexes from free proteins. At a 1:1 molar ratio, virtually all of the protein migrated as the complex. When the input ratio of UL18 to D1-D4 was greater than 1:1, there was excess UL18, and when it was less than 1:1, there was excess D1-D4.

55 kDa (D1-D4), and 96 kDa (UL18-HM/D1-D4 complex) (data not shown).

LIR-1 Binds UL18 with Higher Affinity Than It Binds to Class I MHC Proteins

We used a surface plasmon resonance (SPR)-based assay to determine the affinities of the interactions between D1-D4 and the various forms of UL18. Empty UL18-CC, peptide-filled UL18-CC, and UL18-HM were each immobilized on a biosensor chip, and the interaction with injected D1-D4 was monitored (Figure 3A). Binding of the various UL18 species over a D1-D4 coupled biosensor chip was also assayed. As summarized in Table 1, D1-D4 binds all forms of UL18 with an equilibrium dissociation constant (K_D) in the nM range. There is a slight coupling dependence to the derived affinities, such that injected LIR-1 binds immobilized UL18 with a higher apparent affinity than injected UL18 binds immobilized LIR-1. Coupling-dependent affinity differences have been observed in other biosensor-based assays (Kuziemko et al., 1996; Lebrón et al., 1998). For the UL18 interaction with D1-D4, affinity constants derived from either orientation demonstrate that the presence or absence of peptide and the nature of the carbohydrate on UL18 have little effect on binding LIR-1. These results suggest that the LIR-1 binding site on UL18 primarily involves a protein, rather than carbohydrate, portion of UL18 that is distinct from the peptide-binding site.

We also derived affinities for the interaction of D1-D4 with soluble versions of classical and nonclassical class I MHC molecules (Figures 3C and 3D; Table 1). The MHC proteins used in these binding assays contained either a mixture of endogenous peptides (HLA-B*2702) or single defined peptides (HLA-Cw*0602, HLA-Cw*0301, HLA-Cw*0702, HLA-G1, HLA-E). The proteins were either unglycosylated (HLA-Cw*0602, HLA-Cw*0301, HLA-G1, HLA-E) or included complex N-linked glycans (HLA-B*2702, expressed in CHO cells) or high mannose or truncated trimannosyl N-linked glycans (HLA-Cw*0702, expressed in insect cells). Each class I protein was immobilized to a flowcell on a biosensor chip, and D1-D4 was injected. Most of the binding reactions were assayed only in this orientation because the class I proteins were not generally available in sufficient quantities to allow injections over immobilized D1-D4. We also coupled soluble HFE, a β_2m-containing heterodimer that is structurally similar to class I MHC proteins (Lebrón et al., 1998), to a similar density. We observed small but significant binding responses for high concentrations of D1-D4 injected over the immobilized classical and nonclassical class I proteins, but no significant response for injections over the HFE coupled flowcell (Figure 3C). We also found no significant binding of D1-D4 to soluble versions of two other human class I MHC homologs, FcRn and ZAG (Sánchez et al., 1999) (data not shown). To account for nonspecific interactions, the binding response at equilibrium was calculated by subtracting the response seen in the HFE-coupled flow cell for each concentration of injected D1-D4 (Figure 3D). Affinity constants derived from these data are summarized in Table 1. The approximate K_Ds for the interaction of D1-D4 with the classical and nonclassical class I molecules we tested range from 15 to 100 μM. Thus, LIR-1 binds to these host class I proteins >1000-fold more weakly than it binds to UL18.

The Primary UL18 and Class I Binding Site on LIR-1 Is Located in D1

To localize the binding site(s) on LIR-1 for UL18 and class I MHC proteins, we compared the binding of D1-D4 with fragments of LIR-1 composed of one or two Ig-like domains. As summarized in Table 1, the D1D2 fragment binds both UL18 and each of the class I proteins tested with a similar affinity as D1-D4. In contrast, D3D4 showed no detectable binding to either UL18 or any of the class I proteins (Figures 3B and 3E). To further localize the binding site on LIR-1, we analyzed the binding of individual domains, D1 and D2, to UL18 and class I molecules. In all cases tested, D1 bound with only slightly reduced affinity compared with D1D2 or D1-D4, whereas D2 showed no detectable binding (Figures 3B and 3E). These results indicate that the primary binding site on LIR-1 for both UL18 and class I MHC proteins is located within D1, with the possibility of minor contributions from residues within D2. The finding that the

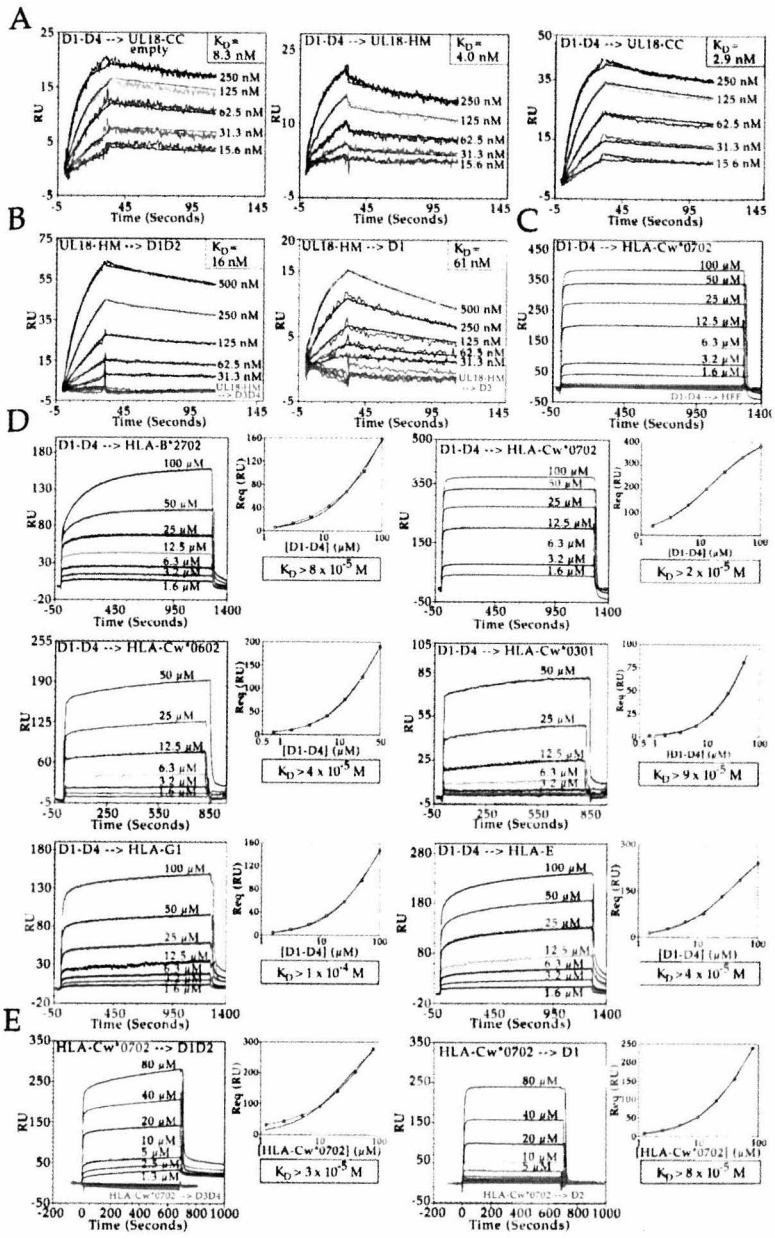

Figure 3. Biosensor Analyses of LIR-1-UL18 and LIR-1-Class I Binding

In each panel, the injected protein is indicated in front of an arrow pointing to the immobilized protein.

(A and B) Sensorgrams (thick colored lines) from kinetics-based binding experiments overlaid with the calculated response (thin black lines) derived using a 1:1 binding model. One representative set of injections from experiments performed in triplicate is shown for each interaction (analyses from triplicate experiments reported in Table 1).

(C–E) Sensorgrams from binding experiments in which the binding response closely approached or reached equilibrium. Plots of the equilibrium binding response (R_{eq}) versus the log of the concentration of injected protein are shown to the right of each sensorgram with best fit binding curves to the experimental data points shown as continuous lines. Derived K_D values are approximate because binding is not saturated at the highest concentration of protein possible to achieve with limited quantities of protein.

(A) D1-D4 injected over the three forms of UL18.

(B) UL18-HM injected over smaller LIR-1 fragments. No significant responses are seen for UL18-HM injected over D3D4 or D2 (red sensorgrams).

(C) Comparison of response for D1-D4 injected over HLA-Cw*0702 or over HFE. No significant response is seen for D1-D4 injected over HFE (red sensorgrams).

(D) D1-D4 injected over classical and nonclassicial class I proteins. For each sensorgram, the residual response from the HFE-coupled flowcell (C) has been subtracted.

(E) HLA-Cw*0702 injected over smaller LIR-1 fragments. No significant responses are seen for HLA-Cw*0702 injected over D3D4 or D2 (red sensorgrams).

same region of LIR-1 is used for binding both UL18 and class I molecules is consistent with the observation that preequilibration of D1-D4 with UL18 blocks binding to immobilized HLA-Cw*0702 (data not shown).

LIR-1 Interacts with the α3 Domain of Both UL18 and Class I Molecules

To identify which portion of UL18 is recognized by LIR-1, we constructed domain-swapped proteins in which domains from HFE were exchanged into UL18. We made the following four constructs: full-length (wild-type) versions of UL18 and HFE and α1α2UL18-α3HFE and α1α2HFE-α3UL18 (in which the α1 and α2 domains from the first protein were fused to the α3, transmembrane, and cytosolic domains of the second protein). Expression in transfected COS-7 cells was verified by staining live and fixed cells with polyclonal antisera against UL18 and/or HFE. LIR-1 binding was assayed by staining with His-tagged D1-D4 incubated with a FITC-labeled anti-His tag antibody. The D1-D4 reagent stained cells expressing wild-type UL18 and α1α2HFE-α3UL18 but not cells expressing α1α2UL18-α3HFE or whole HFE (Figure 4A), indicating that the UL18 α3 domain is a primary interaction site for D1-D4.

To identify the LIR-1 binding site on a class I MHC molecule, we made chimeras of HFE and the human class I MHC molecule HLA-B*0702 (α1α2HFE-α3B7 and α1α2B7-α3HFE) to compare with full-length HLA-B*0702 and HFE. Protein expression was verified using antisera against HFE or a class I MHC-specific monoclonal antibody. Although wild-type HLA-B*0702 and the B7-HFE swapped constructs were expressed in transfected COS-7 cells (Figure 4B), none of the cells stained with labeled D1-D4 (data not shown), which was used for

Table 1. Biosensor Analyses of LIR-1 Binding to UL18 and Class I MHC Molecules

	K_D (M)	k_a ($sec^{-1}M^{-1}$)	k_d (sec^{-1})
UL18 or Class I Immobilized			
D1-D4→UL18-CC empty	$(8.3 \pm 0.5) \times 10^{-9}$	$(6.1 \pm 0.9) \times 10^{5}$	$(5.0 \pm 0.9) \times 10^{-3}$
D1-D4→UL18-CC + peptide	$(2.9 \pm 0.3) \times 10^{-9}$	$(5.8 \pm 0.8) \times 10^{5}$	$(1.7 \pm 0.4) \times 10^{-3}$
D1-D4→UL18-HM + peptide	$(4.0 \pm 3) \times 10^{-9}$	$(5.2 \pm 1) \times 10^{5}$	$(2.1 \pm 0.5) \times 10^{-3}$
D1-D4→HLA-B*2702	$(8, 9) \times 10^{-5}$		
D1-D4→HLA-Cw*0702	$(2, 2) \times 10^{-5}$		
D1-D4→HLA-Cw*0602	$(4, 5) \times 10^{-5}$		
D1-D4→HLA-Cw*0301	9×10^{-5}		
D1-D4→HLA-G1	1×10^{-4}		
D1-D4→HLA-E	4×10^{-5}		
LIR-1 D1-D4 Immobilized			
UL18-CC empty→D1-D4	$(1.0 \pm 0.1) \times 10^{-7}$	$(1.1 \pm 0.3) \times 10^{5}$	$(1.1 \pm 0.2) \times 10^{-2}$
UL18-CC + peptide→D1-D4	$(2.1 \pm 0.5) \times 10^{-8}$	$(1.1 \pm 0.8) \times 10^{5}$	$(2.3 \pm 0.4) \times 10^{-3}$
UL18-HM + peptide→D1-D4	$(1.4 \pm 0.4) \times 10^{-8}$	$(1.5 \pm 0.5) \times 10^{5}$	$(2.1 \pm 0.6) \times 10^{-3}$
HLA-Cw*0702→D1-D4	6×10^{-5}		
UL18 and Class I MHC Binding to LIR-1 Domains			
UL18-HM + peptide→D1D2	$(1.6 \pm 0.3) \times 10^{-8}$	$(1.1 \pm 0.1) \times 10^{5}$	$(1.7 \pm 0.3) \times 10^{-3}$
UL18-HM + peptide→D1	$(6.1, 7.7) \times 10^{-8}$	$(8.0, 6.6) \times 10^{5}$	$(4.9, 5.1) \times 10^{-2}$
UL18-HM + peptide→D2	NB		
UL18-HM + peptide→D3	NB		
UL18-HM + peptide→D3D4	NB		
D1D2→HLA-B*2702	5×10^{-5}		
D3D4→HLA-B*2702	NB		
D1D2→HLA-Cw*0702	3×10^{-5}		
HLA-Cw*0702→D1D2	3×10^{-5}		
HLA-Cw*0702→D1	8×10^{-5}		
HLA-Cw*0702→D2	NB		
D3D4→HLA-Cw*0702	NB		
D3D4→HLA-G1	NB		
D3D4→HLA-E	NB		

The injected protein is indicated in front of an arrow pointing to the immobilized protein. When kinetic constants (k_a and k_d) are reported, the binding data were fit to a 1:1 binding model, and the K_D was determined as k_d/k_a. K_Ds were determined from three or four independent measurements, and the numbers after the ± sign represent standard deviations. When no kinetic constants are reported, the K_D was determined from equilibrium binding data fit to a 1:1 binding model. Experiments were performed in duplicate if two K_D values are listed. Due to insufficient quantities of protein, the highest LIR-1 or class I concentration used was 100 μM, which was not sufficient to saturate binding; thus, the K_D values for LIR-1 binding to class I molecules are approximate. NB, no binding detected.

the staining of the UL18 expressing cells (Figure 4A). Assuming that the inability to stain with monomeric D1-D4 resulted from a low affinity between D1-D4 and HLA-B*0702, as was found for the D1-D4 interaction with other class I MHC proteins (Table 1), we used a bivalent version of LIR-1 (a LIR-1 Fc fusion protein; LIR-1 Fc; Cosman et al., 1997) in order to increase the avidity between LIR-1 and HLA-B*0702. Labeled LIR-1 Fc stains cells expressing wild-type HLA-B*0702 and α1α2HFE-α3B7 but not cells expressing α1α2B7-α3HFE or wild-type HFE (Figure 4B). We conclude that LIR-1 interacts primarily with the α3 domain of HLA-B*0702 and that this interaction is of lower affinity than the LIR-1 interaction with the α3 domain of UL18.

Discussion

LIR-1 is an inhibitory receptor that is expressed on a majority of B cells, monocytes, and dendritic cells, and a small subset of NK and T cells (Borges et al., 1997; Colonna et al., 1997; Cosman et al., 1997; Vitale et al., 1999). Like the KIR and Ly49 families of NK inhibitory receptors (Lanier et al., 1997), LIR-1 binds class I MHC molecules, resulting in inhibition of activation signals (Colonna et al., 1997; Navarro et al., 1999). Unlike these NK receptors, which bind with allelic specificity (Lanier et al., 1997), LIR-1 binds to a broad range of classical and nonclassical class I molecules (Fanger et al., 1998; Navarro et al., 1999; Vitale et al., 1999). In addition, LIR-1 binds to UL18 (Cosman et al., 1997), a peptide-binding class I MHC homolog encoded by HCMV (Beck and Barrell, 1988; Fahnestock et al., 1995). The functions of both LIR-1 and UL18 remain obscure. To address how LIR-1 functions in the absence of HCMV infection and the role of UL18 in HCMV evasion of the host immune response, we characterized the LIR-1 interaction with class I MHC proteins and with UL18. Our studies reveal the molecular basis for the broad class I–binding specificity of LIR-1 and shed light on the function of UL18.

Using soluble versions of LIR-1 and class I MHC proteins, we found weak but significant binding between the LIR-1 extracellular region (D1-D4) and every class I protein tested, including three HLA-C alleles, one HLA-B allele, and the nonclassical class I molecules HLA-G1 and HLA-E. These results are in general agreement with binding and functional studies demonstrating LIR-1 interaction with a broad range of class I proteins including HLA-G (Fanger et al., 1998; Navarro et al., 1999; Vitale et al., 1999) but are in apparent contrast with previous reports that the LIR-1 Fc fusion protein does not bind HLA-Cw*0702 (Fanger et al., 1998) and that HLA-E does not induce LIR-1-mediated inhibition in a functional assay (Navarro et al., 1999). We find that D1-D4 binds to these alleles, but these binding events might not be

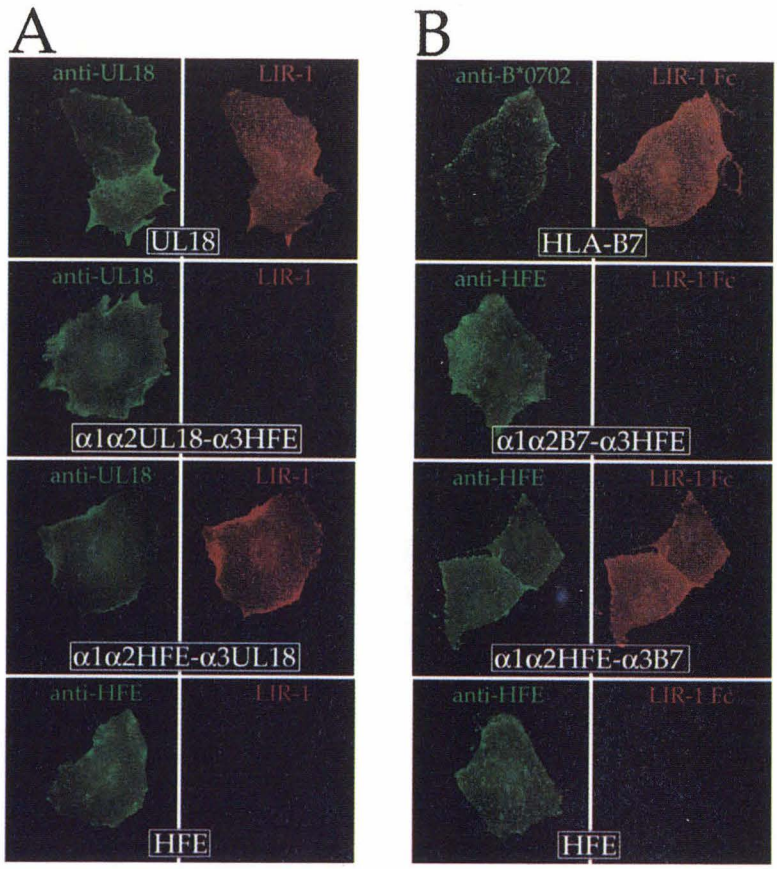

Figure 4. Staining of Transfected COS-7 Cells

Fixed cells were stained with the indicated FITC-labeled antibody or antiserum (green) to verify expression and with a Cy-3-labeled antibody bound to D1-D4 ([red]; cells expressing UL18-containing proteins) or LIR-1 Fc ([red]; cells expressing HLA-B*0702-containing proteins; magnification, 63×, zoomed twice). Staining of live cells verified that the constructs are expressed at the cell surface (data not shown).

detected using other assays and may have no functional consequences. Although D1-D4 binds to every classical and nonclassical class I protein tested in our assay, it does not bind to HFE, FcRn, or ZAG, class I MHC homologs that are structurally but not functionally similar to members of the class I MHC family that function in antigen presentation to T cells (Lebrón et al., 1998; Sánchez et al., 1999). Thus, LIR-1 is specific for peptide-binding class I molecules that function in the immune system, supporting the proposed role of UL18 as a virally-encoded immunomodulator.

The LIR-1 interaction with host class I MHC proteins is considerably weaker than its interaction with the viral class I homolog UL18. D1-D4 binds to UL18 with a K_D in the nM range but binds to classical and nonclassical class I molecules with >1000-fold reduced affinity (Table 1). The extensive N-linked glycosylation of UL18 (Beck and Barrell, 1988) compared to that of class I molecules (Bjorkman and Parham, 1990) suggested a possible explanation for the increased affinity of LIR-1 for UL18 compared to its affinity for class I molecules. However, LIR-1 binds different carbohydrate-containing forms of UL18 with nearly equal affinities (Table 1), suggesting that LIR-1 primarily recognizes a protein, rather than carbohydrate, epitope on UL18 and class I molecules. The recognition is independent of bound peptide, since LIR-1 binds to peptide-filled and empty UL18 with similar affinities (Table 1).

Although LIR-1 binds UL18 with much higher affinity than it binds class I proteins, other aspects of the LIR-1 interaction with the two types of protein are similar. For both UL18 and class I proteins, the primary binding site on LIR-1 is within the first of its four Ig-like domains. Thus, a fragment corresponding to the N-terminal domain alone (D1) binds with similar affinity as the entire extracellular region of LIR-1 (D1-D4) (Table 1). This property distinguishes LIR-1 from p58 KIRs, whose binding site for class I molecules is at the interface between the first and second Ig-like domains (Lanier et al., 1997). Indeed, the structure of the D1D2 portion of LIR-1 is likely to be different from the structures of p58 KIRs, in which an acute angle relating KIR D1 and D2 creates extensive interaction between the domains (Fan et al., 1997). The observation that D1D2 can be cleaved into stable fragments corresponding to D1 and D2 (Figure 1) suggests that there are not extensive interdomain interactions in this portion of LIR-1. A second similarity in LIR-1 recognition of its viral and host ligands is that LIR-1 recognizes the α3 domain of both UL18 and class I molecules. In this respect, LIR-1 also differs from KIRs, which bind to an epitope within the α1-α2 region of class I molecules (Lanier et al., 1997). In class I proteins, the α3 domain is relatively conserved between different alleles as compared with the polymorphic α1-α2 peptide-binding region (Bjorkman and Parham, 1990), providing a rationalization for the broad binding specificity of LIR-1 compared with individual KIRs.

Our data suggest that the interaction between LIR-1 and class I molecules and the class I–related protein UL18 can be schematically diagrammed as shown in

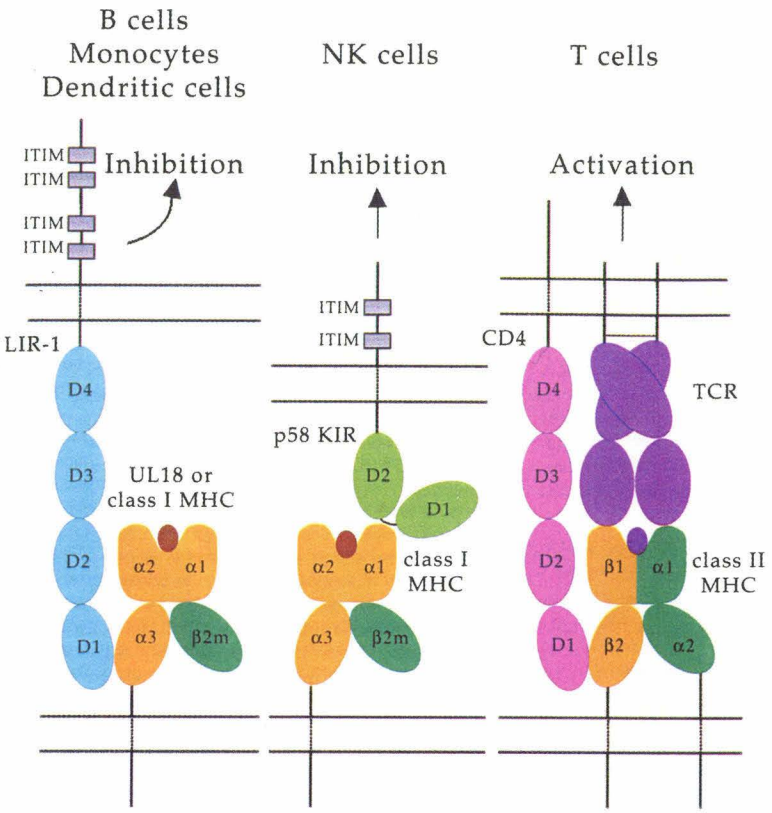

Figure 5. Schematic Comparison of the LIR-1–Class I, KIR–Class I, and CD4–Class II Interactions

D1-D4 is likely to have an elongated structure with minimal interdomain interactions (see text). LIR-1 binds to the α3 domain of UL18 and class I proteins using its N-terminal domain (see text), analogous to the interaction between D1 of CD4 and the β2 domain of class II MHC proteins (Leahy, 1995). By contrast, KIRs are bent, with extensive interdomain interactions, and bind to a region on the class I α1 domain using residues at the interface between domains (Fan et al., 1997; Lanier et al., 1997).

Figure 5. Based upon the ability of isolated LIR-1 domains to fold stably, we assume that there are not extensive interdomain interactions and therefore depict LIR-1 as a four domain extended structure. In contrast, p58 KIR domains are arranged in a kinked structure with extensive interdomain interactions, as revealed by crystal structures (e.g., Fan et al., 1997). Based upon our binding analyses, we show a 1:1 complex in which LIR-1 D1 interacts with the α3 domain of UL18 and class I molecules. This interaction is reminiscent of the interaction between CD4 and class II MHC molecules, in that the class II binding site is localized primarily on the CD4 N-terminal domain and CD4 binds to the class II counterpart of the class I α3 domain (class II β2) (reviewed in Leahy, 1995). In its properties, LIR-1 can be thought of as a hybrid between KIRs and the T cell coreceptors CD4 and CD8. Like KIRs, LIR-1 functions as an inhibitory receptor and binds weakly to class I MHC molecules (KIR-class I MHC affinities are ~10 μM) (Valés-Gómez et al., 1998), but like the T cell coreceptors, LIR-1 responds to a region on MHC molecules that does not involve the peptide-binding domains recognized by T cell receptors or KIRs.

The low affinity of the interaction between LIR-1 and class I MHC molecules suggests that high local concentrations of class I molecules need to be present to trigger LIR-1-mediated inhibition. However, class I MHC molecules are downregulated by HCMV infection (Wiertz et al., 1997). In the absence of a mechanism to engage host cell LIR-1 molecules, B cells, monocytes, and dendritic cells would presumably be activated by a lower threshold of stimulatory signals, leading to a stronger antiviral immune response. Expression of UL18 by HCMV-infected cells may be a mechanism whereby HCMV avoids the consequences of downregulating LIR-1 ligands. In this respect, the high affinity between LIR-1 and UL18 may be significant, in that only a small amount of UL18 on infected cells should be sufficient to bind LIR-1 resulting in inhibition. Indeed, only small amounts of UL18 are expressed on the surfaces of transfected or HCMV-infected cells (Leong et al., 1998); thus, a high affinity interaction with LIR-1 would be required for UL18 to exert an effect.

UL18 probably evolved from a host cell class I MHC gene acquired by HCMV at some point during its evolution with its human host (Wiley, 1988). While UL18 has greatly diverged from class I MHC molecules, as evidenced by sharing only ~25% amino acid sequence identity (Beck and Barrell, 1988), it has retained and improved upon the class I property of binding the inhibitory receptor LIR-1. The higher affinity of LIR-1 for UL18 than for class I molecules provides an example of how a viral protein is able to compete efficiently with host proteins to subvert the host immune response.

Experimental Procedures

Production of Peptide-Filled, Empty, and Different Carbohydrate-Containing Forms of UL18

We previously described the purification of a soluble form of UL18 (residues 1–284 of the mature UL18 heavy chain complexed with human β_2m) from the supernatants of transfected CHO cells (Fahnestock et al., 1995; Chapman and Bjorkman, 1997). For the experiments described here, we modified the UL18 construct to include a C-terminal 6x-His tag. The modified UL18 gene was sequenced

and subcloned into PBJ5-GS, which carries the glutamine synthetase gene as a selectable marker and means of gene amplification in the presence of methionine sulfoximine (Bebbington and Hentschel, 1987). Selection and amplification of UL18-expressing cells were done as described (Chapman and Bjorkman, 1997). UL18-CC was purified from the supernatants of transfected CHO cells using Ni-NTA chromatography (Ni-NTA superflow, Qiagen) followed by immunoaffinity chromatography using a column constructed with the anti-β_2m monoclonal antibody BBM.1 (Parham et al., 1983) as described (Fahnestock et al., 1995). Although soluble UL18 expressed in CHO cells contains endogenous peptides (Fahnestock et al., 1995), overexpression of UL18 leads to secretion of some protein that is either empty or does not contain an optimal peptide (Chapman and Bjorkman, 1997). To ensure that all UL18-CC includes a bound peptide, a synthetic peptide (ALPHAILRL) corresponding to a portion of actin, which was previously shown to be a major component of UL18 acid eluates (Fahnestock et al., 1995), was added during purification of UL18-CC.

Empty UL18-CC was prepared from peptide-filled UL18-CC as described for H-2K^d (Fahnestock et al., 1992). In brief, UL18-CC/β_2m heterodimers were denatured in 6.0 M guanidine hydrochloride and separated from endogenous peptides by gel filtration chromatography in 6.0 M guanidine hydrochloride on a Superdex 200 column (Pharmacia). Heavy and light chain peaks were pooled and renatured in the presence of an ~3-fold excess of human β_2m (expressed in bacteria; see below) by dialysis against 20 mM Tris (pH 7.4), 150 mM NaCl, 1 mM EDTA, and 0.2 mM phenylmethanesulfonyl fluoride containing 8.0 M urea, and then twice against the same buffer without urea. Renatured material was concentrated in a Centricon-10 (Millipore) and passed over a Superdex 200 column. Fractions corresponding to unaggregated UL18-CC/β_2m heterodimers were pooled and concentrated.

A form of soluble UL18 containing high mannose or truncated trimannosyl N-linked carbohydrates (UL18-HM) was produced in baculovirus-infected insect cells. A construct encoding soluble UL18 (corresponding to residues 1–284 of the mature protein with the preceding hydrophobic leader sequence) plus a C-terminal Factor X_a site and 6x-His tag was subcloned after sequencing into the dicistronic baculovirus transfer vector pAcUW31 (PharMingen). cDNA encoding human β_2m plus its hydrophobic leader sequence was subcloned into the second multiple cloning site of the transfer vector. Recombinant baculovirus was generated by cotransfection of the transfer vector with linearized viral DNA (Baculogold; PharMingen). UL18-HM/β_2m heterodimers were purified from supernatants of baculovirus-infected High 5 cells after adding the UL18-binding peptide ALPHAILRL (Fahnestock et al., 1995) using Ni-NTA and immunoaffinity chromatography as described for UL18-CC. UL18-HM exists as a complex with the ALPHAILRL peptide, as suggested by its high thermal stability and confirmed by N-terminal sequencing of acid eluates of purified UL18-HM (data not shown).

Far UV CD spectra of the empty UL18-CC, peptide-filled UL18-CC, and UL18-HM are similar to each other (data not shown) and to previously published spectra of UL18 and class I molecules (Chapman and Bjorkman, 1997).

Expression and Purification of Class I and Class I–like Molecules

Soluble HLA-B*2702/β_2m heterodimers containing a mixture of endogenous peptides were expressed in CHO cells and purified as described (Raghavan et al., 1996).

Soluble HLA-Cw*0702 (residues 1–274 of the mature protein complexed with human β_2m) was expressed in baculovirus-infected insect cells as described for UL18-HM. HLA-Cw*0702 was purified from infected cell supernatants after adding a Cw*0702-specific peptide (AYADFVYAY) (Sidney et al., 1995) by Ni-NTA chromatography followed by gel filtration using a Superdex 200 column (Pharmacia).

Truncated HLA-E and HLA-G1 (residues 1–275 of the mature protein containing a C-terminal 6x-His tag) were expressed in *Escherichia coli* as described (Garboczi et al., 1996) (H. Shen and P. J. B., unpublished data). HLA-E and HLA-G1 were refolded from inclusion bodies together with human β_2m (expressed in *E. coli* using a plasmid provided by Drs. D. N. Garboczi and D. C. Wiley) and the appropriate peptides (VMAPRTVLL for HLA-E [Braud et al., 1997] or MQPTHPIRL for HLA-G [Lee et al., 1995]). Refolded class I heterodimers were purified from aggregates and free β_2m by gel filtration chromatography using a Superdex 200 column.

HLA-Cw*0301 and HLA-Cw*0602 were provided by Dr. Jongsun Kim (Yonsei University College of Medicine, Seoul, Korea). These proteins were expressed in *E. coli* and refolded from inclusion bodies as described (Kim et al., 1997).

Soluble human FcRn (A. P. West and P. J. B., unpublished data), ZAG (Sánchez et al., 1999), and HFE (Lebrón et al., 1998) were expressed and purified (in the case of FcRn and HFE) or purified from human serum (in the case of ZAG) as described.

All of the classicial, nonclassical, and class I–like MHC molecules migrated in the expected positions on a gel filtration column and were at least 95% pure as judged by SDS-PAGE (data not shown). After immobilization on a biosensor chip (see below), the HLA-B, HLA-Cw, HLA-E, and HLA-G proteins were recognized by W6/32, a monoclonal antibody that binds to correctly folded classical and nonclassical class I heterodimers (Parham et al., 1979), and FcRn and HFE bind to their ligands (IgG and transferrin receptor, respectively) (A. P. West and P. J. B., unpublished data; Lebrón et al., 1998) (data not shown).

Expression and Purification of LIR-1 Proteins

D1-D4 was expressed in baculovirus-infected insect cells as described for UL18-HM. PCR was used to modify the cDNA encoding LIR-1 (gift of D. Cosman, Immunex) to introduce a stop codon and a 6x-His tag after the codon for His458 (numbered according to Cosman et al. [1997]; see our numbering scheme below). The modified gene, which encodes the hydrophobic leader sequence and residues 1 to 435 of the mature protein, was subcloned after sequencing into the baculovirus transfer vector pVL1393 (Pharmacia). D1-D4 was purified from supernatants of baculovirus-infected High 5 cells using Ni-NTA and gel filtration chromatography as described for HLA-Cw*0702. N-terminal sequence analysis yielded the sequence GHLPKPTLWAE; thus, the leader sequence was cleaved during the secretion process. In our numbering scheme, the N-terminal residue of the mature protein is residue 1; previous publications referred to this glycine as residue 24 (Cosman et al., 1997).

D1D2 (an initial methionine plus residues 1–197 of the mature protein) was expressed in *E. coli* strain BL21(DE3)pLysS using the expression vector pEt23a (Novagen). The protein was renatured from inclusion bodies as described (Garboczi et al., 1996). The N-terminal sequence of purified D1D2 was GHLPKPTLWAE, the same as that of D1-D4; thus, the methionine residue added to allow production inside *E. coli* was lost.

To prepare D1 and D2, 1 mg of D1D2 was incubated in 50 mM $NaHCO_3$ and 100 mM NaCl with 0.05 mg trypsin (Worthington Biochemical) at 37°C for 3 hr. Cleavage products were isolated on a Uno Q anion exchange column. Two peaks were recovered and identified as D1 and D2 by matrix-assisted, laser desorption, time-of-flight mass spectrometric analyses (molecular mass of D1, 11122.5 Da; molecular mass of D2, 7516.4 Da) and N-terminal sequencing (D1 sequence, GHLPKPTLWAE; D2 sequence, IKPTL SAQPPV) (data not shown). D1 begins at the first residue of D1D2 and is predicted from the mass spectrometry-derived molecular weight and the N-terminal sequence of D2 to end after residue 99, a tyrosine. (Cleavage after tyrosine is usually caused by chymotryptic activity in trypsin preparations.) D1 contains all of the first Ig-like domain and four residues of the second domain as defined by Cosman et al. (1997). D2 begins at residue 100 (an isoleucine) and ends at Arg-169, as determined from the mass spectrometry-derived molecular weight. No evidence of contamination with uncleaved D1D2 was found by either mass spectrometry or N-terminal sequence analyses of purified D1 or D2.

D3 and D3D4 were expressed in CHO cells as described for UL18-CC. Constructs encoding D3 (residues 198–295) or D3D4 (residues 198–396), each with a C-terminal 6x-His tag, were subcloned into a modified version of pBJ5-GS, which included the hydrophobic leader sequence from rat IgG2a upstream of the multiple cloning site (W. L. Martin, H. Shen, and P. J. B., unpublished data). Cell lines secreting D3 or D3D4 were identified after precipitation of transfected cell supernatants with Ni-NTA beads. D3 and D3D4 were purified as described for HLA-Cw*0702.

Far UV CD spectra of D1-D4, D1D2, D3D4, and D3 were similar and demonstrated that each fragment was folded and composed of mainly β-sheet secondary structure (data not shown). Transition midpoints (T_ms) derived from CD-monitored thermal denaturation curves ranged from 57°C to 71°C (data not shown), demonstrating that all fragments are folded.

CD Analyses

An AVIV 62A DS spectropolarimeter equipped with a thermoelectric cell holder was used for CD measurements. Samples containing 10 μM protein in 5 mM phosphate at pH 7 were used for wavelength scans (0.1 mm path length cell) and thermal denaturation curves (1.0 mm path length cell). Heat-induced unfolding of D1-D4, smaller LIR-1 fragments, or the various forms of UL18 were monitored by recording the CD signal at 223, while the sample temperature was raised from 25°C to 75°C at a rate of approximately 0.7°C/min. T_ms were determined by taking the maximum of a plot of $d\theta/dT$ versus T (where θ is ellipticity) after averaging the data with a moving window of five points.

Determination of D1-D4/UL18 Stoichiometry

Protein concentrations were determined spectrophotometrically at 280 nm using the following extinction coefficients: D1-D4, 43543 $M^{-1}cm^{-1}$; UL18-HM, 64951 $M^{-1}cm^{-1}$, derived as described (Lebrón et al., 1998). For determining the LIR-1/UL18 stoichiometry by gel filtration, molar ratios from 1:3 (300 pmol D1-D4:900 pmol UL18-HM) to 3:1 (900 pmol D1-D4:300 pmol UL18-HM) of D1-D4 and UL18-HM were incubated for 30 min at room temperature in 20 mM Tris (pH 7.4), 150 mM NaCl, and 0.05% NaN_3, in a total volume of 100 μl. Samples were injected onto a Superose 6 column (Pharmacia) and eluted with the same buffer at 0.5 ml/minute. The composition of each fraction was analyzed by SDS-PAGE (data not shown).

Sedimentation equilibrium analytical ultracentrifugation was performed with a Beckman Optima XL-A analytical ultracentrifuge, using data analysis software provided by the manufacturer. Separate solutions of D1-D4, UL18-HM, and D1-D4/UL18-HM, each at 0.6 mg/ml, were centrifuged for ≥36 hr at 20°C with a rotor speed of 10,000 rpm. Molecular masses were determined by nonlinear least squares fits of the equilibrium gradients (absorbance versus radius) using the model of single ideal species (Hansen et al., 1994), and partial specific volumes of 0.725 (D1-D4), 0.724 (UL18-HM), and 0.725 (D1-D4/UL18-HM), calculated from the amino acid composition and the carbohydrate content (Zamyatnin, 1972).

Biosensor-Based Affinity Measurements

A Biacore 2000 biosensor system (Pharmacia LKB Biotechnology) was used to assay interactions between UL18 or class I molecules and D1-D4 or fragments of LIR-1. Binding between a molecule coupled to a biosensor chip and a second molecule injected over the chip results in changes in the SPR signal that are read out in real time as resonance units (RU) (Karlsson and Fält, 1997). UL18, class I, D1-D4, or LIR-1 fragments were covalently immobilized at pH 5.5 on a CM5 chip (Pharmacia LKB Biotechnology) using standard amine coupling chemistry as described in the Biacore manual. Higher coupling densities were achieved by increasing the time of exposure of the protein solutions to the activated flowcell. Proteins were injected over coupled biosensor chips at room temperature in 50 mM PIPES (pH 7.0), 150 mM NaCl, and 0.005% Biacore surfactant P20. All samples were purified by size exclusion chromatography to minimize SPR signal resulting from aggregated protein. All injections were followed by an identical injection onto a mock-coupled flowcell or a flowcell coupled with an irrelevant protein in order to subtract out significant nonspecific responses.

Binding interactions between UL18 and all species of LIR-1 were assayed using short injection times (2–4 min) with fast flow rates (100 μl/min) over biosensor chips coupled to low densities (~100 RU) (kinetics-based approach). These conditions were chosen to minimize mass transport effects upon the kinetics of the binding reactions (Karlsson and Fält, 1997). Kinetic constants were derived from sensorgram data using BIAevaluation version 3.0, which simultaneously fits the association and dissociation phases of the sensorgrams and globally fits all curves in the working set. Sensorgrams were fit to a binding model that assumes a single class of noninteracting binding sites in a 1:1 binding interaction. Equilibrium dissociation constants (K_Ds) were derived from the ratios of rate constants (k_a and k_d) as $K_D = k_d/k_a$. For binding interactions involving class I proteins, HFE, FcRn, and ZAG, we derived K_Ds using an equilibrium-based approach that is not affected by mass transport effects. For these experiments, we used long injection times (15–40 min) with slow flow rates (5 μl/min) over biosensor chips coupled to high densities (1500–2000 RU), and the binding reactions were allowed to closely approach or to reach equilibrium. K_Ds were derived by nonlinear regression analysis of plots of R_{eq} (the equilibrium binding response) versus the log of the injected protein concentration, and the data were fit to a 1:1 binding model as described (Lebrón et al., 1998). Comparison of the kinetics-based versus equilibrium-based methods for determining K_Ds demonstrated that both methods yielded comparable values for the same binding interaction (Lebrón et al., 1998).

Expression of UL18, HLA-B*0702, HFE, and Domain-Swapped Proteins on the Surface of COS-7 Cells

Full-length cDNAs corresponding to wild-type UL18, HLA-B*0702, or HFE were subcloned into the expression vector PBJ5-GS (UL18 and HLA-B*0702) or PBJ1-neo (HFE). Genes encoding the following fusion proteins were prepared using PCR: α1α2UL18-α3HFE (UL18 hydrophobic leader sequence plus residues 1–188 fused to HFE residues 182–345); α1α2HFE-α3UL18 (HFE hydrophobic leader sequence plus residues 1–181 fused to UL18 residues 189–349); α1α2B7-α3HFE (HLA-B*0702 hydrophobic leader sequence plus residues 1–180 fused to HFE residues 182–345); and α1α2HFE-α3B7 (HFE hydrophobic leader sequence plus residues 1–181 fused to HLA-B*0702 residues 181–341). (The numbering system for HFE is from Lebrón et al. [1998]). Bridge PCR products were subcloned after sequencing into PBJ5-GS. The expression vectors were cotransfected into COS-7 cells (ATCC) with a human β_2m expression vector (Fahnestock et al., 1992) using a Superfect procedure (Qiagen). Transfected cells were maintained in α minimal essential medium (Irvine Scientific) supplemented with 5% dialyzed fetal bovine serum (GIBCO BRL), 2 mM glutamine, penicillin (100 U/ml), and streptomycin (100 μg/ml) for 48 hr, at which point protein expression was assayed by cell staining (see below).

Immunofluorescence

Transfected cells were washed three times with growth medium and twice with phosphate-buffered saline, 0.52 mM $MgCl_2$, and 0.9 mM $CaCl_2$ (PBS-MC). Cells were stained after fixing to increase the signal or stained live and then fixed to verify cell surface expression. For fixed cell staining, cells were incubated for 10 min in 2.5% (v/v) paraformaldehyde in PBS-MC and then washed twice with PBS-MC and once with PBS-MC containing 1% (w/v) BSA (BSA buffer). Live cells or fixed cells were incubated with primary antibody, D1-D4, or LIR-1 Fc (see below) in BSA buffer for 15–30 min on ice (live cells) or at room temperature (fixed cells) followed by two washes with PBS-MC and one wash with BSA buffer. Secondary antibody incubations were done in BSA buffer for 30 min at 4°C followed by three washes with PBS-MC. Live cells were fixed after staining in 100% methanol at −20°C for 15 min. Following staining, cells were mounted in Fluoromount (Southern Biotechnology Association) containing n-propyl gallate to reduce photobleaching and viewed in a Zeiss Axiophot fluorescent microscope. Images were recorded using software written by S. E. Fraser, J. Stollberg, and G. R. Belford (Biological Imaging Center, Caltech) on an Imaging Technology series 151 image processor. All experiments were repeated four times with similar results.

Expression was assayed by incubating transfected cells with a 1:10 dilution of a rabbit anti-UL18 antiserum (Chapman and Bjorkman, 1997; for wild-type UL18, α1α2UL18-α3HFE, or α1α2HFE-α3UL18) or 50 μl of 1:10 dilution of a rabbit anti-HFE antiserum (J. A. Lebrón and P. J. B., unpublished data; for wild-type HFE, α1α2B7-α3HFE, or α1α2HFE-α3B7) followed by labeling with 50 μl of a FITC-conjugated donkey anti-rabbit antiserum (15 μg/ml) (Jackson ImmunoResearch). HLA-B*0702 expression was assayed by staining with 50 μl FITC-labeled W6/32 (20 μg/ml) (Sigma), a mouse monoclonal antibody that recognizes human class I MHC molecules (Parham et

al., 1979). Untransfected cells were stained under equivalent conditions (data not shown).

For cells expressing wild-type UL18 or UL18 domains, D1-D4 binding was assayed by incubating transfected and nontransfected control cells with 50 μl of His-tagged D1-D4 (100 μg/ml), followed by addition of 50 μl of a murine anti-His-tag monoclonal antibody (20 μg/ml) (Qiagen) and then 50 μl of a Cy3-labeled donkey anti-mouse antiserum (3 μg/ml) (Jackson ImmunoResearch). For cells expressing wild-type HFE, wild-type B*0702, or B7 domains, D1-D4 binding was assayed by incubating with 50 μl of LIR-1 Fc (100 μg/ml) (gift of D. Cosman, Immunex) followed by 50 μl of Cy3-labeled goat anti-human IgG antiserum (3 μg/ml) (Jackson ImmunoResearch). (Results of staining fixed cells expressing UL18 and UL18-containing domains with the D1-D4 reagent are shown in Figure 4A. Equivalent results were obtained by staining with the LIR-1 Fc reagent; data not shown).

Acknowledgments

We thank P. M. Snow and I. Nangiana for assistance with protein expression, T. S. Ramalingam for helpful discussions and assistance with cell staining, D. Cosman, J. Kim, J. A. Lebrón , A. P. West, L. M. Sánchez, and H. Shen for protein samples, G. Hathaway and the Caltech PPMAL for peptide analyses, P. Poon for performing the analytical ultracentrifugation studies, and D. Cosman, B. Wilcox, and members of the Bjorkman laboratory for critical reading of the manuscript. This work was supported by a National Defense Science and Engineering Pre-Doctoral Fellowship (T. L. C.) and a grant from the Arthritis Foundation (P. J. B.).

Received August 19, 1999; revised September 29, 1999.

References

Bebbington, C.R., and Hentschel, C.C.G. (1987). The use of vectors based on gene amplification for the expression of cloned genes in mammalian cells. In DNA Cloning: A Practical Approach, D.M. Glover, ed. (Oxford: IRL Press), pp. 163–188.

Beck, S., and Barrell, B.G. (1988). Human cytomegalovirus encodes a glycoprotein homologous to MHC class I antigens. Nature *331*, 269–272.

Bjorkman, P.J., and Parham, P. (1990). Structure, function and diversity of class I major histocompatibility complex molecules. Annu. Rev. Biochem. *90*, 253–288.

Borges, L., Hsu, M.L., Fanger, N., Kubin, M., and Cosman, D. (1997). A family of human lymphoid and myeloid Ig-like receptors, some of which bind to MHC class I molecules. J. Immunol. *159*, 5192–5196.

Braud, V.M., Allan, D.S.J., Wilson, D., and McMichael, A.J. (1997). TAP- and tapasin-dependent HLA-E surface expression correlates with the binding of an MHC class I leader peptide. Curr. Biol. *8*, 1–10.

Browne, H., Smith, G., Beck, S., and Minson, T. (1990). A complex between the MHC class I homologue encloded by human cytomegalovirus and β2 microglobulin. Nature *347*, 770–772.

Chapman, T.L., and Bjorkman, P.J. (1998). Characterization of a murine cytomegalovirus class I MHC homolog: comparison to MHC molecules and to the human cytomegalovirus MHC homolog. J. Virol. *72*, 460–466.

Colonna, M., Navarro, F., Bellon, T., Llano, M., Garcia, P., Samaridis, J., Angman, L., Cella, M., and Lopez-Botet, M. (1997). A common inhibitory receptor for major histocompatibility complex class I molecules on human lymphoid and myelomonocytic cells. J. Exp. Med. *186*, 1809–1818.

Cosman, D., Fanger, N., Borges, L., Kubin, M., Chin, W., Peterson, L., and Hsu, M.-L. (1997). A novel immunoglobulin superfamily receptor for cellular and viral MHC class I molecules. Immunity *7*, 273–282.

Davis, S.J., Michael, J., Puklavec, D.A., Ashford, K.H., Jones, E.Y., Stuart, D.I., and Williams, A.F. (1993). Expression of soluble recombinant glycoproteins with predefined glycosylation: application to the crystallization of the T-cell glycoprotein CD2. Protein Eng. *6*, 229–232.

Fahnestock, M.L., Tamir, I., Narhi, L., and Bjorkman, P.J. (1992). Thermal stability comparison of purified empty and peptide filled forms of a class I MHC molecule. Science *258*, 1658–1662.

Fahnestock, M.L., Johnson, J.L., Feldman, R.M.R., Neveu, J.M., Lane, W.S., and Bjorkman, P.J. (1995). The MHC class I homolog encoded by human cytomegalovirus binds endogenous peptides. Immunity *3*, 583–590.

Fan, Q.R., Mosyak, L., Winter, C.C., Wagtmann, N., Long, E.O., and Wiley, D.C. (1997). Structure of the inhibitory receptor for human natural killer cells resembles haematopoietic receptors. Nature *389*, 96–100.

Fanger, N.A., Cosman, D., Peterson, L., Braddy, S.C., Maliszewski, C.R., and Borges, L. (1998). The MHC class I binding proteins LIR-1 and LIR-2 inhibit Fc receptor-mediated signaling in monocytes. Eur. J. Immunol. *28*, 3423–3434.

Garboczi, D.N., Ursula, U., Ghosh, P., Seth, A., Kim, J., VanTienhoven, E.A.E., Biddison, W.E., and Wiley, D.C. (1996). Assembly, specific binding, and crystallization of a human TCR-αβ with an antigenic tax peptide from human T lymphotropic virus type 1 and the class I MHC molecule HLA-A2. J. Immunol. *157*, 5403–5410.

Hansen, J.C., Lebowitz, J., and Demeler, B. (1994). Analytical ultracentrifugation of complex macromolecular systems. Biochemistry *33*, 13155–13163.

Jenkins, N., Parekh, R.B., and James, D.C. (1996). Getting the glycosylation right—implications for the biotechnology industry. Nat. Biotech. *14*, 975–981.

Karlsson, R., and Fält, A. (1997). Experimental design for kinetic analysis of protein-protein interactions with surface plasmon resonance biosensors. J. Immunol. Methods *200*, 121–133.

Kim, J., Chwae, Y.J., Kim, M.Y., Choi, I.H., Park, J.H., and Kim, S.J. (1997). Molecular basis of HLA-C recognition by p58 natural killer cell inhibitory receptors. J. Immunol. *159*, 3875–3882.

Kuziemko, G.M., Stroh, M., and Stevens, R.C. (1996). Cholera Toxin binding affinity and specificity for gangliosides determined by surface plasmon resonance. Biochemistry *35*, 6375–6384.

Lanier, L.L., Corliss, B., and Phillips, J.H. (1997). Arousal and inhibition of human NK cells. Immunol. Rev. *155*, 145–154.

Leahy, D.J. (1995). A structural view of CD4 and CD8. FASEB J. *9*, 17–25.

Lebrón, J.A., Bennett, M.J., Vaughn, D.E., Chirino, A.J., Snow, P.M., Mintier, G.A., Feder, J.N., and Bjorkman, P.J. (1998). Crystal structure of the hemochromatosis protein HFE and characterization of its interaction with transferrin receptor. Cell *93*, 111–123.

Lee, N., Malacko, A.R., Ishitani, A., Chen, M.C., Bajorath, J., Marquardt, H., and Geraghty, D.E. (1995). The membrane-bound and soluble forms of HLA-G bind identical sets of endogenous peptides but differ with respect to TAP association. Immunity *3*, 591–600.

Leong, C.C., Chapman, T.L., Bjorkman, P.J., Formankova, D., Mocarski, E.S., Phillips, J.H., and Lanier, L.L. (1998). Modulation of natural killer cell cytotoxicity in human cytomegalovirus infection: the role of endogenous class I major histocompatibility complex and a viral class I homolog. J. Exp. Med. *187*, 1681–1687.

Navarro, F., Llano, M., Bellon, T., Colonna, M., Geraghty, D.E., and Lopez-Botet, M. (1999). The ILT2(LIR1) and CD94/NKG2A NK cell receptors respectively recognize HLA-G1 and HLA-E molecules co-expressed on target cells. Eur. J. Immunol *29*, 277–283.

Parham, P., Barnstable, C.J., and Bodmer, W.F. (1979). Use of a monoclonal antibody (W6/32) in structural studies of HLA-A,B,C Antigens. J. Immunol. *123*, 342–349.

Parham, P., Androlewicz, M.J., Holmes, N.J., and Rothenberg, B.E. (1983). Arginine-45 is a major part of the determinant of human β2-microglobulin recognized by mouse monoclonal antibody BBM.1. J. Biol. Chem. *258*, 6179–6186.

Raghavan, M., Lebrón, J.A., Johnson, J.L., and Bjorkman, P.J. (1996). Extended repertoire of permissible peptide ligands for HLA-B*2702. Prot. Sci. *5*, 2080–2088.

Sánchez, L.M., Chirino, A.J., and Bjorkman, P.J. (1999). Crystal structure of human ZAG, a fat-depleting factor related to MHC molecules. Science *283*, 1914–1919.

Sidney, J., Del Guercio, M.F., Southwood, S., Engelhard, V.H., Appella, E., Rammensee, H.G., Falk, K., Rotzchke, O., Takiguchi, M., Kubo, R.T., et al. (1995). Several HLA alleles share overlapping peptide specificities. J. Immunol. *154*, 247–259.

Valés-Gómez, M., Reyburn, H.T., Mandelboim, M., and Strominger, J.L. (1998). Kinetics of interaction of HLA-C ligands with natural killer cell inhibitory receptors (erratum). Immunity *9*, U9–U9.

Vitale, M., Castriconi, R., Parolini, S., Pende, D., Hsu, M.L., Moretta, L., Cosman, D., and Moretta, A. (1999). The leukocyte Ig-like receptor (LIR)-1 for the cytomegalovirus UL18 protein displays a broad specificity for different HLA class I alleles: analysis of LIR-1 + NK cell clones. Int. Immunol. *11*, 29–35.

Wentworth, B.B., and Alexander, E.R. (1971). Seroepidemiology of infectious due to members of the herpesvirus group. Am. J. Epidemiol. *94*, 496–507.

Wiertz, E., Hill, A., Tortorella, D., and Ploegh, H. (1997). Cytomegaloviruses use multiple mechanisms to elude the host immune response. Immunol. Lett. *57*, 213–216.

Wiley, D. (1988). MHC gene in cytomegalovirus. Nature *331*, 209–210.

Zamyatnin, A.A. (1972). Protein volume in solution. Prog. Biophys. Mol. Biol. *24*, 107–123.

Chapter 5:

Does the UL18/LIR-1 Interaction Augment HCMV Infection?

In this chapter I discuss the results of experiments I performed prior to the time the UL18 ligand was identified and discuss the biological implications of the high affinity UL18/LIR-1 interaction.

Chapter 5

1. UL18 is Not Expressed on the Surface of Class I-Null Cells

It was proposed by Fahnestock et al. (1995) that UL18 expression could protect HCMV-infected cells that had down-regulated surface class I MHC expression from lysis by NK cells by engaging NK cell inhibitory receptors (Fahnestock et al., 1995). In collaboration with Dr. Lewis Lanier at DNAX (currently University of California, San Francisco) we sought to address this proposal by expressing UL18 in an HLA-A, -B, -C null lymphoblastoid line (721.221) (Shimizu and DeMars, 1989) followed by incubation with NK cells to determine whether UL18 would indeed provide protection against NK cell lysis.

Three UL18 expression vectors were prepared for transfection of 721.221 cells: full length UL18, UL18 in which the transmembrane and cytoplasmic domains were replaced with a glycosylphosphatidylinositol anchor, and UL18 in which the transmembrane and cytoplasmic domains were replaced by the transmembrane and cytoplasmic domain of HLA-A2. 721.211 cells were electroporated with each of these constructs along with a vector for ß2m and transfectants that had taken up the UL18-containing vector were selected using neomycin and established protocols (Soderstrom et al., 1997). I used a PCR assay (Burden and Whitney, 1995) to verify the presence of the UL18 gene in the genome of transfectants (data not shown). Cells that were positive

for the UL18 gene by PCR were screened for cell surface expression of UL18 by flow cytometry using an anti-UL18 monoclonal antibody that I generated (Chapman and Bjorkman, 1997). I did not detect UL18 on the surface of cells transfected with any of the three forms of UL18 after screening ~20 different clones of each. I also tried screening transfectants using BBM.1, a monoclonal antibody that recognizes human ß2m (Parham et al., 1983), assuming that expression of UL18 at the cell surface might

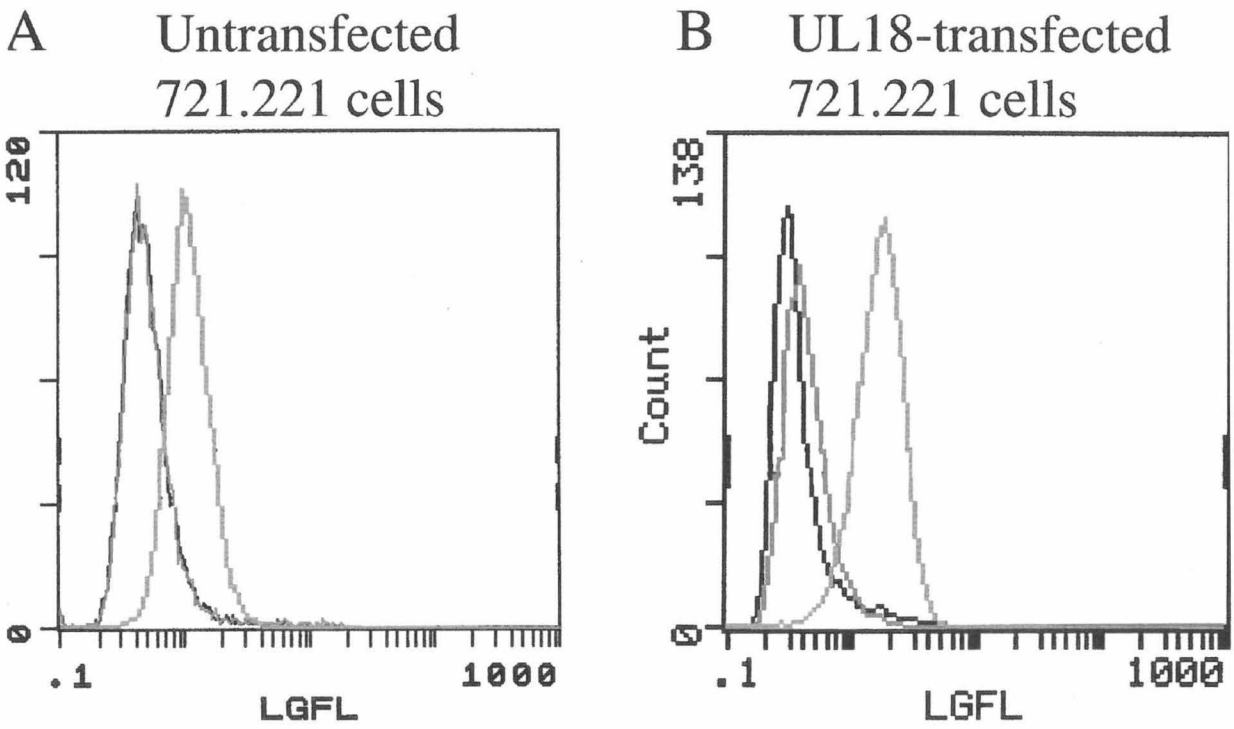

Figure 5-1. FACS plots showing (A) a non-transfected 721.221 cell stained with a control IgG (black), an anti-UL18 antibody, 10C7 (red) and anti-ß2m, BBM.1 (blue) and (B) a UL18-transfected cell stained with a control IgG (black), an anti-UL18 antibody, 10C7 (red) and anti-ß2m BBM.1 (blue). Although the UL18-transfected cells stain more brightly with BBM.1 than the non-transfected cells, UL18 is not being expressed on the cell surface as is evidenced by the fact that these cells are not stained by 10C7.

increase the amount of cell surface ß2m. Representative results using the anti-UL18 and anti-ß2m monoclonal antibodies are shown in Figure 5-1. As can be seen, there is a small increase in the level of ß2m surface expression in transfected compared with untransfected cells, but this increase is not due to UL18 surface expression since the cells do not stain with anti-UL18. Brian Corliss, a technician in Dr. Lanier's lab, also transfected 721.221 cells with a UL18 expression vector and was unable to detect surface expression, and Peter Cresswell's laboratory was unable to detect UL18 at the surface of transfected 721.221 cells (P. Cresswell, personal communication to Pamela Bjorkman). We therefore conclude that UL18 does not get to the surface of 721.221 cells, which may indicate that other viral proteins are required for cell surface expression of UL18. However, even HCMV infected cells express only low levels of UL18, with most of the protein remaining intracellular (Leong et al., 1998).

After we completed these studies, Reyburn et al. published a paper claiming that UL18 expression protected 721.221 cells from NK cell-mediated lysis (Reyburn et al., 1997). They transfected 721.221 cells with a UL18 expression vector, isolated stable transfectants after a drug selection and sorted for cells expressing increased levels of ß2m using BBM.1. They found marginal increases in ß2m expression (Figure 5-2), comparable to the increases that we observed on cells that did not stain with the anti-UL18 monoclonal antibody (Figure 5-1). As discussed above, BBM.1 binding is an indirect means of detecting UL18 since BBM1 recognizes ß2m, which could be

associated with class I MHC molecules that are induced during the selection procedure. Indeed, subsequent data have shown that 721.221 cells express the nonclassical class I MHC molecule, HLA-E, which is a ligand for the CD94/NKG2A inhibitory receptor (Braud et al., 1998). Although the HLA-E is normally intracellular in 721.211 cells, it can be expressed on the cell surface if provided with a proper peptide (typically a peptide derived from a class I MHC signal sequence) (Long, 1998). As Reyburn et al. were only screening for the presence of a molecule that associated with ß2m, it is quite possible that the cells they isolated were HLA-E^+ (HLA-E associates with ß2m)

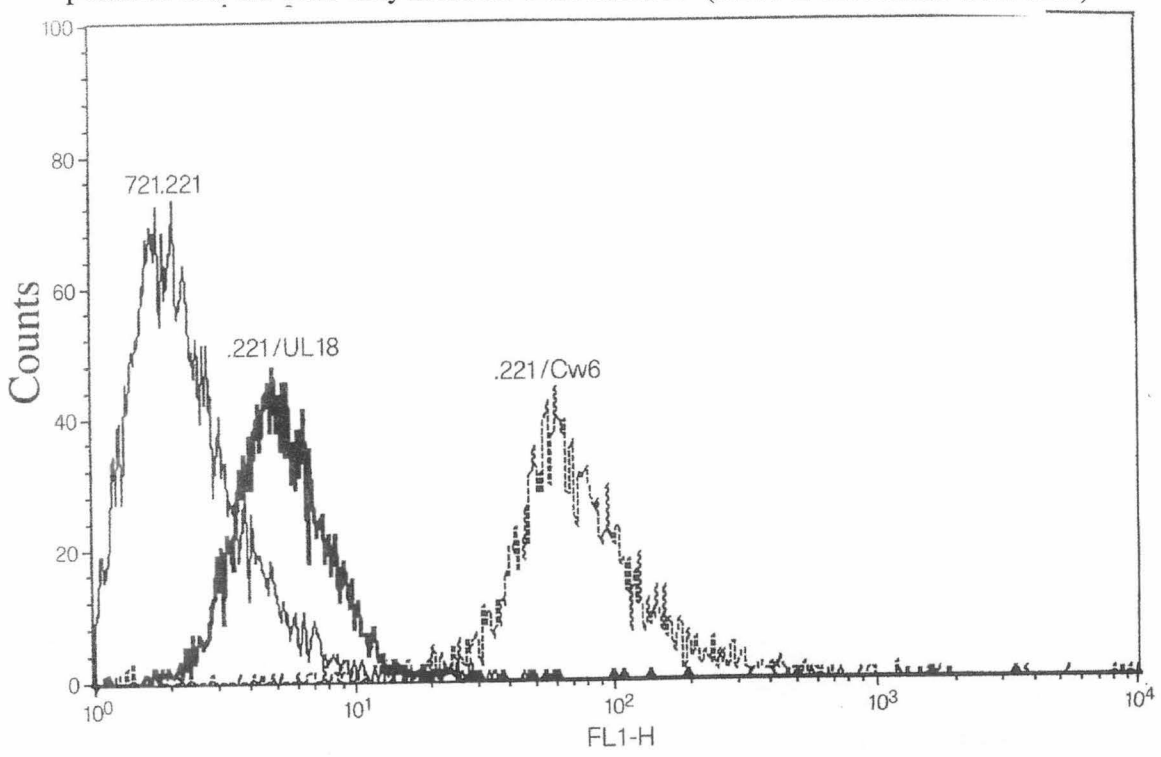

Figure 5-2. FACS plot published by Reyburn et al. (1997) showing BBM.1 (anti-ß2m) staining of non-transfected 721.221 cells (721.221), UL18-transfected 721.221 cells (.221/UL18) and HLA-Cw6 (an MHC class I molecule)-transfected 721-221 cells (.221/Cw6). Reyburn et al. conclude that UL18 is being expressed on the surface of the UL18-transfected cells on the basis of the increase in BBM.1 staining.

as opposed to UL18$^+$, and that they were selecting for cells that express increased levels of HLA-E by sorting for BBM1+ cells. This would correlate with the finding that their observed protection from lysis could be inhibited by an antibody against CD94 (Reyburn et al., 1997). The only direct evidence Reyburn et al. provide of UL18 expression in

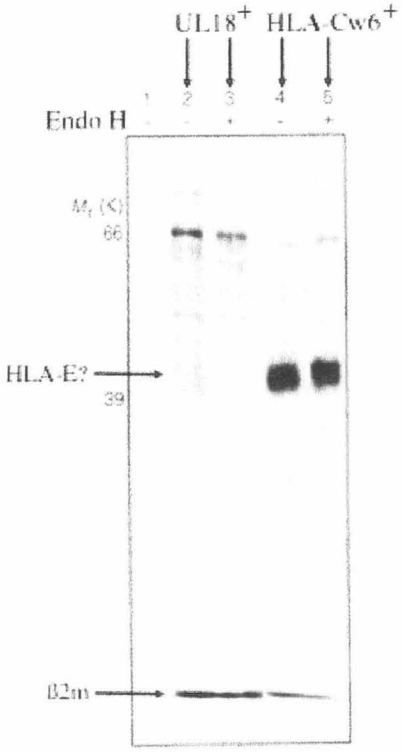

Figure 5-3. UL18-transfected and HLA-Cw6-transfected 721.221 cells were biotinylated and immunoprecipitated with BBM.1. This gel is taken from (Reyburn et al., 1997). The biotinylated proteins were visualized with avidin-ECL after SDS-PAGE immunoblotting. Reyburn et al. claim that the 66 kDa protein in lanes 2 and 3 represents UL18; however, the band is much more compact than would be expected for a protein with 13 potential N-linked glycosylation sites. In addition, this band also appears in lanes 4 and 5 that were derived from the lysates of cells transfected with HLA-Cw6. We suspect that this band is bovine serum albumin, an abundant protein in the serum used to culture 721.221 cells. A faint band at approximately 43 kDa can be seen in the UL18-transfected lanes that may be HLA-E. 721.221 cells express HLA-E and as it associates with ß2m it is likely to be coprecipitated with the ß2m brought down by the BBM.1 antibody. The +/- indicators at the top of the gel indicate whether the proteins have been treated with Endo H.

721.221 cells is an SDS-PAGE gel showing the results of a BBM.1 immunoprecipitation of biotinylated 721.221 cells (Figure 5-3). In the lanes derived from $UL18^{+}$ transfectants, there is a band corresponding to ß2m and another that migrates at ~66 kDa which they claim to be UL18. The 66 kDa protein migrates as a tight band, which seems unlikely for a protein with 13 potential N-linked glycosylation sites. (See for comparison SDS-PAGE gels containing UL18 on pages 40 and 59 and the migration profile of HLA-Cw6 (one potential N-linked glycosylation site) in lanes 4 and 5 of Figure 5-3 as compared to ß2m (no N-linked glycosylation sites)). We note also that the 66 kDa band appears in other lanes of the gel, which are immunoprecipitations of non-UL18 transfected cells. We suspect that the 66 kDa band is biotinylated bovine serum albumin (MW 66.2 kD), a protein that is abundant in the media used for culturing 721.221 cells and that tends to stick to other proteins. We sent our anti-UL18 monoclonal antibody to these authors in April of 1998, but have yet to hear whether they achieved staining with our antibody. In the absence of that result, we believe that there is no evidence that UL18 is expressed at the surface of 721.221 cells, nor that it confers protection to 721.221 cells from NK lysis or interacts with CD94/NKG2A

2. UL18 Confers Susceptibility to, Rather Than Protection From, NK Cell Lysis

Subsequent studies by Leong et al. ((Leong et al., 1998), see appendix B) question the importance of UL18 in protection of infected cells from NK cell killing. In these studies, UL18 was expressed and class I MHC molecules were down-regulated in the course of HCMV infection, rather than expressing UL18 in class I-null cells. Fibroblasts were infected with wildtype HCMV and an HCMV mutant in which the UL18 gene had been deleted and NK cell lysis of the two types of infected cells was compared. In these experiments UL18 expression did not provide protection from NK cell lysis, rather it seemed to enhance NK cell-mediated killing. Fibroblasts infected with wild type HCMV (AD169) were found to be more susceptible to NK cell killing than fibroblasts infected with virus in which UL18 had been deleted (Δ18). In addition, UL18 expression on 293EBV, COS-7 and CHO-K1 cells rendered these cells more susceptible to NK cell-mediated lysis than non-UL18 expressing cells. UL18 is transcribed late in the HCMV replication cycle, at a time when virus should be nearly mature. One possible benefit of making UL18-expressing cells more susceptible to lysis would be to facilitate release of virus.

3. NK Cell Susceptibility: More a Function of Adhesion Molecule Up-regulation than Class I MHC Down-regulation?

While fibroblasts infected with mutant HCMV in which UL18 had been deleted (Δ18) were less susceptible to NK cell lysis than those infected with AD169, both infected populations were more susceptible to lysis than non infected fibroblasts. Using antibodies against adhesion/costimulatory molecules, Leong et al. (1998) observed that intracellular adhesion molecule (ICAM) 1 was up-regulated in virally infected cells. Lysis of infected fibroblasts could be prevented by blocking ICAM-1 from interacting with its ligand, lymphocyte function-associated antigen (LFA)-1ß. These results suggest that adhesion molecule up-regulation, more than MHC class I down-regulation, determines whether an infected cell is susceptible to NK cell lysis.

The importance of adhesion molecules in determining the susceptibility of CMV-infected cells to NK cell lysis is emphasized by Fletcher et al. (1998). Using seven different CMV strains and several different cell types, the authors demonstrate that susceptibility to lysis correlates with surface levels of LFA-3, not with surface levels of class I MHC molecules. CMV strains AD169, C1F and R7 up-regulated LFA-3 and were lysed while strains Towne, Toledo, Davis and C1FE down-regulated LFA-3 and were resistant to lysis. Expression levels of class I MHC molecules were down-regulated to a similar extent by all viruses. These studies suggest that class I MHC

down-regulation does not affect NK cell lysis of CMV-infected cells and that UL18 is not a factor in protecting those cells at risk of lysis.

Instead of directly modulating the anti-viral NK cell response, my work and work by others suggest that UL18 may be important in regulating the activation state of monocytes, B cells and dendritic cells by either masking or enhancing LIR-1 signaling. By masking LIR-1 signaling, UL18 could decrease the activation threshold of LIR-1-expressing cells making immune effector functions (e.g., cytokine secretion, cytolytic activity) more likely and potentially increasing the likelihood of CMV reactivation. In contrast, by enhancing LIR-1 signaling, UL18 could increase the activation threshold of LIR-1 expressing cells making immune effector functions and CMV reactivation less likely. The high affinity of UL18 for LIR-1 provides an example of a viral protein that can effectively compete with host proteins to subvert the host immune response.

4. References

Braud, V. M., Allan, D. S., O'Callaghan, C. A., Soderstrom, K., D'Andrea, A., Ogg, G. S., Lazetic, S., Young, N. T., Bell, J. I., Phillips, J. H., Lanier, L. L., and McMichael, A. J. (1998). HLA-E binds to natural killer cell receptors CD94/NKG2A, B and C. Nature *391*, 795-799.

Burden, D. W., and Whitney, D. (1995). Biotechnology: Proteins to PCR: A Course in Strategies and Lab Techniques (Toronto: Springer Verlag).

Chapman, T. L., and Bjorkman, P. J. (1997). Characterization of a murine cytomegalovirus class I MHC homolog: Comparison to MHC molecules and to the human cytomegalovirus MHC homolog. J. Virol., in press.

Fahnestock, M. L., Johnson, J. L., Feldman, R. M. R., Neveu, J. M., Lane, W. S., and Bjorkman, P. J. (1995). The MHC class I homolog encoded by human cytomegalovirus binds endogenous peptides. Immunity *3*, 583-590.

Leong, C. C., Chapman, T. L., Bjorkman, P. J., Formankova, D., Mocarski, E. S., Phillips, J. H., and Lanier, L. L. (1998). Modulation of natural killer cell cytotoxicity in human cytomegalovirus infection: the role of endogenous class I major histocompatibility complex and a viral class I homolog. J. Exp. Med. *187*, 1681-1687.

Long, E. O. (1998). Signal sequences stop killer cells. Nature *391*, 741-743.

Parham, P., Androlewicz, M. J., Holmes, N. J., and Rothenberg, B. E. (1983). Arginine-45 is a major part of the determinant of human ß2-microglobulin recognized by mouse monoclonal antibody BBM.1. J. Biol. Chem. *258*, 6179-6186.

Reyburn, H. T., Mandelboim, O., Valez-Gomez, M., Davis, D. M., Pazmany, L., and Strominger, J. L. (1997). The class I MHC homologue of human cytomegalovirus inhibits attack by natural killer cells. Nature *386*, 514-519.

Shimizu, Y., and DeMars, R. (1989). Production of human cells expressing individual transferred HLA-A,-B,-C genes using an HLA-A,-B,-C null human cell line. J. Immunol. *142*, 3320-3328.

Soderstrom, K., Corliss, B., Lanier, L. L., and Phillips, J. H. (1997). CD94/NKG2 is the predominant inhibitory receptor involved in recognition of HLA-G by decidual and peripheral blood NK cells. J. Immunol. *159*, 1072-1075.

Chapter 6:

LIR-1 D1D2 Structure

In this chapter I discuss the preliminary structure for LIR-1 D1D2. Dr. Anthony West guided me through data collection, data processing and solving the structure.

Chapter 6

1. Expression, Purification and Crystallization of D1D2

Domains 1 and 2 (D1D2) of LIR-1 were expressed in *E. Coli* and purified as described in Chapter 4. Crystals (space group $P4_12_12$; a = 68.3 Å, b = 68.3 Å, c=129.7 Å, one molecule per asymmetric unit) of D1D2 were grown in 1:1 hanging drops D1D2 (8 mg/ml) and 0.7 M potassium sodium tartrate, 0.1 M tris chloride (pH 8.5) then improved by microseeding. Crystals were soaked 30 seconds to 5 minutes in a cryoprotectant containing 20% ethylene glycol, 0.7 M potassium sodium tartrate and 0.1 M tris chloride (pH 8.5).

2. Data Collection

Data were collected at -150°C from a single crystal to 2.1Å using a Quantum CCD Research detector at the Stanford Synchrotron Radiation Laboratory beamline 9-2. Data were processed and scaled using DENZO and SCALEPACK (Otwinowski and Minor, 1997) (Table 6-1).

3. Structure Determination

A preliminary structure was determined by molecular replacement using AmoRe (Figure 6-1) (Navaza, 1994). Cross-rotation and -translation functions (20-3.0Å) using individual

domains of the 1.7Å structure of KIR2DL1 (Fan et al., 1997) (PDB code 1NKR with nonconserved side chains truncated to alanine, residues 1-6, 54-59 and 80-91 omitted) as a search model yielded a solution.

Table 6-1. Data Collection Statistics	
Unit cell dimensions	
a, b, c (Å)	68.3, 68.3, 129.7
Space group	$P4_12_12$
Temperature (°C)	-150
Data Processing	
Resolution (Å)	20-2.1 (2.15-2.07)
Completeness (%)	99.5 (99.4)
I/σ	18.8 (4.7)
R_{sym}, %	6.0 (29.7)

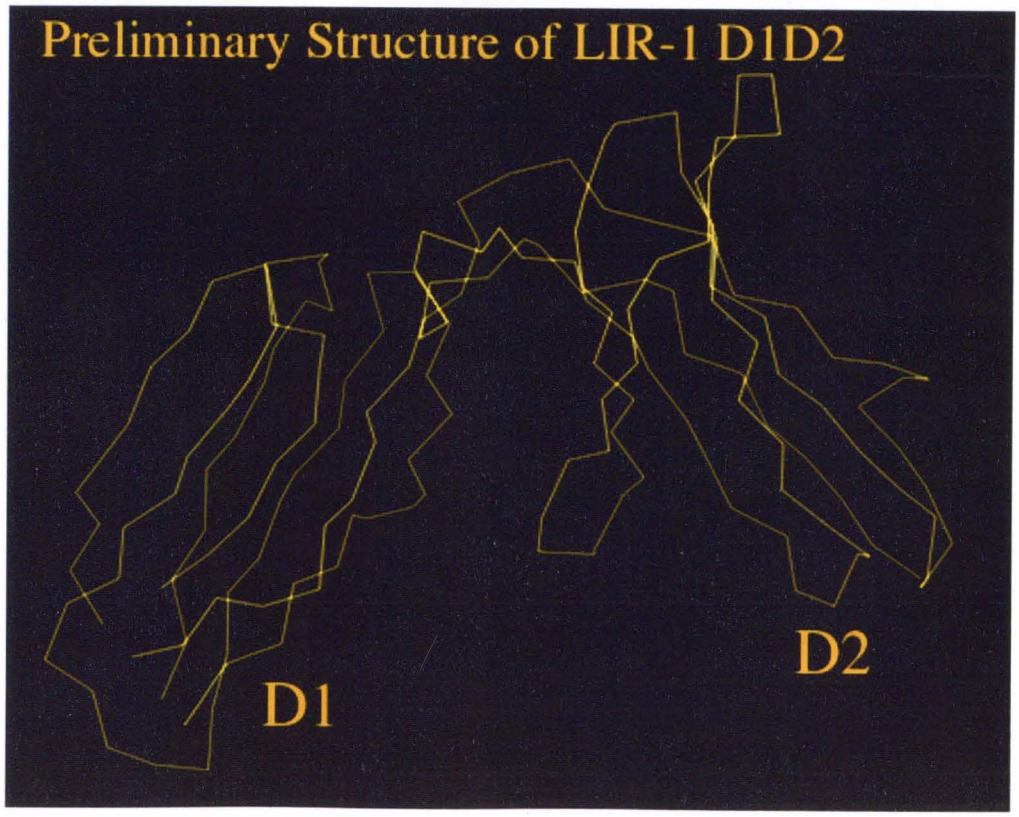

Figure 6-1. Preliminary Structure of LIR-1 D1D2.

4. Structure of LIR-1 D1D2

The overall structure of LIR-1 D1D2 is similar to that of the p58 KIRs (Figure 6-2) (Fan et al., 1997; Maenaka et al., 1999; Snyder et al., 1999) in that both structures are composed of two domains resembling Ig-like domains containing two antiparallel beta-sheets. In Chapter 4 we proposed that D1 and D2 would be in an extended conformation due to our ability to express individual domains stably; however, the D1D2 structure reveals that the two domains are bent with respect to one another. The angle between two domains is defined as the angle between the major axes of the domains and is specified as the elbow angle (Fan et al., 1997). The elbow angle between KIR domains varies from 60° to 80° (Fan et al., 1997; Snyder et al., 1999) with conserved residues Leu-17, Met-69, Val-100, Ile-101, Thr-102, His-138, Phe-178, Ser-180, Pro-185, Tyr-186 and Trp-188 being integral in stabilizing the domain interface. The elbow angle between D1 and D2 of LIR-1 is similar to the 80° angle of the KIR2DL2 (Figure 6-2), and of the 11 conserved residues listed above that have been shown to be located in the KIR D1/D2 interface, only 5 (Val-100, Thr-102, Pro-185, Tyr-186 and Trp-188) are conserved in the LIR-1 D1D2 sequence.

5. Residues Involved in Ligand Binding

KIR residues important in MHC class I recognition include 44, 45, 70, and 183 (Maenaka et al., 1999). These residues are all located in the hinge region between D1 and D2 (Figure 6-3, next page).

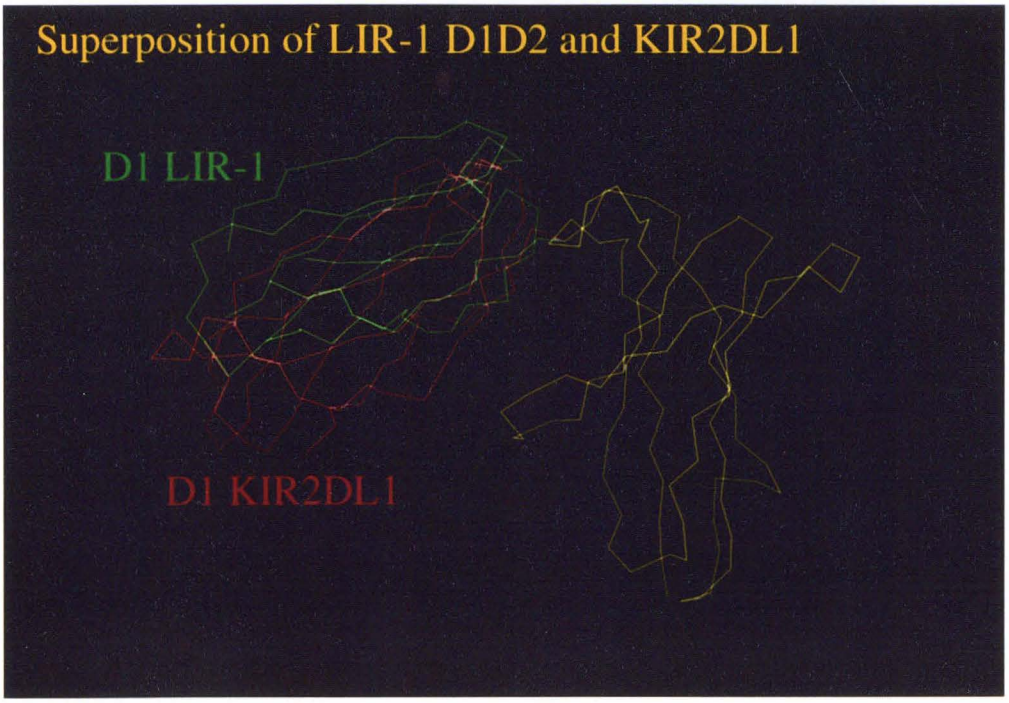

Figure 6-2. Superposition of the KIR2DL1 Structure on the LIR-1 D1D2 Structure.

Sequence comparisons between LIR family members and characterization of site-directed mutants (A. P. Heikema, T. L. Chapman and P. J. Bjorkman, unpublished results) suggest that the MHC class I binding site on LIR-1 includes residues Tyr-76, Asp-80 and Arg-84. These residues are located in near the tip of LIR-1 D1 (Figure 6-3, next page) suggesting

that despite the structural similarity between LIR-1 D1D2 and the p58 KIRs, different regions of the two molecules are responsible for ligand binding.

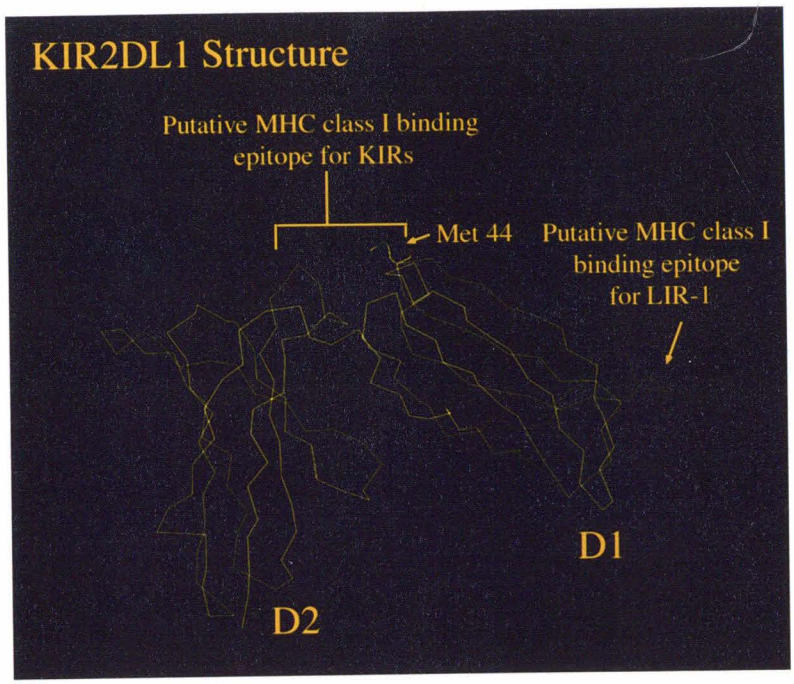

Figure 6-3. Regions Involved in MHC Class I Binding. Residues involved in MHC class I recognition by p58 KIRs are shown in comparison to residues involved in MHC class I recognition by LIR-1.

6. References

Fan, Q. R., Mosyak, L., Winter, C. C., Wagtmann, N., Long, E. O., and Wiley, D. C. (1997). Structure of the inhibitory receptor for human natural killer cells resembles haematopoietic receptors. Nature *389*, 96-100.

Maenaka, K., Juji, T., Stuart, D. I., and Jones, E. Y. (1999). Crystal structure of the human p58 killer cell inhibitory receptor (KIR2DL3) specific for HLA-Cw3-related MHC class I. Structure *7*, 391-398.

Navaza, J. (1994). AMORE- An automated package for molecular replacement. Acta Cryst. *A50*, 157-163.

Otwinowski, Z., and Minor, W. (1997). Processing of X-ray diffraction data collected in oscillation mode. Meth. Enzymol. *276*, 307-326.

Snyder, G. A., Brooks, A. G., and Sun, P. D. (1999). Crystal structure of the HLA-Cw3 allotype-specific killer cell inhibitory receptor KIR2DL2. Proc. Natl. Acad. Sci. U. S. A. *96*, 3864-3869.

Appendix A:

Modulation of Natural Killer Cell Cytotoxicity in Human Cytomegalovirus Infection: the Role of Endogenous Class I Major Histocompatibility Complex and a Viral Class I Homolog.

This paper describes studies done in collaboration with Dr. Lewis Lanier's lab at DNAX and Dr. Ed Mocarski's lab at Stanford to show that surface UL18 expression does not protect cells from NK cell-mediated lysis. My contributions include determination that 721.221 cells cannot be used for stable transfection of UL18, generation of UL18-producing CHO-K1 cells and generation of a UL18-specific antibody.

Modulation of Natural Killer Cell Cytotoxicity in Human Cytomegalovirus Infection: The Role of Endogenous Class I Major Histocompatibility Complex and a Viral Class I Homolog

By Clement C. Leong,* Tara L. Chapman,‡ Pamela J. Bjorkman,‡ Danuska Formankova,§ Edward S. Mocarski,§ Joseph H. Phillips,* and Lewis L. Lanier*

*From the *Department of Immunobiology, DNAX Institute of Molecular and Cell Biology, Palo Alto, California 94304; the ‡Division of Biology 156-29 and Howard Hughes Medical Institute, California Institute of Technology, Pasadena, California 91125; and the §Department of Microbiology and Immunology, Stanford University, Stanford, California 94305*

Summary

Natural killer (NK) cells have been implicated in early immune responses against certain viruses, including cytomegalovirus (CMV). CMV causes downregulation of class I major histocompatibility complex (MHC) expression in infected cells; however, it has been proposed that a class I MHC homolog encoded by CMV, UL18, may act as a surrogate ligand to prevent NK cell lysis of CMV-infected cells. In this study, we examined the role of UL18 in NK cell recognition and lysis using fibroblasts infected with either wild-type or UL18 knockout CMV virus, and by using cell lines transfected with the UL18 gene. In both systems, the expression of UL18 resulted in the enhanced killing of target cells. We also show that the enhanced killing is due to both UL18-dependent and -independent mechanisms, and that the killer cell inhibitory receptors (KIRs) and CD94/NKG2A inhibitory receptors for MHC class I do not play a role in affecting susceptibility of CMV-infected fibroblasts to NK cell–mediated cytotoxicity.

Key words: cytomegalovirus • class I major histocompatibility complex • UL18 • natural killer cell • cytotoxicity

Human cytomegalovirus (hCMV)[1] is an extremely widespread infectious agent. Healthy individuals acquiring hCMV postnatally are usually asymptomatic, although the virus persists in the host for life (1). Both T and NK cells play a critical role in controlling the initial infection and the disease that follows viral reactivation in immunocompromised individuals (2, 3). The importance of NK cells is highlighted by the fact that patients with an NK cell deficiency are extremely susceptible to hCMV infection and its associated diseases (4). In addition, NK cells also play an important role in the control of mouse CMV (5). Strain-dependent mouse CMV resistance or susceptibility has been mapped to the NK complex (NKC) region of murine chromosome 6 (6). The NKC region contains genes involved in modulating murine NK cell functions and codes for molecules that can trigger (NKR-P1) or inhibit (Ly49) NK cell–mediated cytotoxicity (7). Murine Ly49 molecules and their human functional counterparts, the KIRs (killer cell inhibitory receptors) and CD94/NKG2A receptors, inhibit NK cell cytotoxicity after cognate interaction with class I MHC molecules (8). Since many viruses downregulate host cell class I MHC expression upon infection, the hypothesis that NK cell inhibitory receptors serve as a physiological means to monitor for viral infection is compelling.

Both human (9) and mouse CMV (10) encode glycoproteins with homology to class I MHC heavy chains, designated UL18 (human) and M144 (mouse), respectively. It has been suggested that these molecules serve as surrogates for class I MHC molecules to engage inhibitory NK cell class I MHC receptors. In support of this hypothesis, Farrel et al. (10) have shown that mouse CMV lacking the M144 gene is more virulent in vivo. Transfection studies using the human CMV UL18 gene have implicated this protein

[1]*Abbreviations used in this paper:* β_2M, β_2-microglobulin; CHO, Chinese hamster ovary; cIg, control Ig; hCMV, human cytomegalovirus; HFF, human foreskin fibroblasts; ICAM-1, intracellular adhesion molecule 1; KIR, killer cell inhibitory receptor; MOI, multiplicity of infection.

 J. Exp. Med. © The Rockefeller University Press • 0022-1007/98/05/1681/07 $2.00
Volume 187, Number 10, May 18, 1998 1681–1687
http://www.jem.org

in the protection of B lymphoblastoid cells from lysis by NK cells expressing CD94/NKG2A receptor (11). In addition, Cosman and coworkers (12, 13) have recently demonstrated that UL18 is specifically recognized by LIR-1, a membrane of the Ig receptor superfamily, which is predominantly expressed on monocytes, B cells, and a minor subset of NK cells (12, 13). In this study we examined the roles of endogenous class I MHC and an hCMV encoded class I homolog (UL18) in modulating NK cell–mediated cytotoxicity during hCMV infection.

Materials and Methods

Cell lines, NK Cell Lines, and Clones. 293EBV is a human kidney cell line expressing the EBNA-1 nuclear antigen (Invitrogen, Carlsbad, CA). COS-7, Chinese hamster ovary (CHO)-K1, 293EBV, and human foreskin fibroblast (HFF) cell lines were maintained in RPMI (MediaTech, Herndon, VA) supplemented with 10% FCS (GIBCO BRL, Bethesda, MD). NK cells were cloned and cultured as previously described (14, 15). HFF cell lines were prepared and cultured as previously described (16).

Constructs. The UL18 open reading frame was subcloned into the EBV episomal expression vectors pREP10 and pCEP4 (Invitrogen). The cDNA for CD32 and CD94 were cloned into pBJneo. The hCMV gB (UL55) cDNA in the pRcCMV vector (Invitrogen) was a gift from Dr. L. Pereira (University of California San Francisco, San Francisco, CA).

Transient Transfection. 293EBV were plated at 60–80% confluence and transfected with pREP10 UL18 using Lipofectamine (GIBCO BRL). 48 h after transfection, cells were trypsinized and stained with anti-UL18 mAb (10C7), followed by PE-conjugated goat anti–mouse IgG. Viable UL18 positive cells were sorted and cultured for 48 h before use in cytotoxicity assays. COS-7 and CHO-K1 were transfected with pCEP4 UL18 and sorted as above. Flow cytometry was performed as previously described (17).

Antibodies. 10C7 (mouse IgG1) was generated by immunizing mice with soluble, partially deglycosylated UL18. The mAbs against KIRs were: DX9 (KIR3DL1); DX27 (KIR2DL2, KIR2DL3, and KIR2DS2); DX30 (KIR3DL1, KIR3DL2); DX31 (KIR3DL2); and HP-3E4 (KIR2DL1, KIR2DS1, and KIR2DS4). DX22 mAb is against CD94. Anti–class I mAbs (DX15, DX16, and DX17) have been previously described (18). Anti-CMV UL55 (gB) was purchased from the Goodwin Institute (Goodwin Institute, Plantation, FL). Anti-hCMV IE mAb was purchased from Chemicon (Temecula, CA). All other mAbs were provided by Becton Dickinson Immunocytometry Systems (San Jose, CA).

Cytotoxicity Assays. Cell-mediated cytotoxicity was assessed using 4-h ^{51}Cr–release assays. In these assays, effector cells at various concentrations were incubated with 5×10^3 target cells in U-bottomed 96-well microtiter plates at 37°C. Percentage of lysis was determined as previously described (18). Spontaneous ^{51}Cr release was <10% of total counts. Only cells with >80% viability were used for labeling. The spontaneous release of 293EBV UL18 cells and 293EBV controls were similar.

Western Blot. Infected HFFs were lysed in 0.5 ml of lysis buffer (Tris buffered saline, 50 mM Tris, 150 mM NaCl, pH 8.0, with 1% NP-40). Lysates were resolved by SDS-PAGE on 12% gels. Western blots were performed using 10C7 anti-UL18 or anti-hCMV IE mAbs, followed by horseradish peroxidase–conjugated second antibodies as previously described (19).

hCMV Infection. AD169 and Δ18 (20) viruses were titered and propagated in HFFs as previously described (16). HFFs were infected at a multiplicity of infection (MOI) of 3–5. After adsorption of the virus for 1 h at 37°C, the inoculum was removed and medium containing 10% FCS was added. Viral stocks were titered using classical cytopathic effect as an end-point.

Results and Discussion

The Role of Endogenous Class I in Modulating NK Cell Killing of Infected and Uninfected HFFs. Fibroblasts downregulate class I MHC expression upon hCMV infection (21). In Fig. 1 *A*, we show that class I MHC is downregulated 10-fold in hCMV-infected HFFs, but a significant level of class I MHC is still present on the cell surface. This downregulation was seen by 24 h and was maintained for the duration of the studies (5 d, data not shown). The 'missing self' hypothesis stipulates that the loss of class I MHC expression confers susceptibility to NK cell killing (22). The expectation from this hypothesis is that infected cells would become more susceptible to NK cell–mediated lysis. To address this question, we performed NK cell cytotoxicity assays using hCMV-infected and mock-infected cells. In repeated experiments, NK cells efficiently lysed hCMV-infected HFFs, but not mock-infected cells (Fig. 1 *B*). This inability to efficiently kill mock-infected HFFs may be due to their high level of class I MHC expression. If NK cells were restrained from killing uninfected HFFs by a class I MHC–dependent mechanism, blocking the KIRs and/or CD94/NKG2A receptors on the effector cells or class I MHC on the fibroblasts should reverse the protection. Experiments performed with anti–class I or a cocktail of mAbs against CD94 and KIRs did not induce killing (Fig. 1 *C*). This inability to kill was evident using a variety of NK clones and lines (data not shown). The KIR and CD94/NKG2A receptors expressed by these NK cells were functional against B lymphoblastoid target cells transfected with relevant class I MHC genes, with the target cell protection being reversed using anti–class I MHC or anti-CD94 + anti-KIR mAbs. Therefore, class I MHC expression alone by HFFs does not prevent NK cell–mediated killing. It can be argued that mock-infected HFFs lack positive signals needed to trigger NK cells, and that class I MHC may be functional in the context of infected cells, which have upregulated ligands for the 'triggering' receptors. To address this, we repeated these experiments using hCMV-infected HFFs. Again, blocking class I MHC, KIRs, or CD94 neither augmented nor attenuated NK cell–mediated cytotoxicity (Fig. 1 *D*).

The Role of a Virus-encoded Class I MHC Homolog in NK Cell Killing. hCMV encodes a glycoprotein with homology to class I MHC (9). This molecule is able to form a complex with β_2-microglobulin (β_2M)(23) and contains a peptide-binding groove (24). KIR recognition of class I MHC requires the formation of a trimeric complex comprising class I MHC, β_2M, and peptide (25, 26). It was therefore hypothesized that UL18 would interact with NK cell class I receptors to inhibit killing of CMV-infected

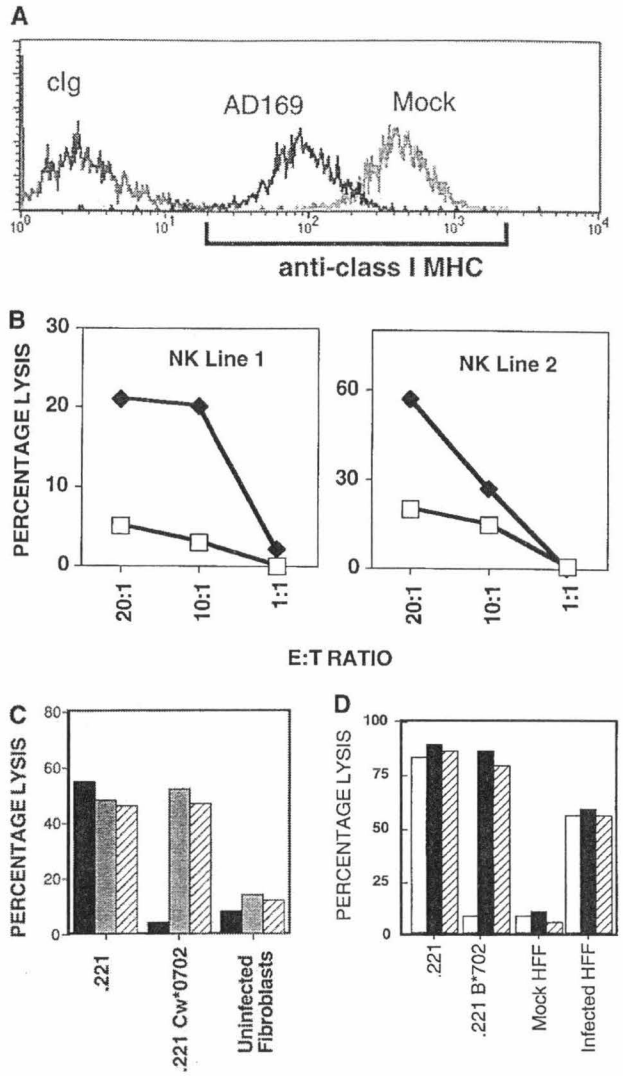

Figure 1. (*A*) Downregulation of class I MHC in hCMV-infected HFFs. AD169 or mock-infected HFFs were stained with anti-class I (DX17) or control Ig (cIg), followed by PE-conjugated goat anti-mouse Ig. HFFs were infected with AD169 at an MOI of 3, and cells were stained at 24 h after infection. (*B*) NK cell cytotoxicity assay against hCMV or mock-infected HFF cells. hCMV or mock-infected HFFs were used as targets in a 4-h ^{51}Cr-release assay. HFFs were infected at an MOI of 3 and used at 48 h after infection. Mock-infected, *white squares*; AD169, *black diamonds*. (*C*) Blocking class I MHC, KIR, or CD94 does not induce NK cell killing of uninfected HFFs. Normal HFFs were incubated in the presence of NK cells and with cIg or a mixture of mAb against class I MHC (DX15, DX16, and DX17 at 20 μg/ml) or a mixture of anti-KIR mAbs (DX27, DX30, DX31, and HP-3E4) and anti-CD94 mAb (DX22), each at 20 μg/ml. cIg, *black bars*; anti-KIR/CD94, *gray bars*; anti-class I, *hatched bars*. (*D*) AD169 or mock-infected HFFs were incubated in the presence of NK cells with cIg or mAb directed at class I MHC (DX15, DX16, and DX17 at 20 μg/ml) or a cocktail of mAbs against KIR and CD94. Cytotoxicity assays were performed at E/T ratios of 5:1. As controls, 721.221 class I HLA transfectants expressing HLA-B*0702 or HLA-Cw*0702 were analyzed, using NK clones expressing the relevant CD94/NKG2A or KIR, respectively. cIg, *white bars*; anti-KIR/CD94, *black bars*; anti-class I, *hatched bars*.

cells. We examined this by infecting HFFs with wild-type AD169 CMV virus or Δ18 (a mutant virus with the UL18 gene deleted). The level of class I MHC downregulation by the two viruses was comparable (Fig. 2 *A*). A 69-kD UL18 protein was detectable by 24 h in AD169-infected HFFs by Western blot analysis, but not in Δ18-infected HFF lysates (Fig. 2 *B*). Although UL18 protein was readily detected by Western blot analysis in HFF infected with AD169 virus, analysis by flow cytometry suggested that very little UL18 was expressed on the cell surface (data not shown). The amounts of hCMV IE protein (Fig. 2 *B*) and class I MHC (data not shown) in lysates prepared from Δ18-infected HFFs were comparable to those detected in HFF infected with AD169 wild-type CMV. Furthermore, the titer of AD169 and Δ18 viruses were comparable, as assessed by plaque formation assays (data not shown) and the HFFs were homogeneously infected as assessed by the uniform downregulation of class I in all the cells (Fig. 2 *A*). Many NK cell lines and clones killed AD169-infected cells somewhat better than they did Δ18-infected cells (Fig. 2 *C*). However, HFFs infected with AD169 or Δ18 showed enhanced killing when compared with mock infected cells (Fig. 2 *C*). Therefore, UL18 confers a slight enhancement of susceptibility to NK cell killing, although UL18-independent mechanism(s) also exists.

To examine directly the ability of UL18 to confer increased susceptibility to NK cell killing in the absence of viral infection, we transfected 293EBV cells with a UL18 expression vector. Fig. 2 *D* shows the expression of UL18 on the surface of transfectants using a UL18-specific mAb. In a series of experiments, 293EBV UL18 cells consistently showed enhanced lysis compared with 293EBV (Fig. 2 *E*). In addition, UL18-dependent enhancement of NK cell killing could also be demonstrated in transfected COS-7 and CHO-K1 cells (data not shown) using several NK clones and lines. These clones included those expressing functional KIRs and CD94 (Table 1). Inhibition of NK cell killing by UL18-expressing target cells was never observed in any of these experiments. The enhanced lysis of 293EBV cells transfected with UL18 was not affected by mAbs against CD94 or KIR (data not shown), although it should be noted that not all KIR isoforms are recognized by the available mAbs. The enhanced killing of 293EBV UL18 transfectants versus 293EBV was not due to changes in the level of class I MHC or adhesion molecules (data not shown). As controls, cells were transfected with expression constructs encoding CD32, CD94, an hCMV surface glycoprotein (gB), or vector only; none of these transfectants showed enhanced susceptibility to NK cell lysis (data not shown).

Hence, the hypothesis that UL18 replaces class I MHC molecules to prevent NK cell lysis does not seem to apply to hCMV-infected HFFs and transfected epithelial and ovary cells (293, COS-7, and CHO-K1). It was recently reported that UL18 inhibits NK cell lysis of 721.221 B lymphoblastoid targets, mediated through CD94 (11). In repeated studies, we never observed inhibition of NK cell

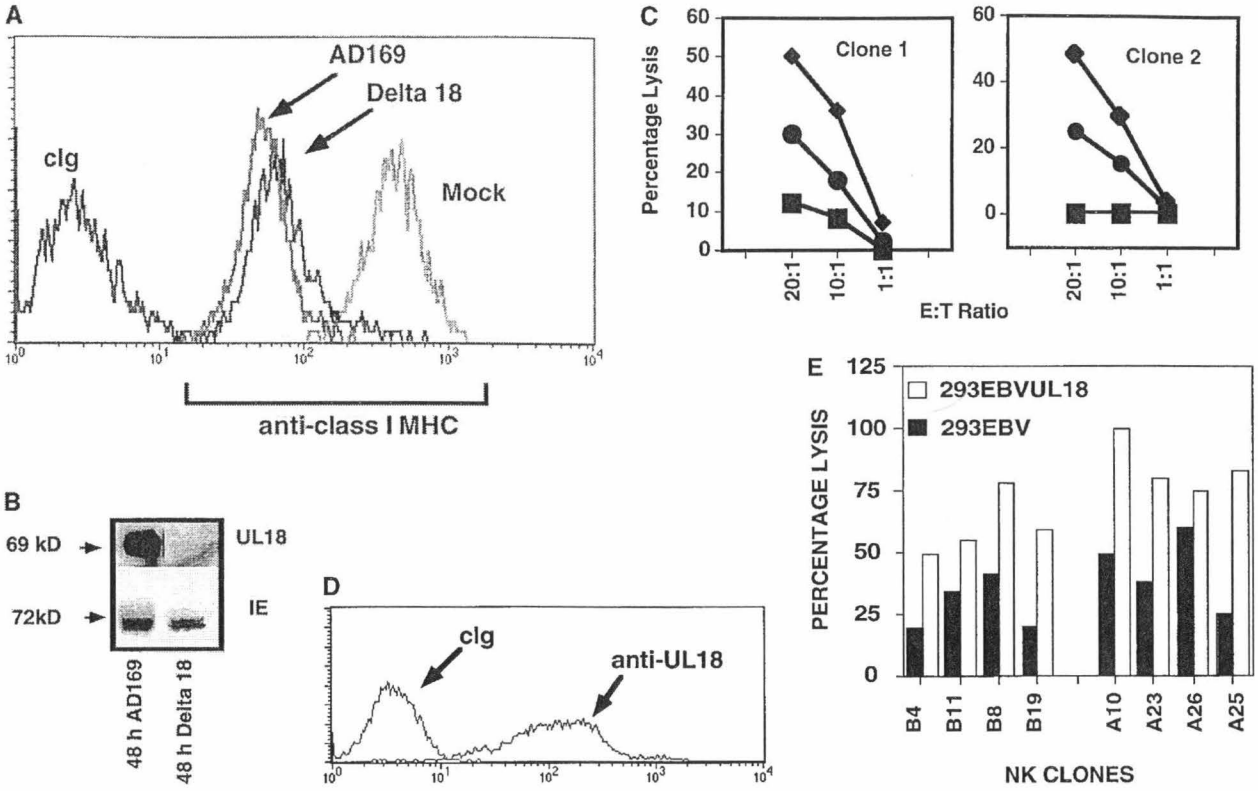

Figure 2. (*A*) Downregulation of class I MHC after Δ18 and AD169 hCMV infection of HFFs. HFFs were infected with Δ18 or AD169 at an MOI of 5. At 48 h after infection cells were stained with anti-class I MHC or cIg, followed by PE-conjugated goat anti-mouse second step. (*B*) Expression of UL18 in AD169 but not Δ18 cell lysates. Lysates were prepared from HFF-infected with Δ18 or AD169 at 48 h after infection and blotted with anti-UL18 or anti-hCMV IE mAb, followed by horseradish peroxidase–conjugated second step. (*C*) AD169-infected HFFs were lysed more efficiently than were Δ18-infected HFFs. HFFs were infected with AD169 or Δ18 at an MOI of 5, and used as targets at 48 h after infection in 4-h ^{51}Cr-release assays. Assays were performed at an E/T ratio of 20:1, 10:1, and 1:1. Standard deviation between triplicates was <10%. Δ18, *black circles*; AD169, *black diamonds*; mock-infected, *black squares*. (*D*) Surface UL18 expression on 293EBV transfectants. 293EBV cells were transfected with pREP10 UL18. Cells were cultured for 48 h before use in cytotoxicity assays. Histograms of sorted UL18-positive cells. Cells were stained with anti-UL18 mAb 10C7 followed by PE-conjugated goat anti-mouse Ig. (*E*) 293EBV transfectant expressing UL18 were lysed at an enhanced level compared with parental controls. UL18-transfected 293EBV cells were used as targets in NK cell cytotoxicity assays. Experiments were performed at an E:T ratio of 5:1. All transfectants other than vector only were positively sorted using mAb directed against the protein encoded by the transfected cDNA. Cells were cultured for 48 h and used in 4-h cytotoxicity assays as described above.

killing against UL18 expressing targets using clones with functional CD94 or KIR. In view of this discrepancy, several aspects of the previous report should be highlighted. First, in the prior study UL18 was transfected into 721.221 targets; however, transfectants were isolated on the basis of surface β_2M expression, not UL18. Second, we have failed to generate stable UL18 transfectants in 721.221 or in 15 other human or mouse lines, because it seems that prolonged expression (>2 wk) of UL18 results in cell death. We could only generate UL18 transfectants in high efficiency transient transfection systems such as 293, COS-7, and CHO-K1. Notably, 721.221 cells express low levels of HLA-E (27) and -F (28). Since Reyburn et al. (11) sorted UL18-transfected 721.221 on the basis of β_2M surface expression, rather than UL18, cells expressing HLA-E or -F may have been inadvertently enriched and could be responsible for the protection against NK cell lysis. In fact, a

Table 1. *Phenotype of NK Cell Lines and Clones*

Clones	KIRs	CD94
A10	DX9−, DX24+	CD94
A23	DX9−, DX24+	CD94
A26	DX9+, DX24+	ND
A25	DX9+, DX24+	ND
BR	KIR−	CD94/NKG2A
B8	KIR−	CD94/NKG2A
B11	KIR−	CD94/NKG2A
B19	KIR−	CD94/NKG2A

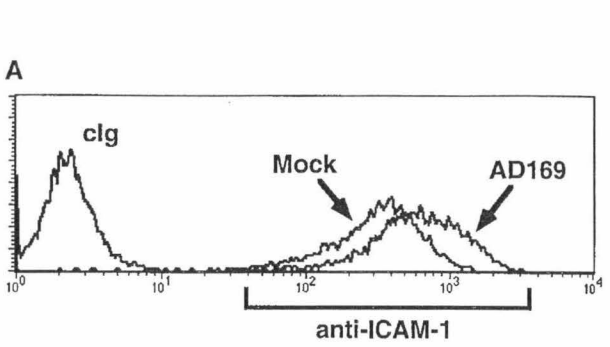

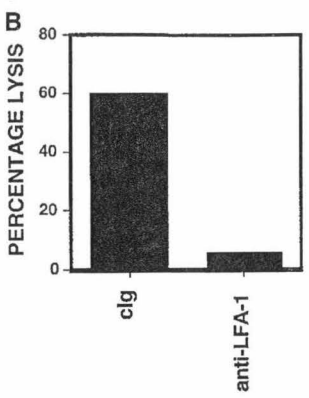

Figure 3. (*A*) Upregulation of ICAM-1 on hCMV-infected cells. AD169 or mock-infected HFFs were stained (24 h after infection) with FITC-conjugated anti–ICAM-1 (LB2 mAb) or FITC-conjugated cIg. Mean fluorescence intensity of ICAM-1 increased from 351 to 705. (*B*) Enhanced cytotoxicity against hCMV-infected HFFs was reversed with anti–LFA-1β (CD18). hCMV or mock-infected HFFs were incubated with cIg or anti–LFA-1β (20 μg/ml). 4-h ^{51}Cr–release assays were performed at an E/T ratio of 5:1.

recent study demonstrated that the endogenous HLA-E expressed by 721.221 cells can protect these target cells from lysis by NK cells expressing the inhibitory CD94/NKG2A receptor (29). Although HLA-E molecules bind peptides derived from the leader segments of certain other MHC class I proteins (27), the leader of UL18 does not conform to the preferred peptide bound by HLA-E. Therefore, it is possible that Reyburn et al. (11) simply selected for a variant of 721.221 that expressed higher levels of the endogenous HLA-E protein.

Recent studies by Cosman and coworkers (12, 13) have shown that the human CMV UL18 protein interacts with a membrane receptor designated ILT2 (30) or LIR-1 (12, 13), which is expressed predominantly on monocytes, B cells, and a subset of NK cells. Binding of a UL18–Ig Fc fusion protein to NK cells and monocytes was completely blocked using an anti-ILT2/LIR-1 mAb, suggesting that ILT2/LIR-1 is the predominant, if not exclusive, receptor for UL18 expressed on leukocytes (12). It is possible that ILT2/LIR-1 on NK cells might interact with UL18 on CMV-infected cells, preventing NK cell–mediated cytotoxicity. However, it should be appreciated that ILT2/LIR-1 is expressed on only a minor subset of NK cells (12, 31); therefore, the physiological significance of ILT2/LIR-1 on NK cells during a CMV infection is uncertain. Although prior studies of UL18 and its mouse homolog M144 have focused on a potential role for these proteins in NK cell–mediated immunity (10, 11), an alternative possibility is that these molecules may be more important in affecting monocyte and dendritic cell function during CMV infection. For example, interactions between UL18 and ILT2/LIR-1 on monocytes or dendritic cells during a CMV infection may suppress IL-12 production, which would in turn limit IFN-γ secretion by NK cells and thus alter the early host immune response. This scenario could potentially explain the increased virulence of mouse CMV virus lacking M144 (10). This is of particular interest given the recent finding that dendritic cells may serve as the reservoir for latent CMV infection (32).

Upregulation of Cell Surface Adhesion Molecules in hCMV-infected HFFs. Since enhanced killing was observed in HFF infected with both AD169 and Δ18, other molecules in addition to UL18 were also playing a role. To examine what molecules were upregulated after infection, we stained mock-infected and hCMV-infected HFFs with a panel of mAb against cell surface adhesion/costimulatory molecules. The only molecule examined that was consistently upregulated in the infected cells was intracellular adhesion molecule 1 (ICAM-1; CD54) (Fig. 3 *A*). Blocking of ICAM-1 interaction with its ligand using anti–LFA-1β (CD18) was able to prevent the killing of infected HFF (Fig. 3 *B*). These data suggest that ICAM-1 is a crucial component in NK cell–mediated killing of hCMV-infected cells, but does not exclude the existence of other molecules capable of triggering NK cell cytotoxicity.

Based on our observations, the hypothesis that KIRs and CD94/NKG2A class I MHC inhibitory receptors are a physiological surveillance mechanism for viral infection may not be universally applicable. Similarly, we have previously shown that in certain target cells (e.g., Jurkat and K562), the expression of an appropriate class I MHC allele recognized by KIR3DL1 (i.e., HLA-B*5801) was insufficient to prevent killing of these transfected target cells (14).

hCMV has evolved many strategies that allow its highly successful dissemination throughout the population. Although infected individuals are generally clinically asymptomatic (1), further viral transmission still occurs. In cases where the infection is not effectively controlled, death often results, thereby limiting the opportunity for further viral dissemination. Therefore, the UL18-dependent and independent mechanisms may serve to limit the severity of CMV-induced disease by rendering infected cells more susceptible to immune destruction.

We thank the members of the DNAX FACS facility for flow cytometry, and Dr. Lenore Pereira, Debra Liggett, Sasha Lazetic, and Brian Corliss for advice and reagents.

DNAX Research Institute is supported by the Schering Plough Corporation. T.L Chapman is supported by a National Defense Science and Engineering Pre-Doctoral Fellowship.

Address correspondence to Clement Leong, DNAX Research Institute, 901 California Ave., Palo Alto, CA 94304. Phone: 650-496-1241; Fax: 650-496-1200; E-mail: leong@dnax.org

Received for publication 3 December 1997 and in revised form 26 February 1998.

References

1. Ho, M. 1982. Epidemiology of cytomegalovirus in man. *In* Cytomegalovirus, Biology and Infection: Current Topics in Infectious Disease. W.B. Greenough III and T.C. Merigan, editors. Plenum Medical Book Co., New York. 77–104.
2. Quinnan, G.V., N. Kirmani, A.H. Rook, J.F. Manishewitz, L. Jackson, G. Moreschi, G.W. Santos, R. Saral, and W.H. Burns. 1982. Cytotoxic T cells in cytomegalovirus infection. *N. Engl. J. Med.* 307:6–13.
3. Riddell, S.R., K.S. Watanabe, J.M. Goodrich, C.R. Li, M.E. Agha, and P.D. Greenberg. 1992. Restoration of viral immunity in immunodeficient humans by the adoptive transfer of T cell clones. *Science.* 257:238–241.
4. Biron, C.A., K.S. Byron, and J.L. Sullivan. 1989. Severe herpesvirus infections in an adolescent without natural killer cells. *N. Engl. J. Med.* 320:1731–1735.
5. Bukowski, J., J. Warner, G. Dennert, and R. Welsh. 1985. Adoptive transfer studies demonstrating the anti-viral effect of natural killer cells in vivo. *J. Exp. Med.* 161:40–52.
6. Scalzo, A.A., N.A. Fitzgerald, C. Wallace, A.E. Gibbons, Y.C. Smart, R.C. Burton, and G.R. Shellam. 1992. The effect of the CMV-1 resistance gene, which is linked to the natural killer cell gene complex, is mediated by natural killers. *J. Immunol.* 149:581–589.
7. Brown, M.G., A.A. Scalzo, K. Matsumoto, and W.M. Yokoyama. 1997. The natural killer gene complex: a genetic basis for understanding natural killer cell function and innate immunity. *Immunol. Rev.* 155:53–65.
8. Lanier, L.L., and J.H. Phillips. 1995. NK cell recognition of major histocompatibility complex class I molecules. *Semin. Immunol.* 7:75–82.
9. Beck, S., and B.G. Barrell. 1988. Human cytomegalovirus encodes a glycoprotein homologous to MHC class I antigens. *Nature.* 331:269–272.
10. Farrel, H., H. Vally, D. Lynch, P. Fleming, G. Shellam, A. Scalzo, and N. Davis-Poynter. 1997. Inhibition of natural killer cells by a cytomegalovirus MHC class I homologue in vivo. *Nature.* 386:446–447.
11. Reyburn, H.T., O. Mandelbolm, M. Vales-Gomez, D. Davis, L. Pazmany, and J. Strominger. 1997. The class I MHC homologue of human cytomegalovirus inhibits attack by natural killer cells. *Nature.* 386:514–517.
12. Cosman, D., N. Fanger, L. Borges, M. Kubin, W. Chin, L. Peterson, and M.-L. Hsu. 1997. A novel immunoglobulin superfamily receptor for cellular and viral MHC class I molecules. *Immunity.* 7:273–282.
13. Borges, L., M.-L. Hsu, N. Fanger, M. Kubin, and D. Cosman. 1997. A family of human lymphoid and myeloid Ig-like receptors, some of which bind to MHC class I molecules. *J. Immunol.* 159:5192–5196.
14. Litwin, V., J. Gumperz, P. Parham, J.H. Phillips, and L.L. Lanier. 1993. Specificity of HLA class I antigen recognition by human NK clones: evidence for clonal heterogeneity, protection by self and non-self alleles, and influence of the target cell type. *J. Exp. Med.* 178:1321–1336.
15. Yssel, H., J.D. Vries, M. Koken, W. van Blittersijk, and H. Spits. 1984. Serum-free medium for the generation and the propagation of functional human cytotoxic and helper T cell clones. *J. Immunol. Methods.* 72:219–227.
16. Mocarski, E.S., M. Bonyhadi, S. Salimi, J.M. McCune, and H. Kaneshima. 1993. Human cytomegalovirus in a SCID-hu mouse: thymic epithelial cells are prominent targets of viral replication. *Proc. Natl. Acad. Sci. USA.* 90:104–108.
17. Lanier, L.L., and D.J. Recktenwald. 1991. Multicolor immunofluorescence and flow cytometry. *Methods: A Companion to Methods in Enzymology* 2:192–199.
18. Phillips, J., J. Gumperz, P. Parham, and L. Lanier. 1995. Superantigen-dependent, cell-mediated cytotoxicity inhibited by MHC class I receptors on T lymphocytes. *Science.* 268: 403–405.
19. Phillips, J., C. Chang, J. Mattson, J. Gumperz, P. Parham, and L.L. Lanier. 1996. Human C-type lectins and MHC class I recognition: evidence for involvement of CD94-associated proteins (CD94AP) in recognition of HLA-A, -B, and -C. *Immunity.* 5:163–172.
20. Browne, H., M. Churcher, and T. Minson. 1992. Construction and characterisation of a human cytomegalovirus mutant with the UL18 (class I homolog) gene deleted. *J. Virol.* 66: 6784–6787.
21. Beersma, M.F., M.J. Bijlmakers, and H.L. Ploegh. 1993. Human cytomegalovirus down-regulates HLA class I expression by reducing the stability of class I heavy chains. *J. Immunol.* 151:4455–4464.
22. Karre, K., H.G. Ljunggren, G. Plontek, and R. Kiessling. 1986. Selective rejection of H-2–deficient lymphoma variants suggests alternative immune defense strategy. *Nature.* 319: 675–678.
23. Browne, H., G. Smith, S. Beck, and T. Minson. 1990. A complex between the MHC class I homologue encoded by human cytomegalovirus and β2-microglobulin. *Nature.* 347: 770–772.
24. Fahnestock, M.L., J.L. Johnson, R.M.R. Feldman, J.M. Neveu, W.S. Lane, and P.J. Bjorkman. 1995. The MHC class I homolog encoded by human cytomegalovirus binds endogenous peptides. *Immunity.* 3:583–590.
25. Malnati, M.S., M. Peruzzi, K.C. Parker, W.E. Biddison, E. Ciccone, A. Moretta, and E.O. Long. 1995. Peptide specificity in the recognition of MHC class I by natural killer cell clones. *Science.* 267:1016–1018.
26. Ciccone, E., D. Pende, L. Nanni, C. Di Donato, O. Viale, A. Beretta, M. Vitale, S. Sivori, A. Moretta, and L. Moretta. 1995. General role of HLA class I molecules in the protection of target cells from lysis by natural killer cells: evidence that the free heavy chains of class I molecules are not sufficient to mediate the protective effect. *Int. Immunol.* 7:393–400.
27. Braud, V., E.Y. Jones, and A. McMichael. 1997. The human major histocompatibility complex class Ib molecule HLA-E

binds signal sequence-derived peptides with anchor residues at positions 2 and 9. *Eur. J. Immunol.* 27:1164–1169.
28. Tzeng, C.-M., E.J. Adams, J.E. Gumperz, L. Percival, and L.D. Barber. 1996. Peptides bound endogenously by HLA-Cw*0304 expressed in LCL 721.221 cells include a peptide derived from HLA-E. *Tissue Antigens.* 48:325–328.
29. Braud, V.M., D.S.J. Allan, C.A. O'Callaghan, K. Soderstrom, A. D'Andrea, G.S. Ogg, S. Lazetic, N.T. Young, J.I. Bell, J.H. Phillips, et al. 1998. HLA-E binds to natural killer cell receptors CD94/NKG2A, B, and C. *Nature.* 391:795–799.
30. Samaridis, J., and M. Colonna. 1997. Cloning of novel immunoglobulin superfamily receptors expressed on human myeloid and lymphoid cells: structural evidence for new stimulatory and inhibitory pathways. *Eur. J. Immunol.* 27: 660–665.
31. Colonna, M., F. Navarro, T. Bellon, M. Llano, P. Garcia, J. Samaridis, L. Angman, M. Cella, and M. Lopez-Botet. 1997. A common inhibitory receptor for major histocompatibility complex class I molecules on human lymphoid and myelomonocytic cells. *J. Exp. Med.* 186:1809–1818.
32. Soderberg-Naucler, C., K.N. Fish, and J.A. Nelson. 1997. Reactivation of latent human cytomegalovirus by allogeneic stimulation of blood cells from healthy donors. *Cell.* 91: 119–126.

Appendix B:

Characterization of the Interaction Between the Herpes Simplex Virus Type I Fc Receptor and Immunoglobulin G

This paper describes characterization of the HSV-1 Fc receptor done in colloboration with Dr. Malini Raghavan from the University of Michigan and Dr. Sherrie Morrison from UCLA. We show that truncated forms of gE and gI assemble into stable heterodimers with a 1:1 stoichiometry, determine the affinity of the gE-gI-IgG interaction and demonstrate that histidine 435 at the C_H2-C_H3 domain interface of IgG is a critical residue for IgG binding to gE-gI. My contributions to this work include expression and purification of gE and gI and determination of the stoichiometry of the interaction.

THE JOURNAL OF BIOLOGICAL CHEMISTRY
Vol. 274, No. 11, Issue of March 12, pp. 6911–6919, 1999
Printed in U.S.A.

Characterization of the Interaction between the Herpes Simplex Virus Type I Fc Receptor and Immunoglobulin G*

(Received for publication, October 27, 1998)

Tara L. Chapman‡, Il You§, Ian M. Joseph§, Pamela J. Bjorkman‡¶, Sherie L. Morrison‖, and Malini Raghavan§**

From the ‡Division of Biology 156-29 and the ¶Howard Hughes Medical Institute, California Institute of Technology, Pasadena, California 91125, the §Department of Microbiology and Immunology, University of Michigan Medical School Ann Arbor, Michigan 48109, and the ‖Department of Microbiology, Immunology, and Molecular Genetics, UCLA, Los Angeles, California 90095

Herpes simplex virus type I (HSV-1) virions and HSV-1-infected cells bind to human immunoglobulin G (hIgG) via its Fc region. A complex of two surface glycoproteins encoded by HSV-1, gE and gI, is responsible for Fc binding. We have co-expressed soluble truncated forms of gE and gI in Chinese hamster ovary cells. Soluble gE-gI complexes can be purified from transfected cell supernatants using a purification scheme that is based upon the Fc receptor function of gE-gI. Using gel filtration and analytical ultracentrifugation, we determined that soluble gE-gI is a heterodimer composed of one molecule of gE and one molecule of gI and that gE-gI heterodimers bind hIgG with a 1:1 stoichiometry. Biosensor-based studies of the binding of wild type or mutant IgG proteins to soluble gE-gI indicate that histidine 435 at the C_H2-C_H3 domain interface of IgG is a critical residue for IgG binding to gE-gI. We observe many similarities between the characteristics of IgG binding by gE-gI and by rheumatoid factors and bacterial Fc receptors such as *Staphylococcus aureus* protein A. These observations support a model for the origin of some rheumatoid factors, in which they represent anti-idiotypic antibodies directed against antibodies to bacterial and viral Fc receptors.

The expression of viral proteins that counter immune responses of the host is well documented. Viral factors have been identified that can potentially inhibit or modify the antiviral effects of antibodies, complement proteins, cytokines, and cytotoxic T cells (1). Characterization of viral proteins that interact with specific components of the immune system is likely to provide insights into immune mechanisms involved in host-virus interactions and into the molecular basis of viral persistence in the presence of a functional immune system. *Herpesviruses*, in particular, have evolved multiple mechanisms for interfering with humoral as well as cell-mediated immune responses (reviewed in Refs. 2 and 3). The present studies focus upon the herpes simplex virus type I-encoded Fc receptor (FcR),[1] a protein complex that has been suggested to interfere with antibody-mediated viral clearance (4). HSV-1 virions, as well as cells infected with HSV-1, bind to immunoglobulins of the IgG subclass via the Fc region (5). The glycoprotein gE of HSV-1 was identified as the IgG-binding polypeptide of HSV-1 (6, 7). It was subsequently shown that gE associates with a second viral glycoprotein, gI (8, 9), and that cells transfected with genes encoding both gE and gI have enhanced IgG binding activity compared with cells transfected with gE alone (10–12). Both gE and gI are type I transmembrane proteins, with an N-terminal extracellular portion, a single transmembrane domain, and a C-terminal cytoplasmic domain. Homologous glycoproteins encoded by other α-herpesviruses, including pseudorabies virus (PRV) (13) and varicella zoster virus (14), have been shown to possess species-specific FcR activity.

HSV-1-infected cells acquire low levels of FcR activity immediately upon exposure to virus (in the absence of viral gene expression), presumably by the transfer of virion gE-gI to the cell surface during viral entry (7). The HSV FcR may thus be particularly significant for protection of virally infected cells from early immune destruction (2). Recent *in vivo* studies demonstrated that passively transferred anti-HSV IgG greatly reduced viral titers and disease severity in mice infected with a mutant HSV-1 that lacked FcR activity. By contrast, anti-HSV IgG was ineffective in reducing viral titers and disease severity in mice infected with wild type virus with intact FcR activity (15). These observations indicate that the HSV-1 FcR activity facilitates evasion of antibody-mediated viral clearance *in vivo*.

Several means of evading antibody-mediated immune responses could arise from the Fc binding function of gE-gI (16–18). Binding of nonimmune IgG by gE-gI present on HSV-1 virions can inhibit virus neutralization by anti-viral antibodies (19). Engagement of the Fc portion of anti-HSV antibodies can protect virally infected cells from antibody-dependent cell-mediated cytotoxicity (ADCC) (20) as well as complement-mediated lysis (21). Inhibition of ADCC has been suggested to occur by a phenomenon called antibody bipolar bridging (21), a mechanism whereby antibodies bound via their Fab ends to HSV-1 glycoproteins on surface membranes of infected cells would simultaneously interact with the viral Fc receptors of the same infected cell. By engaging the Fc domain, the HSV-1 FcR could interfere with recognition by FcγRs on immune effector cells. Antibody bipolar bridging has also been suggested to facilitate antiviral antibody-induced patching, capping, and extrusion of

* This work was supported by a grant from the American Heart Association (to M. R.), the University of Michigan Multipurpose Arthritis and Musculoskeletal Diseases Center (to M. R.), and a National Defense Science and Engineering Predoctoral Fellowship (to T. L. C.). The costs of publication of this article were defrayed in part by the payment of page charges. This article must therefore be hereby marked "*advertisement*" in accordance with 18 U.S.C. Section 1734 solely to indicate this fact.

** To whom correspondence should be addressed. Tel.: 734-647-7752; Fax: 734-764-3562; E-mail: malinir@umich.edu.

[1] The abbreviations used are: FcR, Fc receptor; FcγR, Fcγ receptor; PRV, pseudorabies virus; ADCC, antibody-dependent cell-mediated cytotoxicity; PCR, polymerase chain reaction; CHO, Chinese hamster ovary; FACS, fluorescence-activated cell sorting; FITC, fluorescein isothiocyanate; hIgG, human IgG; PAGE, polyacrylamide gel electrophoresis; RF, rheumatoid factor(s); HSV, herpes simplex virus; HSV-1, HSV, type 1.

viral glycoproteins from the surface of cells infected with PRV (13). Antibody-induced shedding of viral glycoproteins may represent a strategy for rendering virally infected cells refractory to antiviral antibodies and for inhibiting the presentation of viral antigens via class II major histocompatibility complex molecules.

A second function attributed to gE-gI is that of facilitating cell-to-cell spread of virus. Recent studies suggest that gE and gI are required for transneuronal transport of PRV from the retina to the visual centers of rats (22), for cell-to-cell spread of PRV, and for full virulence of PRV (23). Furthermore, studies with mutant HSV-1 virions indicate that gE and gI of HSV-1 facilitate cell-to-cell spread of virus *in vivo* and viral spread across junctions of cultured cells (24–26). It has been proposed that the cell-to-cell spread-promoting functions of gE-gI are unrelated to the Fc binding activity and that the HSV-1-encoded gE-gI glycoproteins and the analogous proteins of other α-herpesviruses may interact with other ligands, enabling viral transport across cells (24, 25). Such ligands remain to be identified.

To better understand the mechanisms by which IgG binding by gE-gI facilitates immune evasion, we initiated a molecular characterization of IgG binding by gE-gI. We expressed soluble forms of gE and gI and showed that the glycoproteins assemble into a stable heterodimer. The soluble receptor heterodimer binds to human IgG (hIgG) with relatively high affinity and can be purified to homogeneity using an hIgG-based affinity matrix. We determined a 1:1 binding stoichiometry for the gE-gI·IgG complex, and also determined that a histidine residue at the C_H2-C_H3 domain interface is a critical determinant of IgG binding specificity. The implications of the gE-gI binding site on IgG and the gE-gI·IgG complex stoichiometry are discussed.

EXPERIMENTAL PROCEDURES

Construction and Expression of Soluble gE, gI, and gE-gI—Molecular cloning manipulations were performed by standard protocols (27). PCR was used to insert a 5′ *Xho*I site, a 3′ *Not*I site, and a stop codon after the codon corresponding to amino acid 399 of the gE gene and amino acid 246 of the gI gene (the *Hin*dIII fragment containing the gE gene and the *Bam*HI fragment containing the gI gene of HSV strain KOS was kindly provided by H. Ghiasi, Cedar Sinai Medical Center). Our numbering scheme starts with the first residue of the mature protein, which is designated residue 1, and all other residues are numbered sequentially (see "N-Terminal Sequencing and Mass Spectrometric Analysis of Purified gE-gI"). The gE PCR product was cloned into pCRII (Invitrogen), and the gI PCR product was cloned into pBSIISK$^+$ (Stratagene). Both sequences were verified. The modified gE and gI genes were excised using *Xho*I and *Not*I enzymes and individually subcloned into the unique *Xho*I and *Not*I sites of separate PBJ5-GS expression vectors (28). PBJ5-GS carries the glutamine synthetase gene as a selectable marker and as a means of gene amplification in the presence of the drug methionine sulfoximine, a system developed by Celltech (29). Expression vectors carrying gE, gI, or both gE and gI were transfected into CHO cells using a Lipofectin procedure (Life Technologies, Inc.). Cells resistant to 100 μM methionine sulfoximine were selected according to the protocol established by Celltech, modification of which has been previously described (28). Transfected CHO cells were maintained in glutamine-free α-minimal essential medium (Irvine Scientific) supplemented with 5% dialyzed fetal bovine serum (Life Technologies), 100 μM methionine sulfoximine (Sigma), penicillin (100 units/ml), and streptomycin (100 μg/ml). Cells secreting gE, gI, or both gE and gI were identified by immunoprecipitation of supernatants of cells metabolically labeled with [^{35}S]methionine and [^{35}S]cysteine (see below) by using either an antibody against gE (1108 (Goodwin Institute) or Fd172 (30) (kindly provided by Subbu Chatterjee) or an antibody against gI (Fd69 (31), kindly provided by Subbu Chatterjee) Clones were considered positive if immunoprecipitation yielded a protein of approximately 56 kDa corresponding to gE or a protein of approximately 43.5 kDa corresponding to gI. The identity of each protein was verified using N-terminal sequencing (see below).

^{35}S Metabolic Labeling—gE-, gI-, and gE-gI-transfected CHO cell lines derived from colonies were expanded into 12-well trays, grown to confluence, and incubated for 5 h in 1.0 ml of methionine- and cysteine-free medium (Life Technologies) plus 1% dialyzed fetal bovine serum including 5 μCi of a [^{35}S]methionine and [^{35}S]cysteine (ICN) mixture. Supernatants were clarified by a 5-min spin in a microcentrifuge, and either anti-gE or anti-gI antibodies were added. Immunoprecipitations were carried out by standard methods (32) with protein G-bearing Sepharose beads (Amersham Pharmacia Biotech). Samples were boiled in SDS-polyacrylamide gel electrophoresis (SDS-PAGE) running buffer and loaded onto 15% polyacrylamide gels, which were fixed, dried, and exposed to a PhosphorImager screen (Molecular Dynamics, Inc., Sunnyvale, CA). The image was then developed with a Molecular Dynamics 425E PhosphorImager scanner.

Co-Expression of Full-length gE and gI—PCR was used to insert a 5′ *Xho*I site and a 3′ *Not*I site into the genes encoding gE and gI. The PCR products were sequenced and subsequently individually subcloned into the unique *Xho*I and *Not*I sites of separate PBJ5-GS expression vectors. The two constructs were co-transfected into CHO cells, and cells resistant to 100 μM methionine sulfoximine were selected. Cells expressing both gE and gI were sorted using fluorescence activated cell sorting (FACS) analysis with FITC-labeled hIgG. Individual clones from the sort were amplified and subsequently shown to express both gE and gI by FACS analysis with 1108 or Fd69 as the primary antibodies and a goat anti-mouse IgG as the secondary antibody. Sorting and analysis were performed on a Coulter Epics Elite flow cytometer.

Purification of Soluble gE-gI Heterodimers—gE-gI-secreting CHO cell lines were grown to confluence in 50 10-cm plates and introduced into a hollow bioreactor device (Cell Pharm I; Unisyn Fibertec, San Diego, CA) in serum-free medium, and supernatants were collected daily. Soluble gE-gI heterodimers were purified from supernatants on either a human Fc or hIgG affinity column. The human Fc column was prepared by coupling 20 mg of human Fc (Jackson ImmunoResearch Laboratories, Inc.) to cyanogen bromide-treated Sepharose 4B (Amersham Pharmacia Biotech) at approximately 10 mg of protein/ml of resin according to the protocol of the manufacturer. The hIgG column was prepared similarly using 70 mg of hIgG (Sigma). Supernatants were passed over the affinity column, which was then washed with 50 column volumes of a solution consisting of 50 mM Tris (pH 7.4), 0.1% NaN_3, and 1 mM EDTA. Bound gE-gI was eluted from the column with 50 mM diethylamine (pH 11.5) into tubes containing 1.0 M Tris (pH 7.4). gE-gI heterodimers were further purified using a Superdex 200 HR 10/30 fast protein liquid chromatography (FPLC) filtration column. Approximately 10 mg of gE-gI heterodimers were recovered per liter of transfected cell supernatants.

N-terminal Sequencing and Mass Spectrometric Analysis of Purified gE-gI—N-terminal sequencing was performed on 2.5 μg of purified, soluble gE-gI in a phosphate buffer dried onto a polyvinylidene difluoride membrane and inserted into an Applied Biosystems model 476A sequencer reaction cartridge. Two sequences were isolated from the gE-gI sample: the sequence GTPKTSWRR, corresponding to the first 9 amino acids of mature gE (33), and the sequence LVVRGPTVS, corresponding to the first 9 amino acids of mature gI (33). The molecular masses of gE and that of gI were determined by matrix-assisted, laser desorption, time-of-flight mass spectrometry with a PerSeptive biosystems (Farmington, MA) ELITE mass spectrometer.

CD Analyses—An AVIV 62A DS spectropolarimeter equipped with a thermoelectric cell holder was used for CD measurements. Wavelength scans and thermal denaturation curves were obtained from samples containing 10 μM protein in 5 mM phosphate at pH 7 by using a 0.1-mm path length cell for wavelength scans and a 1-mm path length cell for thermal denaturation measurements. The heat-induced unfolding of gE-gI was monitored by recording the CD signal at 223 nm, while the sample temperature was raised from 25 to 80 °C at a rate of approximately 0.7 °C/min. The transition midpoint (T_m) for unfolding was determined by taking the maximum of a plot of $d\theta/dT$ *versus* T (where θ is ellipticity) after averaging the data with a moving window of 5 points.

Gel Filtration Analyses of gE-gI·hIgG Stoichiometry—Protein concentrations were determined spectrophotometrically at 280 nm using the following extinction coefficients: gE-gI, 88816 M^{-1} cm^{-1}; hIgG, 202,500 M^{-1} cm^{-1}. The extinction coefficient for the gE-gI heterodimer was calculated from the amino acid sequences as described (34), and the extinction coefficient for hIgG is known (32). A_{280} measurements for a fixed amount of each protein were then compared in 6 M guanidine HCl and aqueous solutions, and the extinction coefficients were adjusted as necessary. For determining the gE-gI·hIgG stoichiometry, various molar ratios from 1:3 (300 pmol of gE-gI:900 pmol of hIgG) to 3:1 (900 pmol of gE-gI:300 pmol of hIgG) of gE-gI and hIgG were incubated for 30 min at room temperature in 20 mM Tris, pH 7.4, 150 mM NaCl, 0.05% NaN_3

in a total volume of 100 μl. Samples were injected onto a Superose 6B FPLC column (Amersham Pharmacia Biotech) and eluted with the same buffer at 0.5 ml/min. The composition of each fraction was analyzed by SDS-PAGE (data not shown).

Equilibrium Analytical Ultracentrifugation—Sedimentation equilibrium was performed with a Beckman Optima XL-A analytical ultracentrifuge, using data analysis software provided by the manufacturer. Experiments were performed using 0.6 mg/ml gE-gI at both 4 and 20 °C at a rotor speed of 10,000 rpm, with equilibrium times of at least 36 h. Molecular masses were determined by nonlinear least square fit of the equilibrium gradient, absorbance *versus* radius (Fig. 3), using the model of single ideal species, and a partial specific volume, 0.69, calculated from the amino acid composition and the carbohydrate content (35).

Equilibrium Column Chromatography—The equilibrium column chromatography method of Hummel and Dreyer (36) was used to observe the interaction between gE-gI and hIgG. A Superdex 200 PC 3.2/30 gel filtration column of 2.4 ml was connected to an Amersham Pharmacia Biotech μ Precision pump system. Absorbance of the eluant was monitored at 280 nm with an Amersham Pharmacia Biotech μ Peak monitor. The column was equilibrated with five different concentrations of purified hIgG (Sigma): 250 nM, 500 nM, 1 μM, 2.5 μM, and 5 μM each in 20 mM Tris, pH 7.4, 150 mM NaCl. At each concentration, four 20-μl injections in the appropriate column equilibration buffer (including the relevant concentration of hIgG) were performed. These four injections included gE-gI at a concentration equal to that of the IgG in the column buffer plus no additional hIgG or hIgG at a concentration equal to 1, 2, or 3 times that of the IgG concentration contained in the column buffer. Binding experiments were done at 20 °C with a flow rate of 100 μl/min.

Biosensor Studies—Biosensor studies were performed on a Biacore 2000 instrument. Purified gE-gI was diluted in 10 mM acetate buffer, pH 4.1, for amine-based coupling to a Biacore chip. Immobilization was accomplished by initial activation of the sensor chip with 0.2 M *N*-ethyl-*N'*-(dimethylaminopropyl)-carbodiimide and 0.05 M *N*-hydroxysuccinimide. The *N*-hydroxysuccinimide-ester was then reacted with gE-gI using the manual injection mode to allow for better control of immobilization levels. Typically, an immobilization level of 200–300 response units was used for kinetic analyses described in Table I. The remaining unreacted ester groups were inactivated by 1 M ethanolamine (pH 8.5). Different concentrations of the chimeric IgG molecules were injected over the immobilized gE-gI surface, as well as a control protein surface (murine IgG). A citrate buffer, pH 3.5, was used for regeneration of the surface between sequential injections. Sensorgrams obtained for IgG binding to the control surface were subtracted from those obtained for IgG binding to the gE-gI surface. The BIAevaluation version 3.0 software package was used for kinetic analysis. Kinetic constants were derived by simultaneous fitting to the association and dissociation phases of the subtracted sensorgrams and global fitting to all curves in a working set (Fig. 5). A working set consisted of injections of four or five different concentrations of a hIgG construct over a surface containing immobilized gE-gI. S.D. values are reported from experiments performed in duplicate or triplicate on different sensor chips (Table I). In all cases, a 1:1 binding model was used for curve fitting.

The expression of chimeric hIgG molecules was described previously (37, 38). These molecules are composed of a murine anti-dansyl V_H domain fused to the constant domains (C_H1 through C_H3) of hIgG4. An expression vector containing cDNA encoding the hybrid chain was co-transfected into a non-Ig-producing mouse myeloma line along with an expression vector containing cDNA encoding a chimeric K light chain (composed of a murine anti-dansyl V_K region fused to the human C_K region). Site-directed mutations were introduced into the chimeric heavy chain gene to make the hIgG4H435R mutant and the hIgG3R435H mutant. The hIgG3-hIgG4 chimeras were generated by exon shuffling as described previously (38).

Determination of K_D Values by Cell Binding Assays—Chimeric hIgG4 was iodinated to a specific activity of 16.1 μCi/μg using the chloramine-T method. CHO cell lines expressing full-length gE and gI were grown to confluence in tissue culture plates. Cells were detached by incubation with phosphate-buffered saline (pH 7.5), 5 mM EDTA for 20–30 min and collected in binding buffer at pH 7.0 (Hanks' balanced salt solution, 10 mM HEPES, 0.25% bovine serum albumin). The cells were pelleted, washed once with binding buffer (pH 7.0), and resuspended in binding buffer (pH 7.0). Cells (1×10^6) were mixed in duplicate or triplicate assays with labeled hIgG4, different concentrations of unlabeled hIgG4, and binding buffer (pH 7.0) to a total volume of 0.5 ml. The samples were incubated for 2 h at room temperature. After completion of the incubations, cells were pelleted for 5 min at 14,000 rpm in an Eppendorf microcentrifuge, the supernatants were aspirated, and 1.0 ml of cold binding buffer was added. After removal of the supernatants by aspiration, the tubes were placed in vials, and the levels of radioactivity were determined using a Beckman Gamma 5500 counter. Nonspecific binding was determined by a similar treatment of wild type CHO cells. The binding data were analyzed using Scatchard plots. Assays were performed in triplicate, and the average of the two most similar readings was used to compute the concentration of bound IgG.

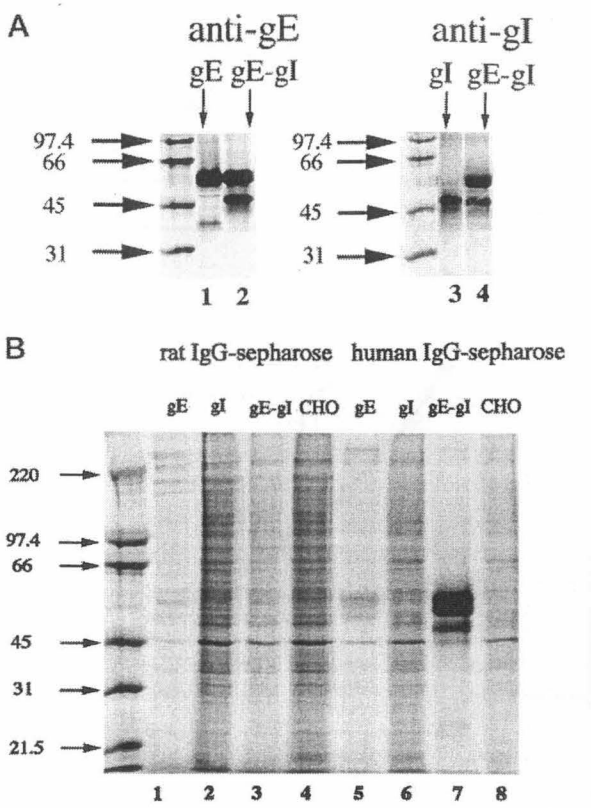

FIG. 1. **Soluble gE and gI assemble into a stable complex.** Cells producing gE, gI, or both gE and gI or nontransfected CHO cells were labeled with [^{35}S]methionine/cysteine, and cell supernatants were analyzed. *A*, SDS-PAGE (10%) analysis of protein isolated from supernatants of ^{35}S-labeled cells producing gE, gI, or gE-gI using antibodies against either gE (*lanes 1* and *2*) or gI (*lanes 3* and *4*). *B*, SDS-PAGE (10%) analysis of gE, gI, and gE-gI binding to either Sepharose-immobilized rat IgG (*lanes 1–4*) or hIgG (*lanes 5–8*).

RESULTS

Co-Expression of Truncated gE and gI Results in Assembly of a Stable Heterodimer—We constructed soluble versions of both gE and gI by truncating each of the genes prior to their predicted transmembrane regions (following the codons for amino acid 399 of mature gE and amino acid 246 of mature gI). The modified genes were co-transfected into CHO cells. Transfected cells were screened by immunoprecipitating supernatants from metabolically labeled cells with antibodies against either gE or gI (Fig. 1*A*). SDS-PAGE analysis of immunoprecipitated protein from gE-gI positive clones revealed two bands with apparent molecular masses of 56 and 43.5 kDa using either the anti-gE or anti-gI antibody. The calculated molecular mass of truncated gE is 42 kDa, and that of gI is 26 kDa; however, both proteins are glycosylated (two potential *N*-linked glycosylation sites in the sequence of gE and three potential sites in the sequence of gI) and would be expected to migrate with a higher apparent molecular mass.

HSV-1-infected cells have previously been shown to encode proteins that bind hIgG but not rodent IgG (39). To investigate the binding characteristics of soluble gE, gI, and the gE-gI

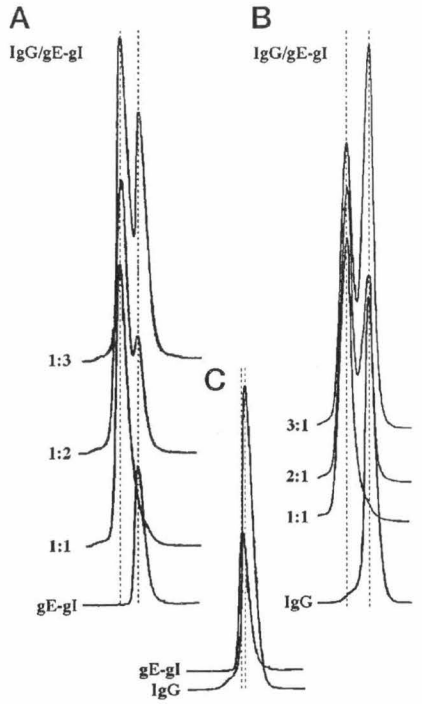

FIG. 2. **Stoichiometry determination of the gE-gI·IgG complex using conventional gel filtration.** gE-gI and IgG were incubated for 30 min at pH 7.4 at the indicated molar ratios and then passed over a size exclusion column to separate the gE-gI·IgG complex from uncomplexed proteins. At a 1:1 molar ratio of gE-gI to IgG, all of the protein chromatographs as a single complex. When the input ratio of gE-gI to IgG is greater than 1:1, there is excess gE-gI (*A*), whereas when the input ratio of IgG to gE-gI is greater than 1:1, there is excess IgG (*B*) (verified by SDS-PAGE analysis; data not shown). *C*, gE-gI and IgG each elute as a single peak and can be distinguished from one another on the basis of their retention times.

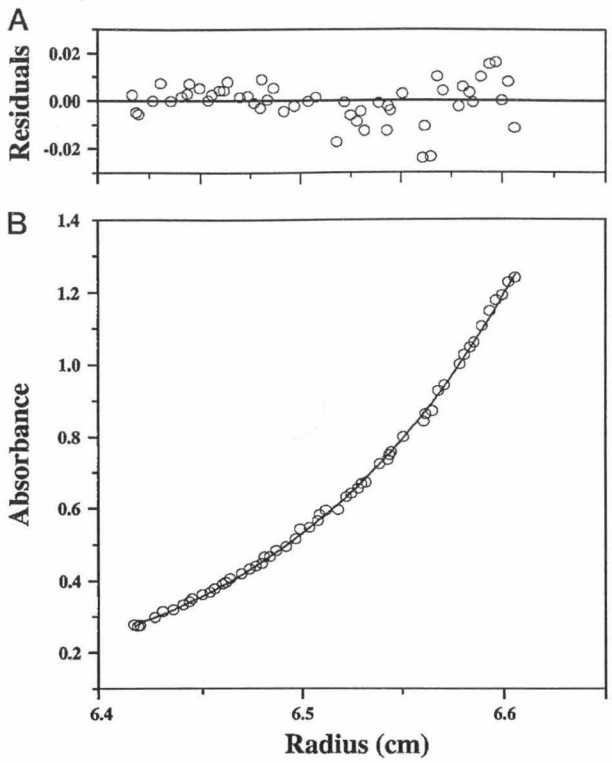

FIG. 3. **Sedimentation equilibrium analysis of gE-gI.** gE-gI at 0.6 mg/ml was centrifuged at 10,000 rpm until equilibrium was reached (36 h). The gradient formed can be best fit to a single species with a mass of 83.4 kDa. The errors of the fit, shown in the residuals plot, are small and random.

heterodimer, metabolically labeled supernatants from gE-, gI-, or gE-gI-secreting cells were incubated with Sepharose-immobilized hIgG or rat IgG. SDS-PAGE analysis revealed that while none of the proteins bind rat IgG, the gE-gI complex efficiently bound to the hIgG matrix. gE alone bound only weakly to the human IgG matrix, while gI alone showed no specific interaction (Fig. 1*B*).

A purification scheme based upon the FcR activity of gE-gI was used to isolate soluble gE-gI heterodimers for biochemical studies. Supernatants from cells expressing gE-gI were passed over an hIgG affinity column, eluted at high pH, and then further fractionated by size exclusion chromatography using a Superose 6B gel filtration column. A single homogenous peak corresponding to a gE-gI complex was obtained, demonstrating that any free gE or gI present in the supernatants does not efficiently associate with the hIgG matrix. By contrast, gE is not purified when supernatants from cells expressing only gE are passed over the hIgG column.

Soluble gE-gI migrates on the gel filtration column slower than predicted by the molecular mass of a 1:1 heterodimer (100 kDa). Indeed, the retention time for gE-gI is greater than that for IgG (165 kDa) (Fig. 2*C*). The increased retention might arise because gE-gI is not a 1:1 heterodimer or because of anomalous migration of a 1:1 heterodimer with an elongated or otherwise nonspherical shape. In order to determine the stoichiometry of soluble gE-gI, we analyzed the protein by N-terminal sequencing and equilibrium analytical ultracentrifugation. N-terminal sequencing of purified gE-gI confirmed the presence of the correctly processed forms of both proteins in approximately stoichiometric amounts (data not shown). The molecular mass of soluble gE-gI determined by equilibrium analytical ultracentrifugation is 83.4 kDa (Fig. 3), in close agreement with the predicted molecular mass of a 1:1 gE-gI heterodimer calculated using molecular masses of each monomer determined by mass spectrometry (gE, 48.4 kDa; gI, 33.5 kDa). To investigate the stability of soluble gE-gI, we used a circular dichroism-based thermal unfolding assay, from which we determined that the heterodimer denatures cooperatively with a T_m of 66 °C (data not shown).

Taken together, these results indicate that gE-gI is a stable heterodimer with 1:1 stoichiometry and that the heterodimer, but neither free gE nor free gI, binds to monomeric hIgG with high affinity. Thus, the observed interaction of free gE with IgG reported here (Fig. 1*B*, *lane 5*) as well as previously (10) must be low affinity or specific for aggregated IgG (11).

The Stoichiometry of the gE-gI·IgG Complex Is 1:1—The stoichiometry of the gE-gI·hIgG complex was determined to be 1:1 using a non-equilibrium-based gel filtration assay and confirmed using an equilibrium column chromatography method (36). As shown in Fig. 2, gE-gI, IgG, and the gE-gI·hIgG complex each elute as single peaks from a Superose 6B column and can be distinguished from one another on the basis of their retention times. To determine the stoichiometry of the gE-gI·IgG complex, various molar ratios of gE-gI to IgG were pre-equilibrated and then passed over the Superose 6B column. When gE-gI and IgG were present at equimolar ratios, a single peak corresponding to the gE-gI·IgG complex eluted from the column (Fig. 2, *A* and *B*). SDS-PAGE analysis of the eluted material revealed that both gE-gI and IgG were present in the peak (data not shown), indicating that gE-gI and IgG form a stable complex under these conditions. When the input ratio of gE-gI to IgG was greater than 1:1, a peak corresponding to excess gE-gI was observed in addition to the gE-gI·IgG complex

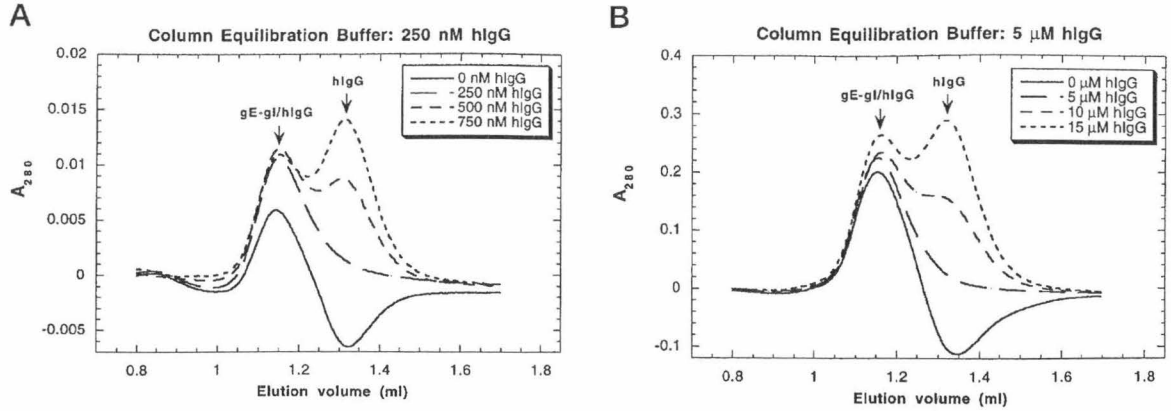

FIG. 4. **Stoichiometry determination of the gE-gI·IgG complex using equilibrium gel filtration.** A Superdex 200 column was equilibrated with 20 mM Tris, 150 mM NaCl, pH 7.4 containing either 250 nM hIgG (*A*) or 5 μM hIgG (*B*). *A*, 250 nM gE-gI was injected in equilibration buffer (20 mM Tris, 150 mM NaCl, pH 7.4, 250 nM hIgG) along with the indicated additional concentrations of hIgG. *B*, 5 μM gE-gI was injected in equilibration buffer (20 mM Tris, 150 mM NaCl, pH 7.4, 5 μM hIgG) along with the indicated additional concentrations of hIgG.

peak, whereas a peak corresponding to excess IgG was observed in addition to the complex peak when the input ratio was less than 1:1 (Fig. 2, *A* and *B*).

To verify the 1:1 stoichiometry of the gE-gI·hIgG complex, we also used an equilibrium-based method. In this method, a gel filtration column was equilibrated with buffer containing a uniform concentration of hIgG (equilibration buffer). gE-gI and hIgG mixtures in equilibration buffer were injected over the gel filtration column. Four injections were made, containing gE-gI at a concentration equal to that of hIgG in the equilibration buffer and either no additional hIgG or 1, 2, or 3 mol eq of hIgG. In all cases, all of the injected gE-gI binds to hIgG, migrating as the gE-gI·IgG complex. When the amount of additional hIgG injected is less than or greater than the amount required for formation of the gE-gI·IgG complex, a trough (in the case of too little hIgG) or a peak (in the case of excess hIgG) should be observed at the position where free hIgG migrates. When the amount of additional hIgG injected is equal to that required for formation of the gE-gI·IgG complex, a flat base line should be observed at the position where hIgG migrates. Over the concentration range from 250 nM (Fig. 4*A*) to 5 μM (Fig. 4*B*), injections of additional hIgG in an amount equivalent to that of gE-gI in the sample result in a flat base line at the hIgG migration position. These results verify that the stoichiometry of the gE-gI·hIgG complex is 1:1 over a protein concentration range of 250 nM to 5 μM.

Residue 435 at the C_H2-C_H3 Domain Interface Is Critical for gE-gI·IgG Binding—Previous IgG binding studies with HSV-1-infected cells indicated that hIgG1, hIgG2, and hIgG4 bind to the HSV-1 FcR, while many hIgG3 allotypes do not bind (39–41). This subtype binding preference resembles the binding preferences for IgG binding by *Staphylococcus aureus* protein A (protein A) and certain classes of rheumatoid factors (RF; antibodies that bind to the Fc portion of Ig) (38, 42–45). We used biosensor-based assays to quantitate the affinity between gE-gI and hIgG subtypes and to characterize the molecular basis of the observed binding specificities. Purified soluble gE-gI was immobilized on the surface of a Biacore biosensor chip using an amine-based coupling chemistry, as described in the Biacore Methods manual. We analyzed the binding of chimeric murine-hIgG molecules composed of the variable domains of a murine anti-dansyl immunoglobulin fused to the constant domains of hIgG1, hIgG2, hIgG3, or hIgG4 (37, 38). The chimeric hIgG subtypes were analyzed for binding to immobilized gE-gI at low coupling densities of gE-gI (100–300 response units), conditions under which mass transport-limited binding is not significant (46). The derived binding constants are summarized in Table I. Chimeric hIgG1, hIgG2, and hIgG4 bind to immobilized gE-gI with equilibrium dissociation constant (K_D) values of 200–400 nM. Of the different hIgG subtypes, hIgG4 has the highest affinity for gE-gI, while hIgG3 does not show detectable binding (>5 response units) at concentrations up to 3.0 μM (Table I and Fig. 5, *A* and *B*).

TABLE I

Binding of hIgG constructs to gE-gI immobilized on a Biacore chip

Kinetic constants were derived from sensorgram data using simultaneous fitting to the association and dissociation curves and global fitting to all curves in a working set. Kinetic analysis was performed using the BIAevaluation version 3.0 package. The equilibrium constants, K_D, were determined from the ratios of the kinetic constants. For hIgG3, hIgG4H435R, and 3–4-3–3, signals of less than 4 RU were observed at protein concentrations of 3.0 μM.

	$k_a \times 10^{-4}$	$k_d \times 10^3$	K_D
	Ms^{-1}	s^{-1}	nM
hIgG1	1.87 ± 0.51	5.09 ± 0.77	282 ± 36
hIgG2	1.96 ± 0.51	6.03 ± 0.08	327 ± 80
hIgG3			
hIgG4	1.75 ± 0.21	3.64 ± 0.44	199 ± 35
hIgG3R435H	1.55 ± 0.44	12.31 ± 4.09	947 ± 533
hIgG4H435R			
3–4-3–3			
3–3-4–4	2.02 ± 0.35	4.66 ± 0.36	240 ± 60
4–3-4–4	1.62 ± 43	2.94 ± 2.04	231 ± 188

For an independent verification of the biosensor-derived affinities, full-length gE and gI were expressed in CHO cells (Fig. 6), and the binding affinity for hIgG4 was derived using iodinated hIgG4. Scatchard analysis of the binding data yields a K_D value of 40.4 ± 13 nM, compared with 199 ± 35 nM in the biosensor-based analysis (Fig. 7). The 5-fold lower affinity determined using the biosensor assay could reflect that covalent immobilization of gE-gI results in reduced affinity for IgG or that the membrane-bound form of gE-gI has a higher affinity for IgG than the soluble version. Although biosensor assays may underestimate the true binding affinity of gE-gI for IgG, they allow quantitative comparison of the relative binding affinities of different hIgG mutants for gE-gI.

Position 435 of hIgG sequences contains a polymorphism that distinguishes many hIgG3 allotypes from hIgG1, hIgG2, and hIgG4. In many hIgG3, residue 435 is an arginine; a histidine is found in all other subclasses. Histidine 435 is a contact residue for protein A binding to IgG Fc (47) and is also important for the binding of some rheumatoid factors to IgG (38, 48, 49). The inability of some RF to recognize hIgG3 can be reversed if the G3m(st) allotype is used. Recognition of this

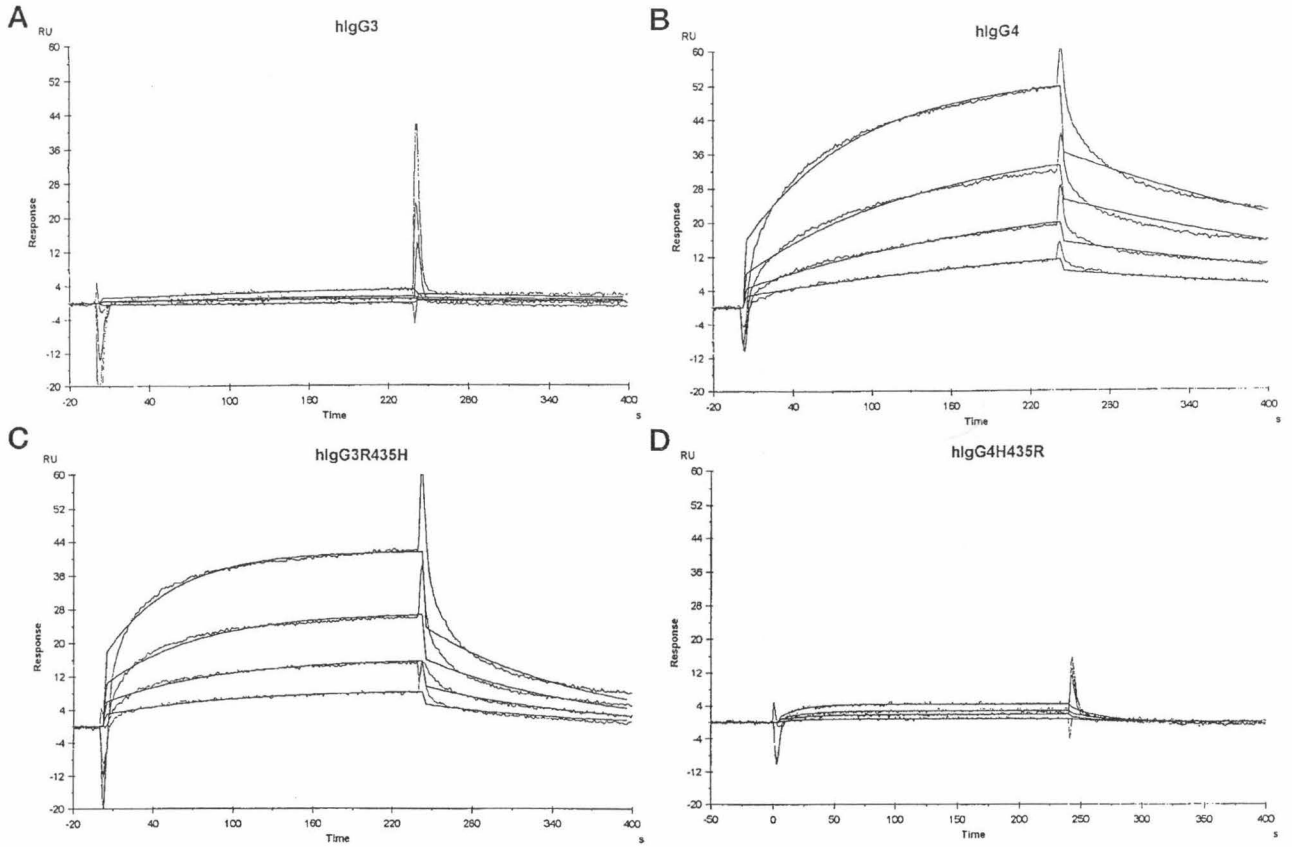

FIG. 5. **Biosensor analysis of the binding of hIgG3, hIgG4, and the corresponding residue 435 mutants.** Soluble gE-gI was immobilized on the surface of a Biacore chip using a primary amine-based coupling protocol. The injected samples were 188 nM to 1.5 μM hIgG3 (*A*), 46–366 nM hIgG4 (*B*), 70.8–566 nM hIgG3R435H (*C*), or 250 nM to 2 μM hIgG4H435R (*D*). For each set of binding experiments, sensorgrams are overlaid with the calculated response using a 1:1 binding model. One representative set of injections from experiments performed in duplicate or triplicate is shown for each interaction.

hIgG3 correlates with the presence of histidine at position 435, while nonbinding hIgG3 have an arginine at position 435 (38, 48). Histidine 435 is located at the interface between the C_H2 and the C_H3 domains of IgG (Fig. 8). The C_H2-C_H3 domain interface of IgG has previously been implicated as the binding site for HSV-1 FcR, based upon inhibition studies with a proteolytic fragment of protein A (50). Alteration of residue 435 could therefore account for the observed differences in gE-gI binding to the hIgG isotypes. Alternatively, since hIgG3 has an extended hinge compared with other hIgG isotypes, hinge-proximal structural differences might account for the observed subtype-specific binding preferences. To investigate these possibilities, we used biosensor assays to examine the binding of gE-gI to mutant hIgG3 and hIgG4 proteins and switch variants in which the constant domains of different subclasses were exchanged by exon shuffling (37, 38).

To investigate the effect of residue 435 upon gE-gI·IgG affinity, the binding of gE-gI to hIgG3 and hIgG4 mutants was examined. The hIgG3 mutant, hIgG3R435H, contains a histidine at residue 435 in place of an arginine in the wild type protein, while the hIgG4 mutant, hIgG4H435R, contains an arginine at residue 435 in place of the histidine in the wild type protein (38). The single residue change of arginine to histidine at residue 435 of hIgG3 is sufficient to restore binding from undetectable in the case of the wild type protein to an affinity of 947 ± 533 nM in the case of the single site mutant (Fig. 5, *A* and *C*, and Table I). The reciprocal change in hIgG4, histidine to arginine at position 435 (hIgG4H435R), results in no binding at concentrations up to 3 μM, as compared with a binding affinity of 199 ± 35 nM for wild type hIgG4 (Fig. 5, *B* and *D*, and Table I).

To probe for differences in affinity due to hinge-proximal structural effects, the binding of gE-gI to switch variants of IgG was examined. As described previously, switch variants have been generated by exchanging the constant domains of different subclasses by exon shuffling (38). The switch variants used in these studies were 3-3-4-4 (C_H1 and hinge domains of hIgG3, C_H2, and C_H3 domains of hIgG4), 4-3-4-4 (C_H1, C_H2, and C_H3 domains of hIgG4, hinge of hIgG3), and 3-4-3-3 (C_H1, C_H2, and the C_H3 domains of hIgG3, hinge of hIgG4). Biosensor assays indicate that the switch variants 3-3-4-4 and 4-3-4-4 bind gE-gI with an affinity comparable with that of wild type hIgG4 (Table I). By contrast, the switch variant 3-4-3-3 does not bind at concentrations up to 3.0 μM (Table I). These results demonstrate that histidine 435 at the C_H2-C_H3 domain interface of IgG is critical for gE-gI binding and that the presence of the extended hinge in the chimeric hIgG3 does not significantly hinder binding.

DISCUSSION

We have initiated a molecular characterization of IgG binding by the herpesvirus gE-gI protein. gE and gI are known to associate in HSV-1-infected cells and upon co-expression in heterologous systems (8, 9). Here we show that gE and gI assemble into a stable complex when expressed as soluble proteins. We also show that the soluble gE-gI complex can be purified to homogeneity based upon its Fc receptor function, using IgG affinity chromatography. Gel filtration and analyti-

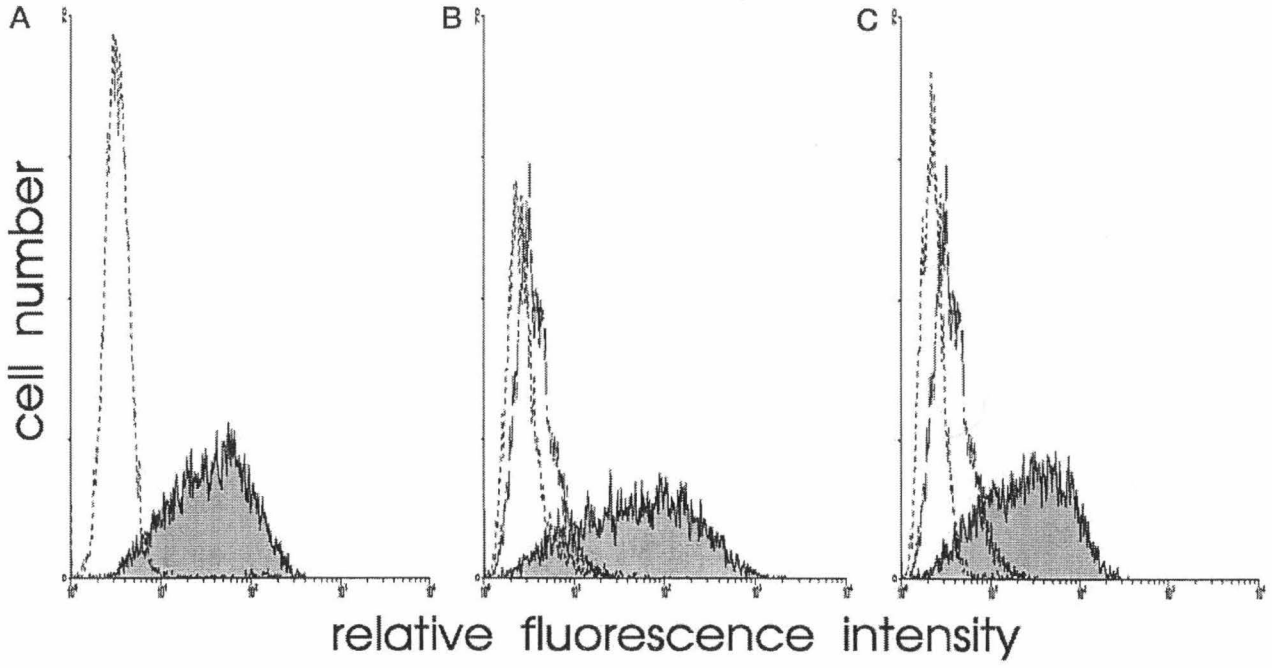

FIG. 6. **Expression of full-length gE and gI in CHO cells.** CHO cells transfected with genes encoding gE and gI were assayed for surface expression of both proteins using flow cytometry. Untransfected (*dotted lines*) or transfected (*solid lines*) cells were stained with FITC-labeled human IgG (*A*), the mouse anti-gE antibody 1108 followed by FITC-labeled goat anti-mouse antibody (*B*), or the mouse anti-gI antibody fd69 followed by FITC-labeled goat anti-mouse antibody (*C*). In *B* and *C*, the *dashed lines* represent staining of transfected cells with FITC-labeled goat anti-mouse antibody alone.

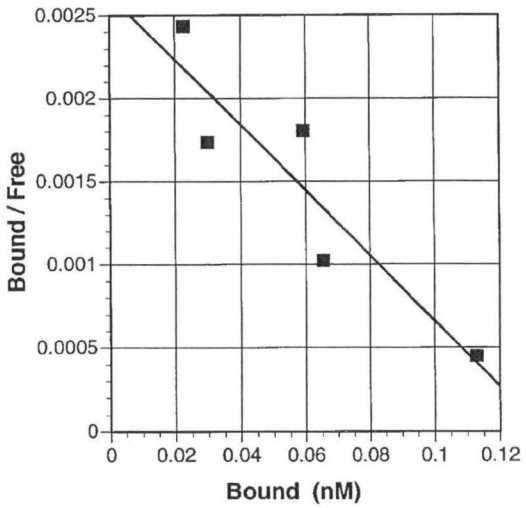

FIG. 7. **Cell binding assay for determination of the binding affinity of membrane-bound gE-gI for IgG.** 1×10^6 CHO cells expressing membrane-bound gE-gI were incubated with different concentrations of ^{125}I-labeled chimeric hIgG4. Binding data are presented as a Scatchard plot. Each point represents the average of two duplicate measurements. Three independent experiments yielded an average binding constant of 40 ± 13 nM.

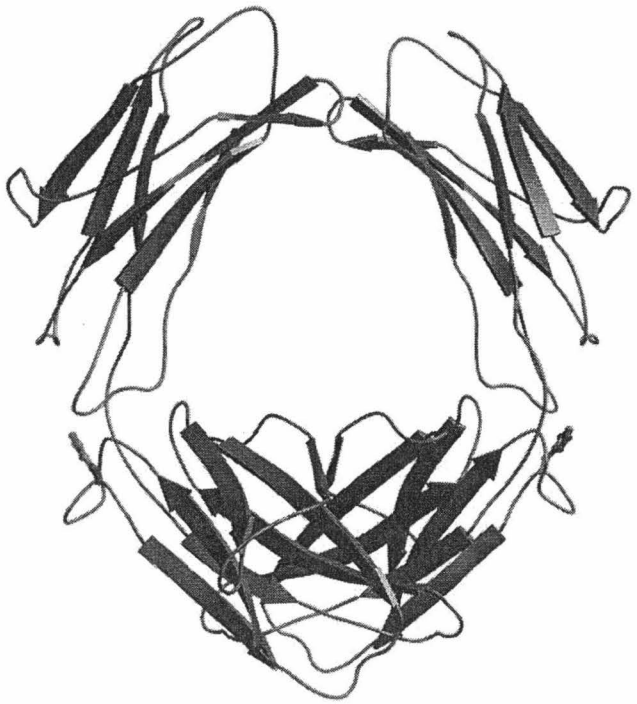

FIG. 8. **The location of histidine 435 on the structure of human Fc.** A *ribbon diagram* of the C_H2 and C_H3 domains of hIgG are shown (47). The side chain of histidine 435 is shown on the carbon-α backbone. The *figure* was prepared using Molscript (75) and rendered using Raster 3D (76).

cal ultracentrifugation experiments establish that soluble gE-gI is a 1:1 heterodimer, consistent with observations for gE-gI complexes derived from other α-herpesviruses (*e.g.* varicella zoster virus (51)). These results demonstrate that the transmembrane and cytoplasmic domains of gE and gI are not required for gE-gI heterodimer assembly and that the extracellular domains are sufficient for the assembly of gE and gI into a stable heterodimer.

Whereas neither gE nor gI alone efficiently bind monomeric hIgG, the gE-gI heterodimer binds hIgG with relatively high affinity. Biosensor-based studies using immobilized gE-gI show that soluble gE-gI binds to hIgG1, hIgG2, and hIgG4 with affinities in the range of 200–400 nM. Results from binding assays using CHO cells expressing membrane-bound gE-gI are in close agreement with the binding constant of 50 nM reported

for the interaction of rabbit IgG with HSV-1-infected cells (52). In addition, the observed binding specificities for the gE-gI interaction with different hIgG subclasses and rodent IgG parallels the binding specificities reported for IgG interaction with HSV-1-infected cells (39, 53). Thus, our results confirm that the FcR activity induced by HSV-1 infection of cells corresponds to IgG binding by cell surface gE-gI heterodimers. The relatively high affinity interaction between gE-gI and the hIgG subtypes 1, 2, and 4 indicates that nonimmune monomeric hIgG can coat HSV-1 virions at the high concentrations of hIgG present in serum (60–70 μM), thereby inhibiting virus neutralization by antiviral antibodies.

Antibody bipolar bridging by gE-gI on HSV-1-infected cells has been implicated in inhibition of ADCC mediated by mammalian FcγRs (20). Human peripheral blood mononuclear cells have been shown to mediate lower levels of ADCC activity against target cells infected with wild type HSV-1 compared with cells infected with a gE-negative HSV-1. These differences were attributed to the engagement of the Fc regions of cell surface-associated antibodies by cognate gE-gI rather than by the FcγR present on opposing immune effector cells. Among mammalian receptors, FcγRI (K_D ~0.5×10^{-9} M) is a high affinity receptor, and FcγRII and FcγRIII (K_D $<1 \times 10^{-6}$ M) are low affinity receptors (reviewed in Refs. 54 and 55). Thus, based upon affinity considerations alone, the formation of a gE-gI·IgG complex is likely to inhibit ADCC mediated by FcγRII and FcγRIII. In addition, the observed 1:1 stoichiometry for IgG interaction with gE-gI, FcγRI, and FcγRIII, as well as the fact that only one of two available binding sites on IgG is a high affinity site in the FcRn-IgG complex (reviewed in Refs. 54 and 55), suggests a marked asymmetry in the Fc regions of receptor-bound IgGs, such that only one of the binding sites is in an optimal conformation for binding to many receptors. The observed 1:1 stoichiometry of the gE-gI·IgG complex at micromolar concentrations of the proteins indicates that the asymmetry of the gE-gI·IgG complex may prevent high affinity interaction with a second gE-gI molecule. Similar mechanisms could also account for a reduced reactivity of the gE-gI·IgG complex with other Fcγ binding proteins, irrespective of the binding site location.

The 1:1 stoichiometry of the gE-gI·IgG complex could have implications for signaling mediated by IgG binding to cell surface gE-gI. Specifically, binding of monomeric IgG would not be expected to induce dimerization of gE-gI heterodimers. However, aggregated IgG (such as IgG in immune complexes) or anti-gE and anti-gI antibodies could result in gE-gI multimerization. In addition, IgG involved in antibody bipolar bridging (21) could result in the oligomerization of gE-gI with other viral glycoproteins. A conserved Y*XX*(L/V) motif is observed in the cytoplasmic domains of gE from HSV-1, HSV-2, and PRV (33, 56, 57). In mammalian receptors, the Y*XX*(V/L) motif is responsible for various signaling events such as the internalization of endocytic receptors from the plasma membrane, protein targeting to various cellular compartments (58), mediation of immune cell activation (59), and inhibition of cellular immune responses (60). The importance of the Y*XX*L motif in mammalian immune responses raises the question of whether the gE-encoded Y*XX*L motif is functional in signal transduction mediated by Fc binding. The FcR activity of gE-gI has been suggested to initiate signaling events that facilitate capping and extrusion of PRV glycoproteins, induced by a polyclonal mixture of porcine anti-PRV antibodies (13). Whether anti-HSV antibodies can mediate glycoprotein capping and extrusion in HSV-infected cells remains an important question to be addressed. If antibody-induced capping and extrusion of viral glycoproteins occurs in HSV-1-infected cells, the importance of Fc binding by gE-gI for the occurrence of the process can be rigorously investigated with the current knowledge of gE-gI binding specificities for different IgG and the interaction stoichiometry. These studies will allow a better understanding of the mechanisms by which the FcR activity of α-herpesviruses could modify the protective effects of antiviral antibodies.

Antibody bipolar bridging has been implicated in inhibition of ADCC by HSV (20) as well as in anti-PRV antibody-mediated glycoprotein capping and extrusion (13); but is antibody bipolar bridging sterically probable? Can an IgG molecule simultaneously use its Fab and the Fc regions in interactions with antigens and Fc receptors? Although direct evidence for the occurrence of antibody bipolar bridging is lacking, fluorescence energy transfer studies indicate that the IgG molecule is highly flexible (61), suggesting that simultaneous interactions of the Fab and Fc domains as postulated in antibody bipolar bridging are feasible.

Using mutant forms of hIgG, we show that histidine 435 at the interface between the C_H2 and C_H3 domains of IgG is critical for the binding interaction. Other proteins known to interact at the C_H2-C_H3 domain interface include protein A (47), protein G (62), the neonatal Fc receptor (63), and RF (44). Crystal structures have been reported for Fc complexes with protein A (47), protein G (64), neonatal Fc receptor (65), and a Fab fragment derived from a human IgM RF antibody (RF-AN) (49, 66). From comparisons of the binding characteristics observed for the gE-gI·IgG complex and IgG complexes with protein A, protein G, neonatal Fc receptor, and RF, it appears that the gE-gI·IgG complex most closely resembles IgG complexes with certain rheumatoid factors. The similarities include a lack of binding of several hIgG3 allotypes, the species specificity (binding to human and rabbit IgG, but lack of binding of rodent IgG (39, 53, 66)), and the importance of histidine 435 in the binding interaction. That the IgG binding specificity of gE-gI closely resembles that of some RF is significant in understanding the origin of RF, since it has been suggested that some RF arise as anti-idiotypic antibodies against antibodies to bacterial or viral Fcγ-binding proteins, in a process known as idiotypic networking (44, 67, 68).

Anti-idiotypic antibodies recognize the idiotypic determinants expressed in the V region of a particular antibody or the V regions of a group of related antibodies. It has been proposed that anti-idiotypic antibodies are expressed in order to regulate the expression of antibodies that dominate the response to a particular antigen (69). Suppression of B cells expressing these dominant antibodies would allow for the proliferation of other antibodies using alternative V region sequences and ultimately to the diversification of the antibody response (70). While the expression of anti-idiotypic antibodies would normally decline with the decreased expression of the antibodies to which they are responding, anti-idiotypic antibodies that cross-react with something so ubiquitous as self-IgG have the potential to be continually propagated. This model of idiotypic suppression provides a possible explanation for the production of RF as a result of HSV-1 infection. Expression of gE-gI on the virion and on the surface of HSV-1-infected cells would lead to production of anti-gE-gI antibodies and subsequently to the production of anti-anti-gE-gI antibodies that have the potential to be RF if the epitope recognized by the anti-gE-gI antibody is the region on gE-gI that interacts with IgG-Fc. In addition, persistence of HSV-I infection may lead to continual production of RF.

The similarities we observe between the gE-gI·IgG complex and IgG complexes with certain classes of RF support the hypothesis that some RF might be anti-idiotypic antibodies against antibodies to gE-gI and provide the basis to more closely examine the linkage between herpesviral infections and

pathogenic RF production. Further support comes from studies by Tsuchiya *et al.* (71), which show that some RF share idiotypic determinants with gE-gI, suggesting that these RF may be anti-idiotypic antibodies against antibodies to gE-gI. However, whether the observed similarities in binding characteristics of gE-gI·IgG and the RF-IgG complexes will correspond to similarities in the interactions at the atomic level remains to be determined from crystallographic comparisons of gE-gI·IgG with RF·IgG complexes that show the closest resemblance in binding characteristics.

Recent studies suggest that antibodies are highly protective against herpes infections in human neonates (72). Based upon the binding studies reported here and previous studies with HSV-1-infected cells (39, 40, 53), gE-gI can mitigate the effects of antiviral antibodies of the IgG1, IgG2, and IgG4 subtypes, whereas IgG3 allotypes might confer the greatest protection to a host due to the inability of many IgG3 allotypes to bind gE-gI. HSV-specific antibodies of the IgG1, IgG3, and IgG4 subclasses have been detected in genital herpes infections (73). Because human neonatal Fc receptor (the receptor responsible for transplacental IgG transfer (74)) binds the four human IgG isotypes with similar affinities,[2] IgG3 is likely to be transferred to the fetus with equal efficacy compared with the other isotypes that are generated, and it may constitute the isotype that confers the greatest protection against neonatal herpes. However, it is possible that anti-HSV hIgG3 antibodies are not produced or are not effective in certain HSV infections, and therefore, a virus expressing an IgG3-binding FcR would not experience a selective advantage. This may explain the lack of hIgG3 binding to gE-gI and the evolution of the viral FcR with specificity for other hIgG subclasses.

Acknowledgments—We thank Philip E. Lapinski for doing the cell binding experiments, the flow cytometry core at the University of Michigan for performing the fluorescence-activated cell sorting analyses, the Reproductive Sciences program at the University of Michigan for IgG radiolabeling, Parke-Davis research facility for use of the Biacore for initial characterization of the gE-gI·IgG complex, and the California Institute of Technology Protein/Peptide Micro Analytical Laboratory for protein analysis. We also thank Pak Poon for doing the equilibrium analytical ultracentrifugation experiments. We thank Dr. Oveta J. Fuller and Pak Poon for many helpful discussions.

REFERENCES

1. Gooding, L. R. (1992) *Cell* **71,** 5–7
2. Banks, T. A., and Rouse, B. T. (1992) *Clin. Infect. Dis.* **14,** 933–941
3. Ploegh, H. (1998) *Science* **280,** 248–253
4. Dubin, G., Fishman, N. O., Eisenberg, R. J., Cohen, G. H., and Friedman, H. M. (1992) *Curr. Top. Microbiol.* **179,** 111–120
5. Westmoreland, D., and Watkins, J. F. (1974) *J. Gen. Virol.* **24,** 167–178
6. Baucke, R. B., and Spear, P. G. (1979) *J. Virol.* **32,** 779–789
7. Para, M. F., Baucke, R. B., and Spear, P. (1980) *J. Virol.* **34,** 512–520
8. Johnson, D. C., and Feenstra, V. (1987) *J. Virol.* **61,** 2208–2216
9. Johnson, D. C., Frame, M., Ligas, M. W., Cross, A. M., and Stow, N. D. (1988) *J. Virol.* **62,** 1347–1354
10. Bell, S., Cranage, M., Borysiewicz, L., and Minson, T. (1990) *J. Virol.* **64,** 2181–2186
11. Dubin, G., Frank, I., and Friedman, H. M. (1990) *J. Virol.* **64,** 2725–2731
12. Hanke, T., Graham, F. L., Lulitanond, V., and Johnson, D. C. (1990) *Virology* **177,** 437–444
13. Favoreel, H. W., Nauwynck, H. J., Van Oostveldt, P., Mettenleiter, T. C., and Pensaert, M. B. (1997) *J. Virol.* **71,** 8254–8261
14. Litwin, V., Jackson, W., and Grose, C. (1992) *J. Virol.* **66,** 3643–3651
15. Nagashunmugam, T., Lubinski, J., Wang, L., Goldstein, L. T., Weeks, B. S., Sundaresan, P., Kang, E. H., Dubin, G., and Friedman, H. M. (1998) *J. Virol.* **72,** 5351–5359
16. Lehner, T., Wilton, J. M. A., and Shillitoe, E. J. (1975) *Lancet* **ii,** 60–62
17. Costa, J. C., and Rabson, A. S. (1975) *Lancet* **i,** 77–78
18. Adler, R., Glorioso, J. C., Cossman, J., and Levine, M. (1978) *Infect. Immun.* **21,** 442–447
19. Dowler, K. W., and Veltri, R. W. (1984) *J. Med. Virol.* **13,** 251–259
20. Dubin, G., Socolof, E., Frank, I., and Friedman, H. M. (1991) *J. Virol.* **65,** 7046–7050
21. Frank, I., and Friedman, H. M. (1989) *J. Virol.* **63,** 4479–4488
22. Whealy, M. E., Card, J. P., Robbins, A. K., Dubin, J. R., Rziha, H.-J., and Enquist, L. W. (1993) *J. Virol.* **67,** 3786–3797

[2] A. P. West and P. J. Bjorkman, unpublished results.

23. Tirabassi, R. S., Townley, R. A., Eldridge, M. G., and Enquist, L. W. (1997) *J. Virol.* **71,** 6455–6464
24. Dingwell, K. S., Brunetti, C. R., Hendricks, R. L., Tang, Q., Tang, M., Rainbow, A. J., and Johnson, D. C. (1994) *J. Virol.* **68,** 834–835
25. Dingwell, K. S., Doering, L. C., and Johnson, D. C. (1995) *J. Virol.* **69,** 7087–7098
26. Balan, P., Davis-Poynter, N., Bell, S., Atkinson, H., Browne, H., and Minson, T. (1994) *J. Gen. Virol.* **75,** 1245–1258
27. Sambrook, J., Fritsch, E. F., and Maniatis, T. (1989) *Molecular Cloning: A Laboratory Manual*, 2nd Ed., Cold Spring Harbor Laboratory, Cold Spring Harbor, NY
28. Gastinel, L. N., Simister, N. E., and Bjorkman, P. J. (1992) *Proc. Natl. Acad. Sci. U. S. A.* **89,** 638–642
29. Bebbington, C. R., and Hentschel, C. C. G. (1987) in *DNA Cloning: A Practical Approach* (Glover, D. M., ed) pp. 163–188, IRL Press, Oxford
30. Metcalf, J. F., Chatterjee, S., Koga, J., and Whitley, R. J. (1988) *Intervirology* **29,** 39–49
31. Longnecker, R., Chatterjee, S., Whitley, R. J., and Roizman, B. (1987) *Proc. Natl. Acad. Sci. U. S. A.* **84,** 4303–4307
32. Harlow, E., and Lane, D., *Antibodies: A Laboratory Manual* (1988) *Antibodies: A Laboratory Manual*, pp. 310–311, Cold Spring Harbor Laboratory, Cold Spring Harbor, NY
33. McGeoch, D. J., Dolan, A., Donald, S., and Brauer, D. H. (1985) *J. Mol. Biol.* **181,** 1–13
34. Gill, S. C., and Von Hippel, P. H. (1989) *Anal. Biochem.* **182,** 319–326
35. Zamyatnin, A. A. (1972) *Prog. Biophys. Mol. Biol.* **24,** 107–123
36. Hummel, J. P., and Dreyer, W. J. (1962) *Biochim. Biophys. Acta* **63,** 530–532
37. Artandi, S. E., Canfield, S. M., Tao, M., Calame, K. L., Morrison, S. L., and Bonagura, V. R. (1991) *J. Immunol.* **146,** 603–610
38. Bonagura, V. R., Artandi, S. E., Agostino, N., Tao, M., and Morrison, S. L. (1992) *DNA Cell Biol.* **11,** 245–252
39. Johansson, P. J., Myhre, E. B., and Blomberg, J. (1985) *J. Virol.* **56,** 489–494
40. Wiger, D., and Michaelsen, T. E. (1985) *Immunology* **54,** 565–573
41. Johansson, P. J., Ota, T., Tsuchiya, N., Malone, C. C., and Williams, R. C. (1994) *Immunology* **83,** 631–638
42. Kronvall, G., and Williams, R. C. (1966) *J. Immunol.* **103,** 828–833
43. Allen, J. C., and Kunkel, H. G. (1966) *Arthritis Rheum.* **9,** 758–768
44. Nardella, F. A., Teller, D. C., Barber, C. V., and Mannik, M. (1985) *J. Exp. Med.* **162,** 1811–1824
45. Langone, J. J. (1982) *Adv. Immunol.* **32,** 157–252
46. Karlsson, R., and Falt, A. (1997) *J. Immunol. Methods* **200,** 121–123
47. Deisenhofer, J. (1981) *Biochemistry* **20,** 2361–2370
48. Bonagura, V. R., Artandi, S. E., Davidson, A., Randen, I., Agostino, N., Thompson, K., Natvig, J. B., and Morrison, S. L. (1993) *J. Immunol.* **151,** 3840–3852
49. Sutton, B. J., Corper, A. L., Sohi, M. K., Beale, D., and Taussig, M. J. (1998) *Adv. Exp. Med. Biol.* **435,** 41–50
50. Johansson, P. J., Nardella, F. A., Sjöquist, J., Schröder, A. K., and Christensen, P. (1989) *Immunology* **66,** 8–13
51. Kimura, H., Straus, S. E., and Williams, R. K. (1997) *Virology* **233,** 382–391
52. Johansson, P. J., and Blomberg, J. (1990) *APMIS* **98,** 685–694
53. Johansson, P. J., Hallberg, T., Oxelius, V. A., Grubb, A., and Blomberg, J. (1984) *J. Virol.* **50,** 796–804
54. Hulett, M. D., and Hogarth, P. M. (1994) *Adv. Immunol.* **57,** 1–127
55. Raghavan, M., and Bjorkman, P. (1996) *Annu. Rev. Cell Dev. Biol.* **12,** 181–220
56. Petrovskis, E. A., Timmins, J. G., and Post, L. E. (1986) *J. Virol.* **60,** 185–193
57. McGeoch, D. J., Moss, H. W., McNab, D., and Frame, M. C. (1987) *J. Gen. Virol.* **68,** 19–38
58. Trowbridge, I. S., Collawn, J. F., and Hopkins, C. R. (1993) *Annu. Rev. Cell Biol.* **9,** 129–161
59. Cambier, J. C. (1992) *Curr. Opin. Immunol.* **4,** 257–264
60. Leisbon, P. J. (1997) *Immunity* **6,** 655–661
61. Zheng, Y., Shopes, B., Holowka, D., and Baird, B. (1992) *Biochemistry* **31,** 7446–7456
62. Stone, G. C., Sjöbring, U., Björck, L., Sjöquist, J., Barber, C. V., and Nardella, F. A. (1989) *J. Immunol.* **143,** 565–570
63. Raghavan, M., Chen, M. Y., Gastinel, L. N., and Bjorkman, P. J. (1994) *Immunity* **1,** 303–315
64. Sauer-Eriksson, A. E., Kleywegt, G. J., Uhlen, M., and Jones, T. A. (1995) *Structure* **3,** 265–278
65. Burmeister, W. P., Huber, A. H., and Bjorkman, P. J. (1994) *Nature* **372,** 379–383
66. Corper, A. L., Sohi, M. K., Bonagura, V., Steinitz, M., Jefferis, R., Feinstein, A., Beale, D., Taussig, M. J., and Sutton, B. J. (1997) *Nat. Struct. Biol.* **4,** 374–381
67. Cooke, A., Lydyard, A. M., and Roitt, I. M. (1984) *Lancet* **2,** 723–725
68. Plotz, P. H. (1983) *Lancet* **2,** 824–826
69. Jerne, N. K. (1974) *Ann. Immunol. (Paris)* **125C,** 373–389
70. Lange, H., Solterback, M., Berek, C., and Lemke, H. (1996) *Eur. J. Immunol.* **26,** 2234–2242
71. Tsuchiya, N., Williams, R. C., and Hutt-Fletcher, L. M. (1990) *J. Immunol.* **144,** 4742–4748
72. Brown, Z. A., Selke, S., Zeh, J., Kopelman, J., Maslow, A., Ashley, R. L., Watts, M. D., Berry, S., Herd, M., and Corey, L. (1997) *N. Engl. J. Med.* **337,** 509–515
73. Hashido, M., and Kawana, T. (1997) *Microbiol. Immunol.* **41,** 415–420
74. Story, C. M., Mikulska, J. E., and Simister, N. E. (1994) *J. Exp. Med.* **180,** 2377–2381
75. Kraulis, P. J. (1991) *J. Appl. Crystallogr.* **24,** 946–950
76. Merritt, E. A., and Murphy, M. E. P. (1994) *Acta Crystallogr. Ser. D.* **50,** 869–873